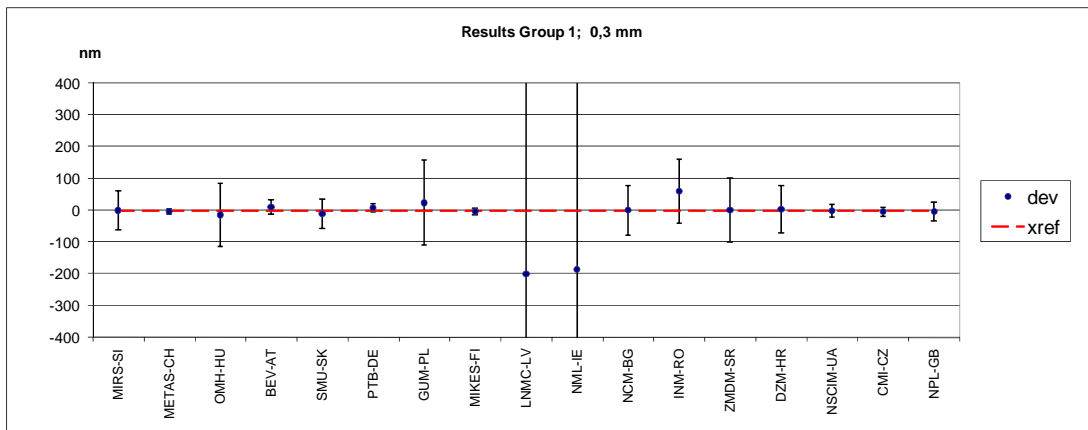
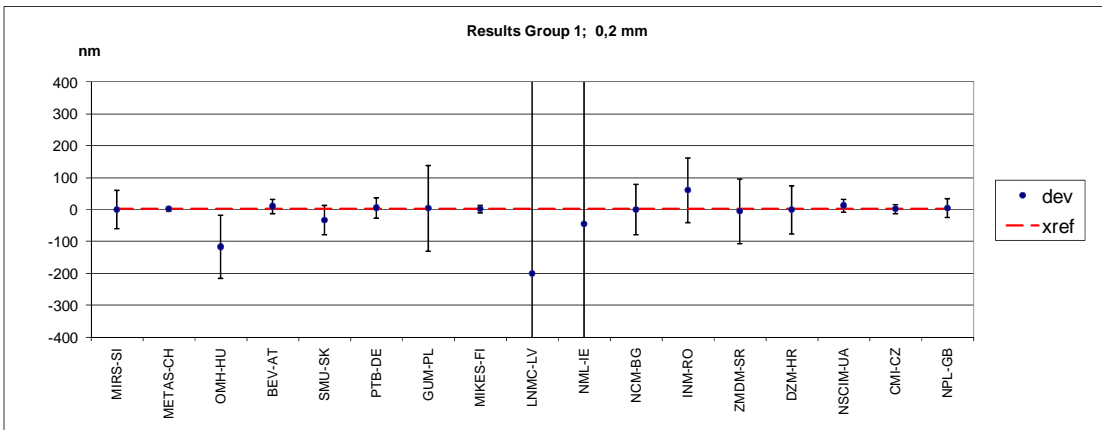
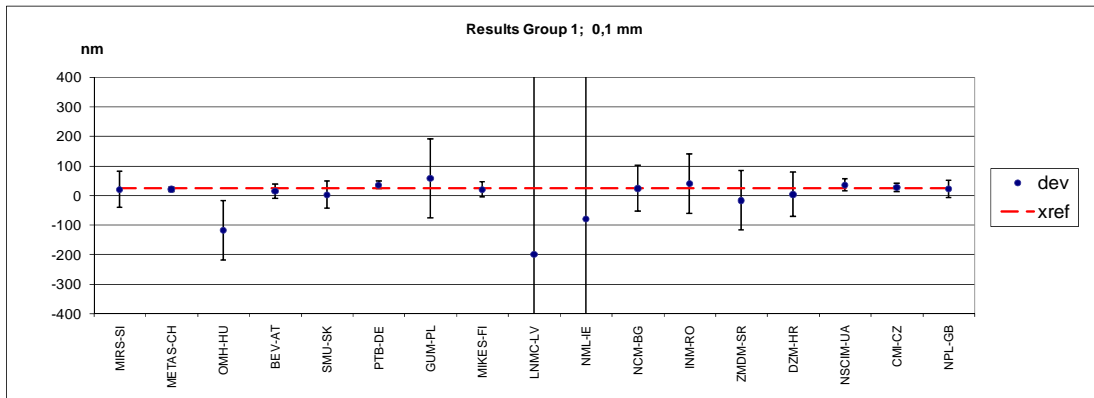
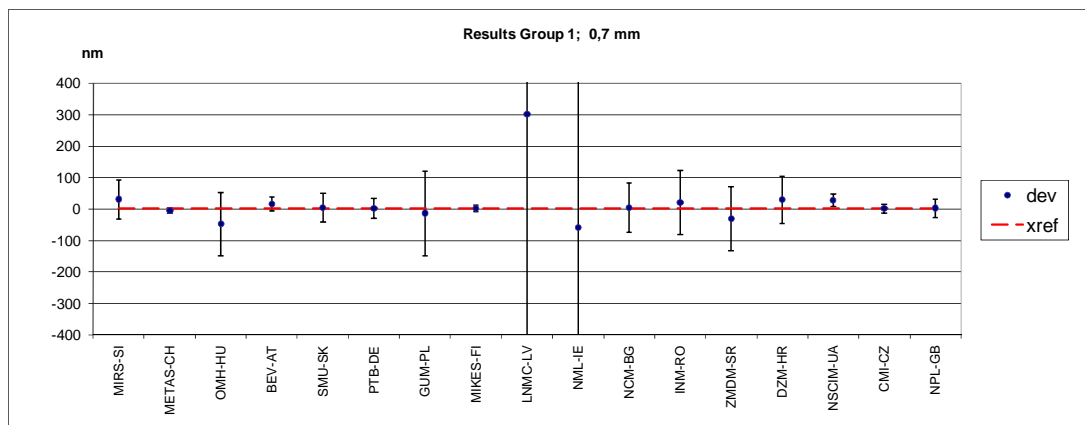
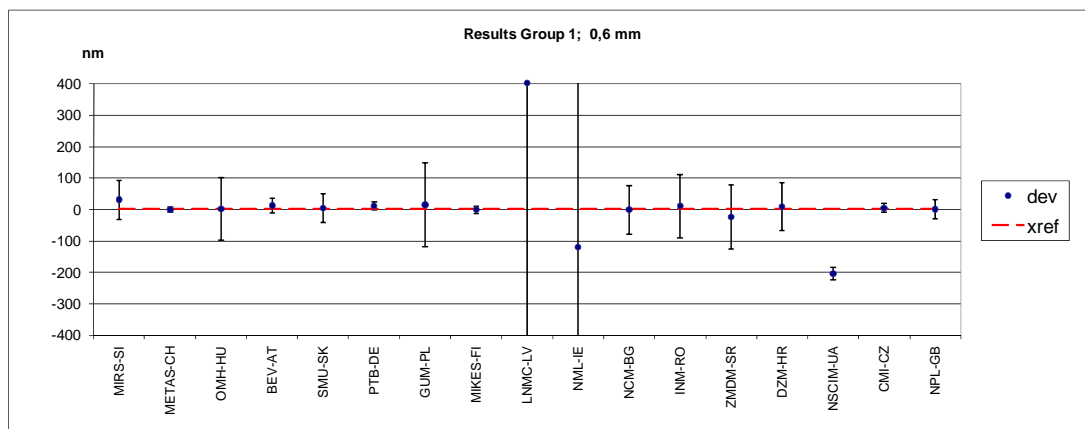
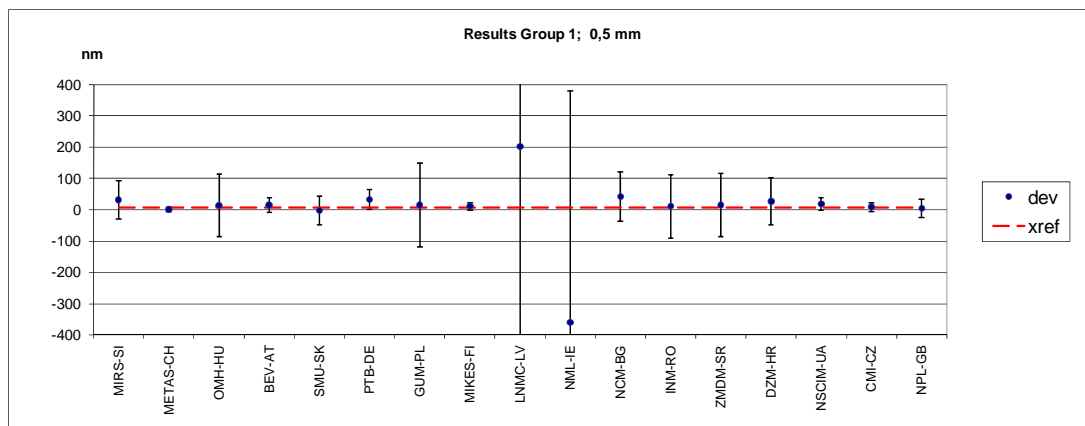
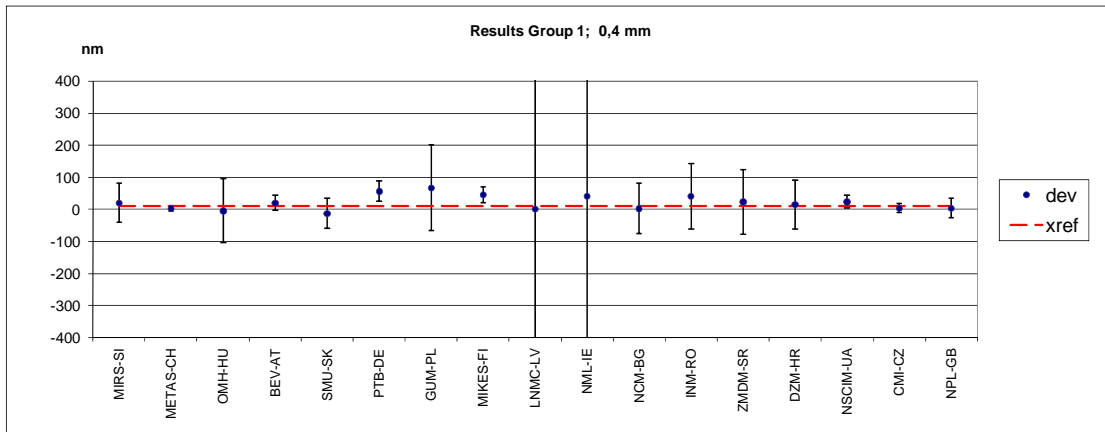


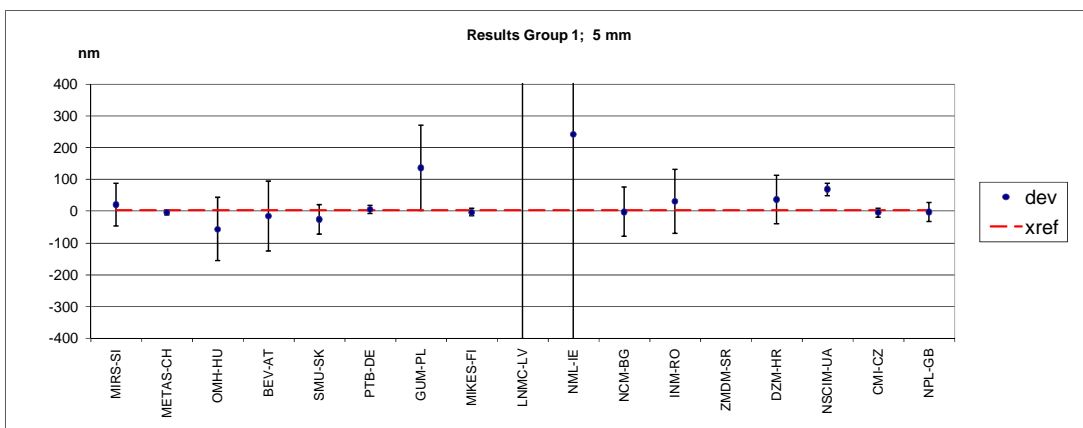
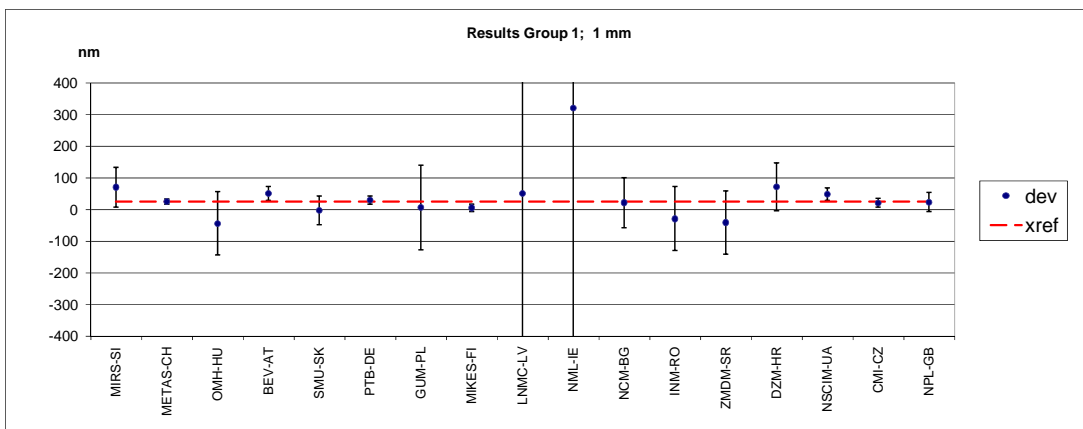
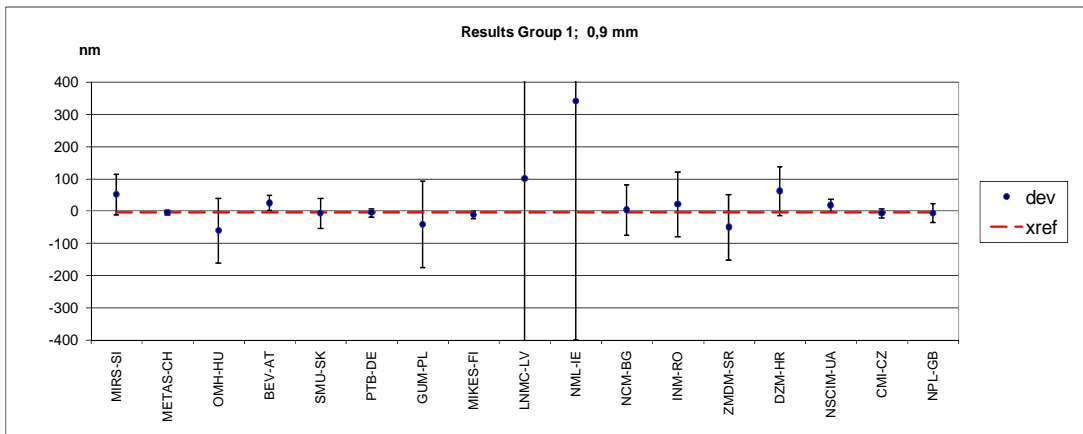
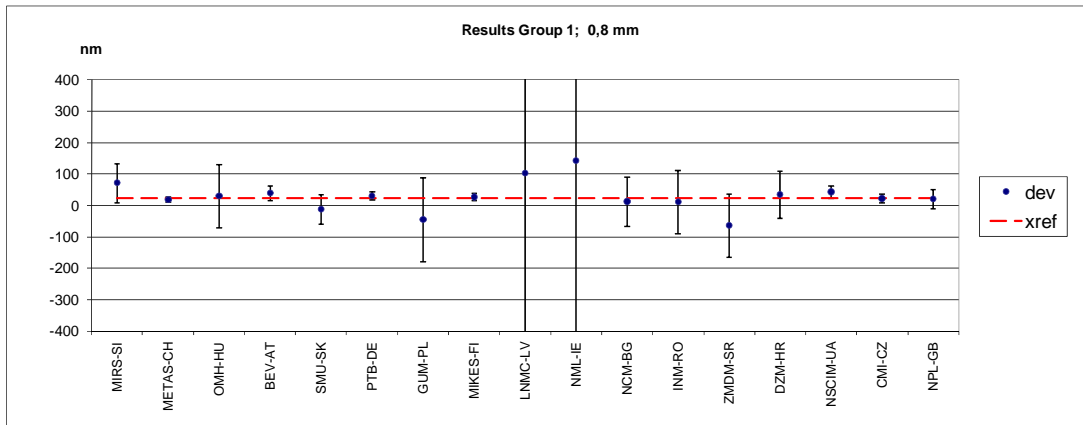
Appendix 1: Intercomparison results for the case of separate treatment of groups 1 and 2 (without link)

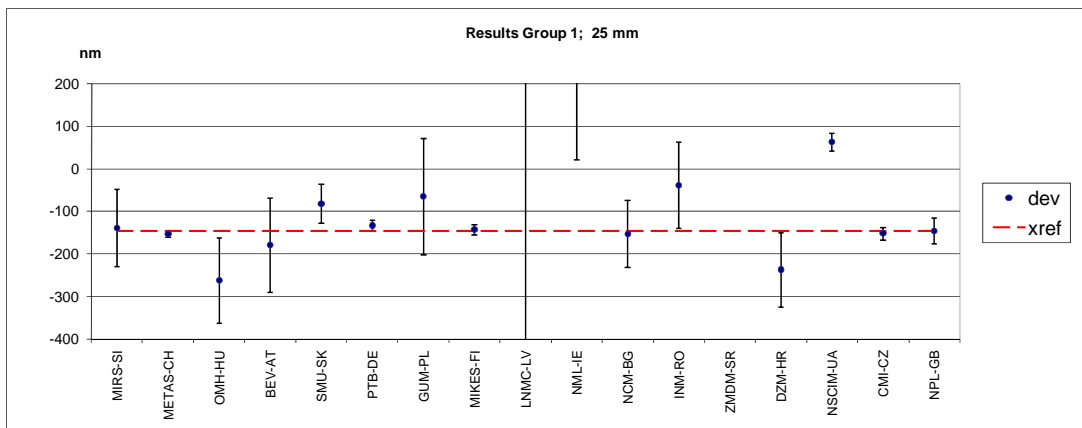
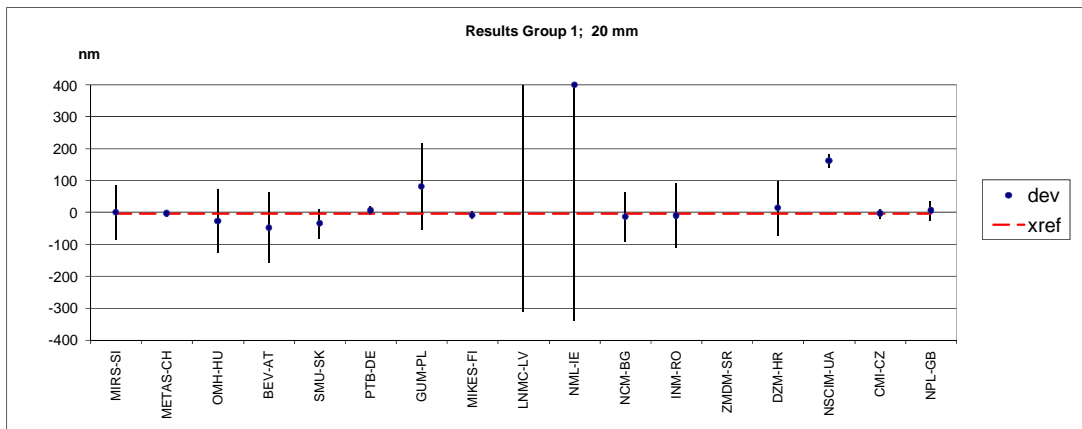
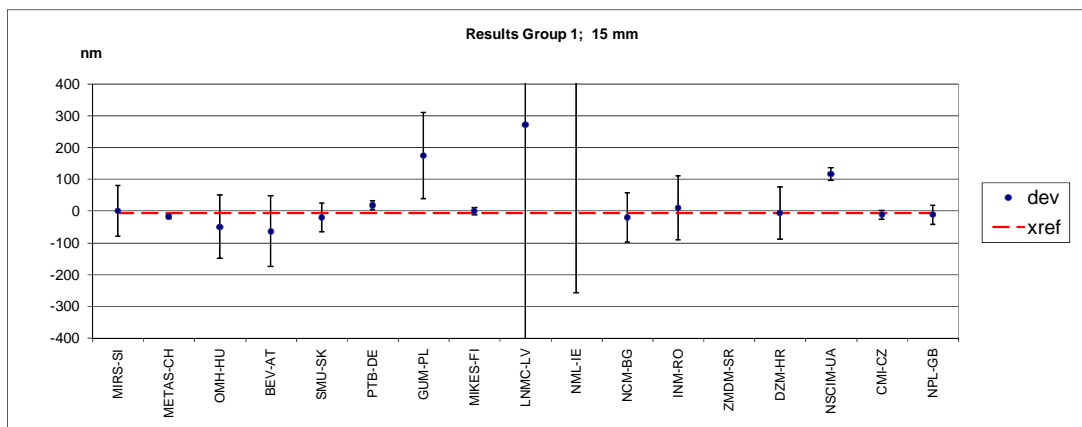
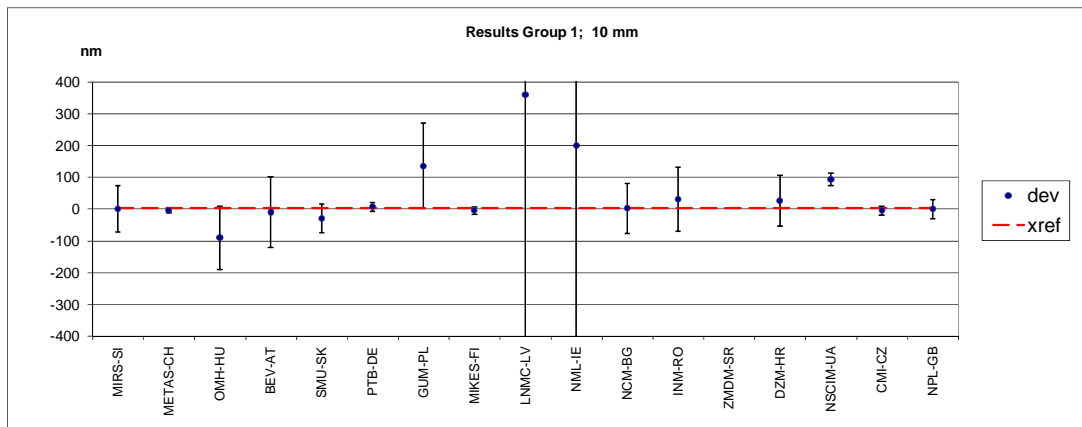
1.1 Group 1 – deviations from reference value

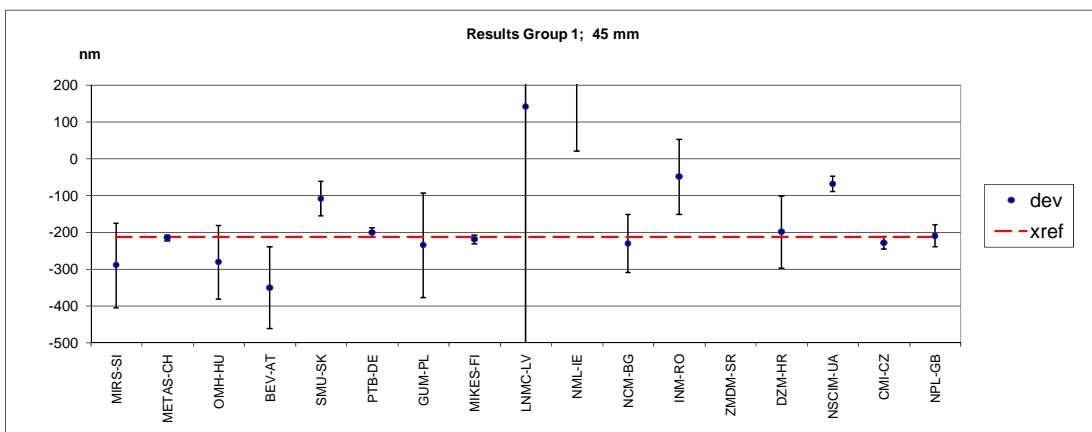
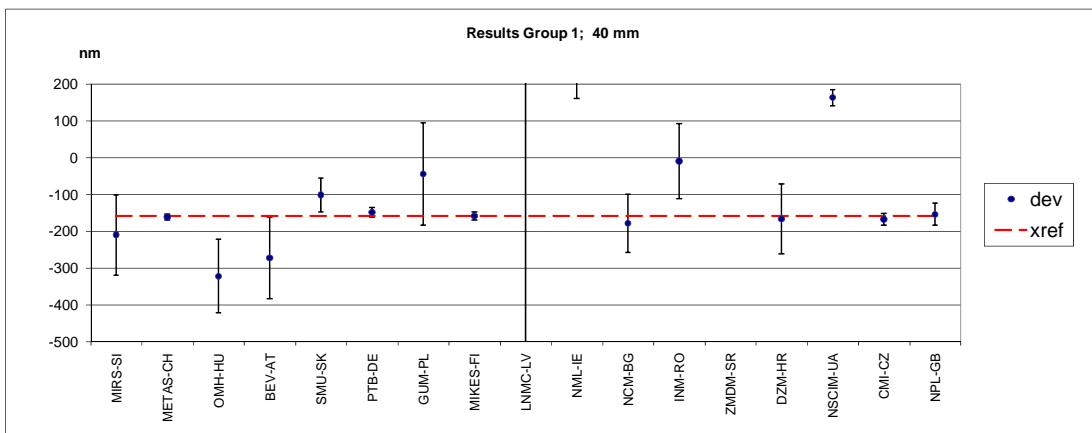
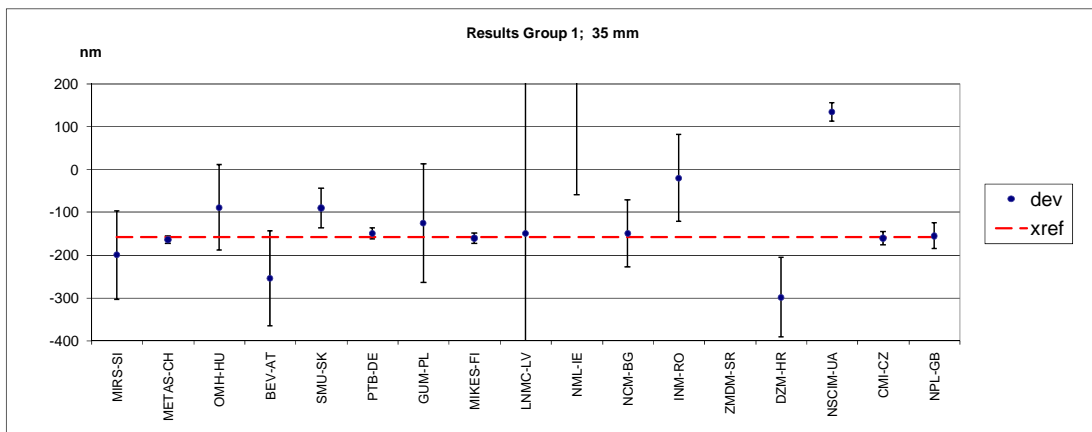
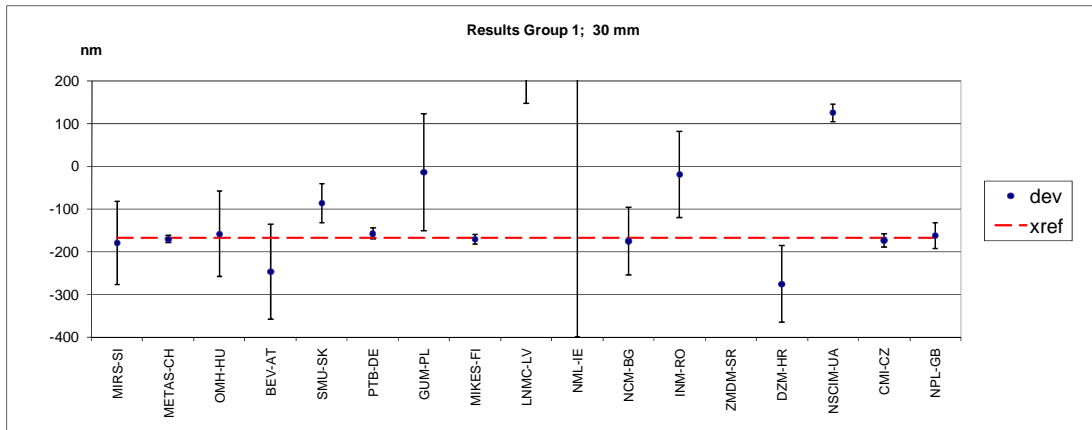
Graphical presentation of measurement results follows in 30 diagrams. Uncertainty bars in the diagrams for single measuring points represent standard uncertainty u ($k = 1$).

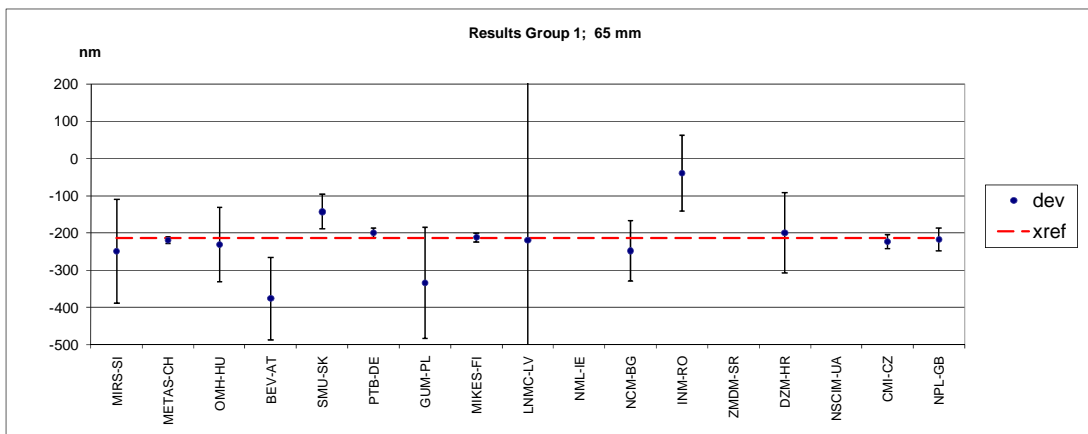
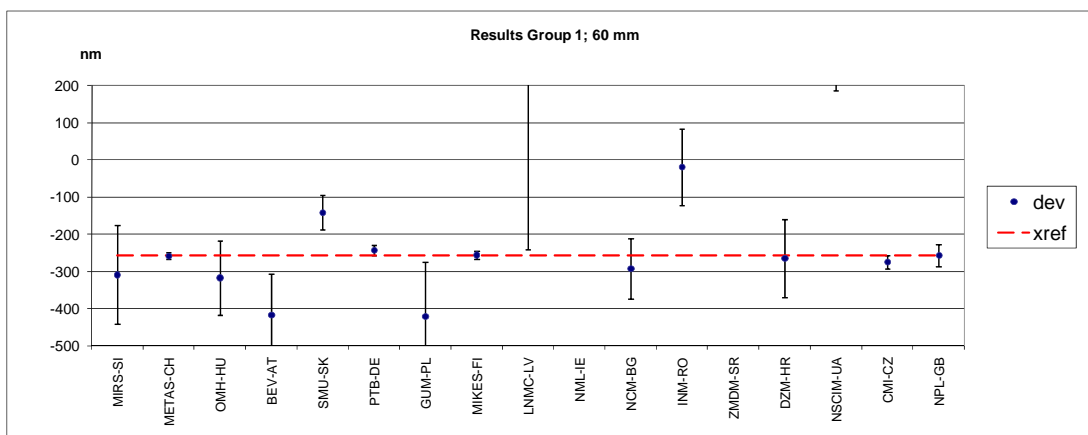
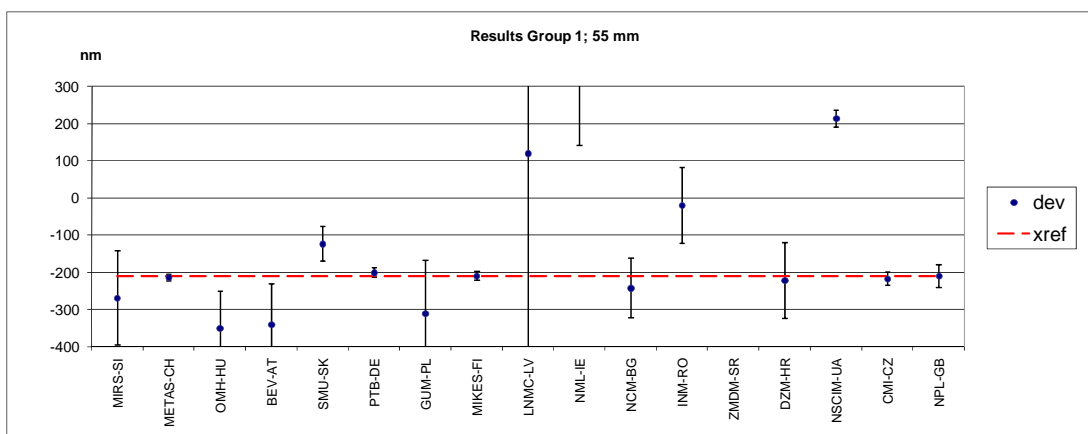
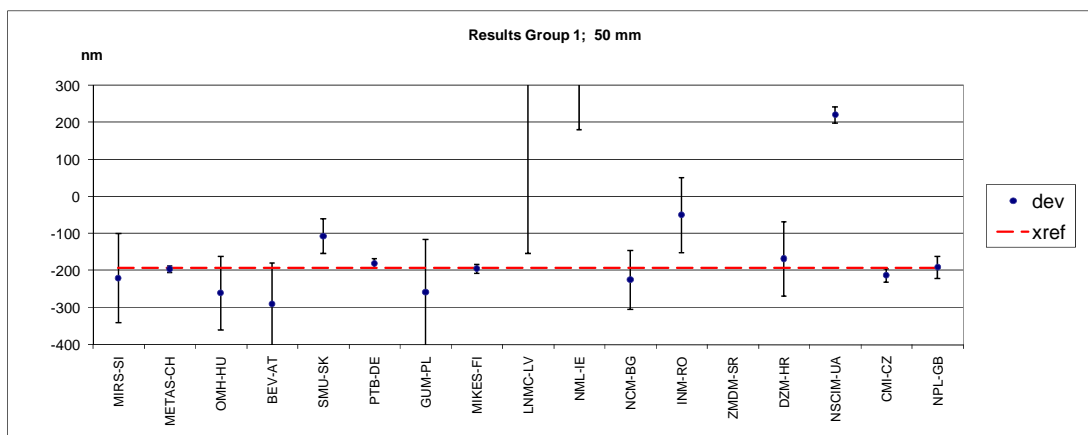


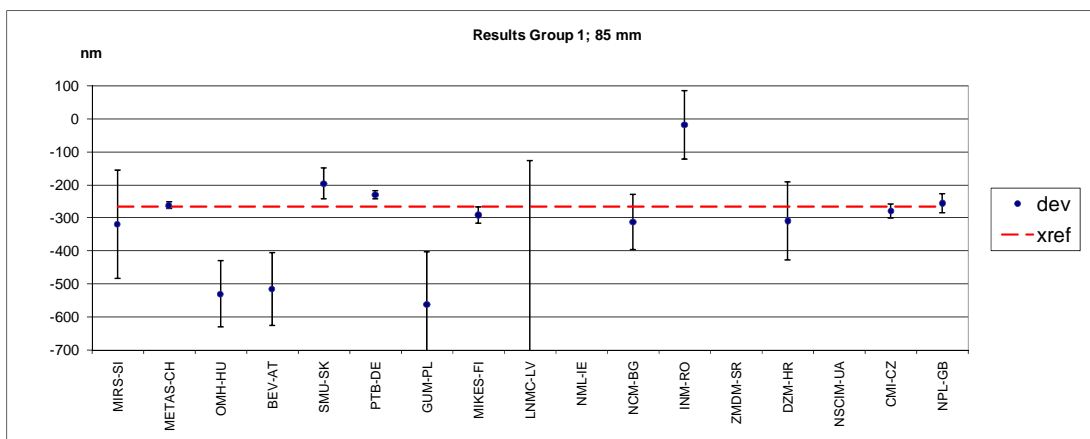
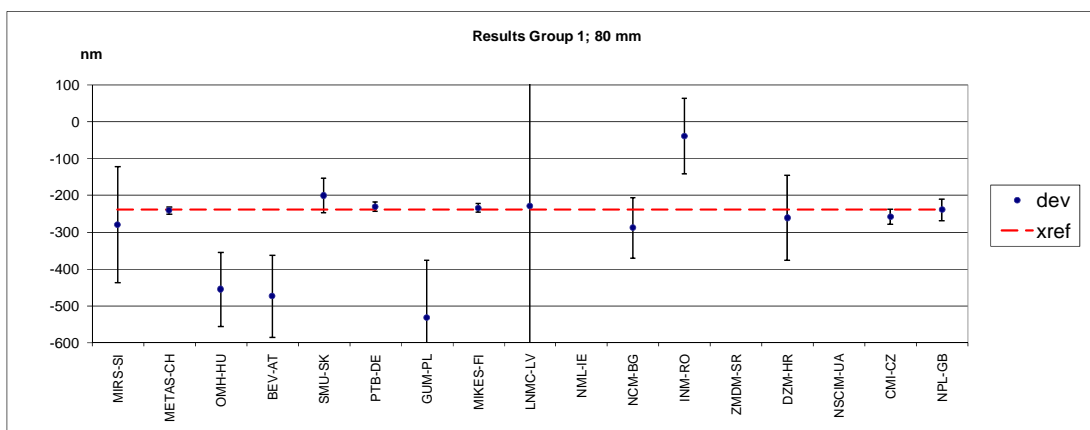
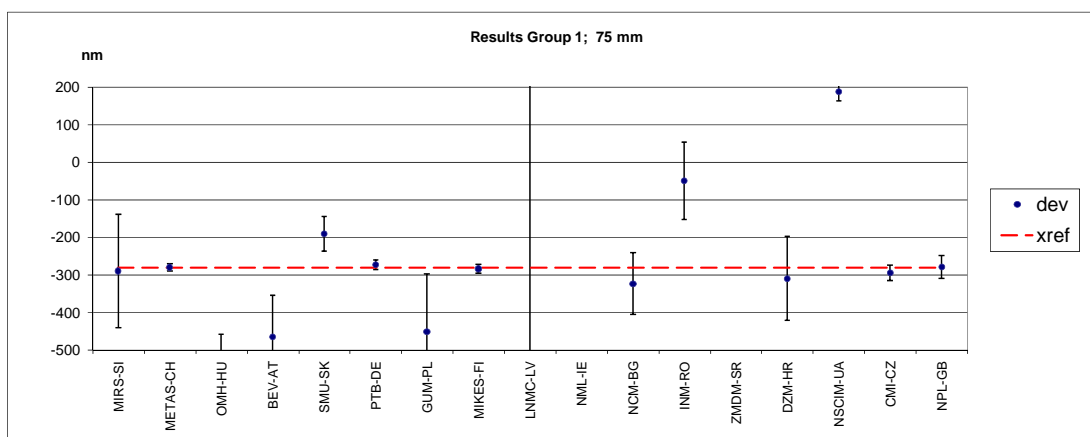
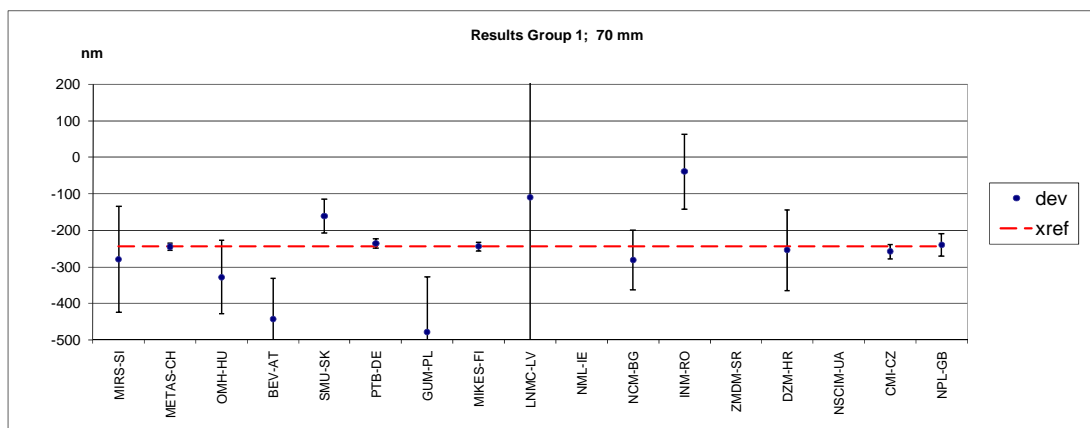


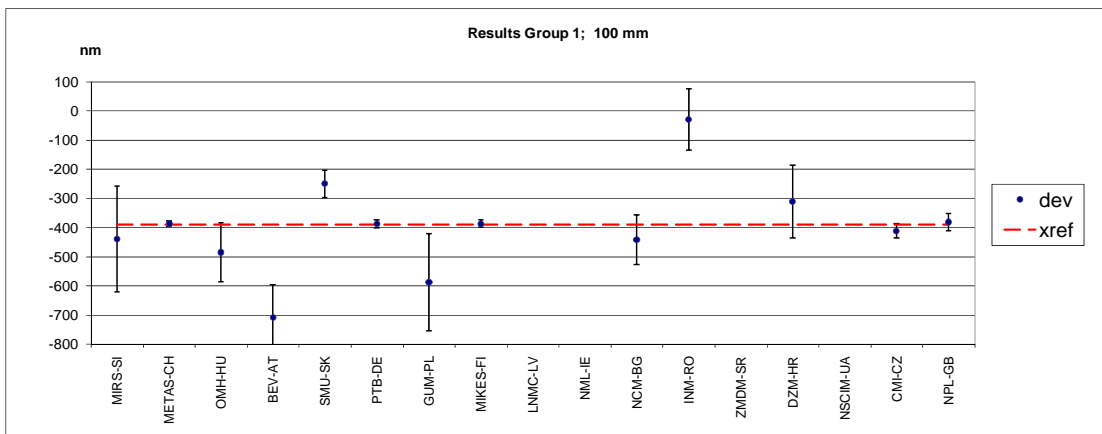
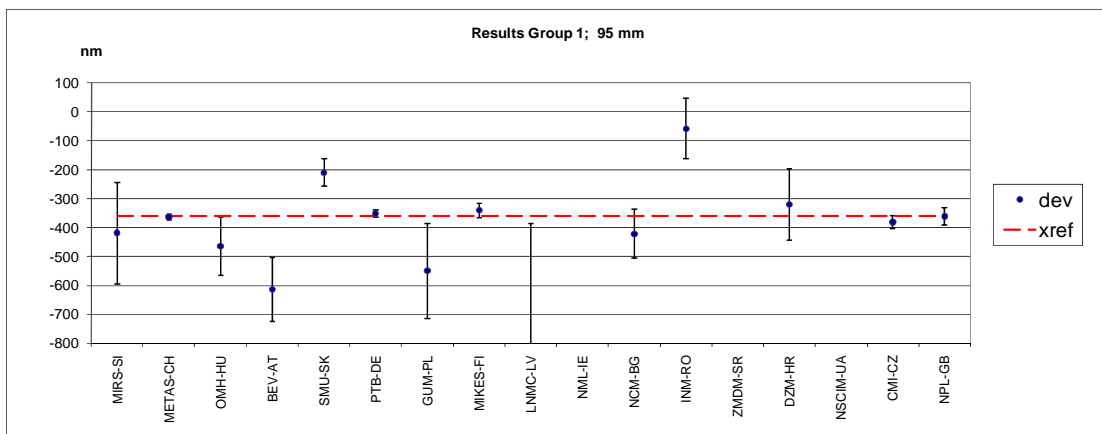
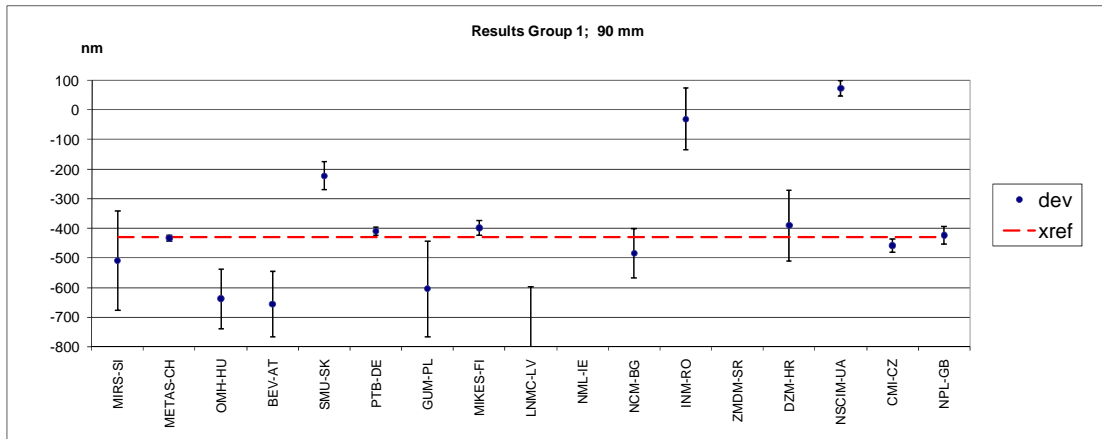












1.2 Group 1 - Calculated values

The results given in Table 1.2 were calculated from the largest consistent subset. This subset was created by eliminating laboratories with the greatest E_n values until the Birge criterion (Ch. 7) was met. E_n values $|E_n| > 1$ are marked with yellow colour. Eliminated laboratories for single measurement points are shown in Table 1.1.

Table 1.1: Laboratories that were excluded from calculation of the reference values:

Measuring point (mm)	No. of excl. labs	Excluded laboratories	Measuring point (mm)	No. of excl. labs	Excluded laboratories
0,6	1	NSCIM-UA	55	2	ZMDM-SR, NSCIM-UA
5	1	ZMDM-SR	60	3	ZMDM-SR, NSCIM-UA, NML-IE
10	1	ZMDM-SR	65	2	ZMDM-SR, NSCIM-UA
15	2	ZMDM-SR, NSCIM-UA	70	2	ZMDM-SR, NSCIM-UA
20	2	ZMDM-SR, NSCIM-UA	75	3	ZMDM-SR, NSCIM-UA, NML-IE
25	2	ZMDM-SR, NSCIM-UA	80	3	ZMDM-SR, NSCIM-UA, NML-IE
30	2	ZMDM-SR, NSCIM-UA	85	5	ZMDM-SR, NSCIM-UA, NML-IE, SMU-SK, INM-RO
35	2	ZMDM-SR, NSCIM-UA	90	5	ZMDM-SR, NSCIM-UA, NML-IE, SMU-SK, INM-RO
40	2	ZMDM-SR, NSCIM-UA	95	4	ZMDM-SR, NSCIM-UA, NML-IE, SMU-SK
45	2	ZMDM-SR, NSCIM-UA	100	5	ZMDM-SR, NSCIM-UA, NML-IE, SMU-SK, INM-RO
50	2	ZMDM-SR, NSCIM-UA			

Table 1.2: Results calculated from the given values – Group 1

Meas. Point	0,1 mm		0,2 mm		0,3 mm		0,4 mm		0,5 mm		0,6 mm	
x_{ref}	24,3 nm		1,8 nm		-1,2 nm		9,8 nm		6,6 nm		1,7 nm	
$u_c(x_{ref})$	5,3 nm		5,2 nm		4,9 nm		5,7 nm		5,2 nm		5,0 nm	
u_{ext}	2,7 nm		2,2 nm		1,6 nm		3,6 nm		2,1 nm		1,6 nm	
No of participants	17		17		17		17		17		16	
R_B	0,52		0,42		0,32		0,63		0,40		0,32	
$R_{B,crit}$	1,31		1,31		1,31		1,31		1,31		1,32	
	x_i-x_{ref}	E_n	x_i-x_{ref}	E_n								
MIRS-SI	-4,29	-0,04	-1,76	-0,01	1,16	0,01	10,21	0,08	23,38	0,19	28,28	0,23
METAS-CH	-3,29	-0,28	-0,76	-0,06	-2,84	-0,23	-6,79	-0,62	-6,62	-0,56	-3,72	-0,31
OMH-HU	-143,29	-0,72	-118,76	-0,59	-12,84	-0,06	-14,79	-0,07	5,38	0,03	-0,72	0,00
BEV-AT	-10,29	-0,23	8,24	0,18	11,16	0,25	10,21	0,23	7,38	0,16	10,28	0,23
SMU-SK	-22,29	-0,24	-35,76	-0,39	-8,84	-0,10	-22,79	-0,25	-10,62	-0,12	2,28	0,02
PTB-DE	10,91	0,46	3,64	0,06	10,16	0,42	45,71	0,73	25,38	0,40	8,78	0,37
GUM-PL	33,71	0,13	2,24	0,01	25,16	0,09	56,21	0,21	7,38	0,03	12,28	0,05
MIKES-FI	-4,29	-0,09	-0,76	-0,04	-2,84	-0,14	35,21	0,72	3,38	0,17	-3,72	-0,18
LNMC-LV	-224,29	-0,14	-201,76	-0,12	-198,84	-0,12	-9,79	-0,01	193,38	0,12	398,28	0,24
NML-IE	-104,29	-0,07	-47,76	-0,03	-184,84	-0,12	30,21	0,02	-366,62	-0,25	-121,72	-0,08
NCM-BG	-0,29	0,00	-1,76	-0,01	2,16	0,01	-7,79	-0,05	34,38	0,22	-3,72	-0,02
INM-RO	15,71	0,08	58,24	0,29	61,16	0,30	30,21	0,15	3,38	0,02	8,28	0,04
ZMDM-SR	-41,59	-0,21	-7,06	-0,04	2,56	0,01	13,31	0,07	7,28	0,04	-26,42	-0,13
DZM-HR	-21,29	-0,14	-2,76	-0,02	4,16	0,03	4,21	0,03	19,38	0,13	6,28	0,04
NSCIM-UA	11,71	0,30	10,24	0,27	0,16	0,00	13,21	0,34	10,38	0,27	-205,72	-5,31
CMI-CZ	3,71	0,14	-0,76	-0,03	-2,84	-0,11	-6,79	-0,27	1,38	0,05	2,28	0,09
NPL-GB	-2,29	-0,04	2,38	0,04	-2,01	-0,03	-6,39	-0,11	-3,60	-0,06	-2,06	-0,03

Meas. Point	0,7 mm		0,8 mm		0,9 mm		1,0 mm		5,0 mm		10,0 mm	
x_{ref}	0,5 nm		22,7 nm		-4,4 nm		23,3 nm		2,0 nm		2,5 nm	
$u_c(x_{ref})$	5,2 nm		4,9 nm		4,9 nm		4,9 nm		5,0 nm		5,0 nm	
u_{ext}	2,5 nm		2,6 nm		3,0 nm		3,6 nm		4,9 nm		6,4 nm	
No of participants	17		17		17		17		16		16	
R_B	0,48		0,53		0,60		0,73		0,98		1,28	
$R_{B,crit}$	1,31		1,31		1,31		1,31		1,32		1,32	
	x_i-x_{ref}	E_n	x_i-x_{ref}	E_n	x_i-x_{ref}	E_n	x_i-x_{ref}	E_n	x_i-x_{ref}	E_n	x_i-x_{ref}	E_n
MIRS-SI	29,51	0,24	47,29	0,38	54,43	0,44	46,66	0,38	18,00	0,13	-2,48	-0,02
METAS-CH	-6,49	-0,55	-5,71	-0,46	-1,57	-0,13	1,66	0,13	-6,00	-0,49	-7,48	-0,61
OMH-HU	-49,49	-0,25	5,29	0,03	-56,57	-0,28	-68,34	-0,34	-59,00	-0,30	-93,48	-0,47
BEV-AT	14,51	0,32	15,29	0,34	28,43	0,63	26,66	0,59	-18,00	-0,08	-13,48	-0,06
SMU-SK	2,51	0,03	-36,71	-0,40	-3,57	-0,04	-26,34	-0,29	-28,00	-0,31	-32,48	-0,36
PTB-DE	0,31	0,00	5,89	0,24	-1,67	-0,07	5,76	0,24	3,40	0,14	3,52	0,15
GUM-PL	-15,49	-0,06	-69,71	-0,26	-38,57	-0,14	-17,34	-0,06	133,00	0,50	132,52	0,49
MIKES-FI	0,51	0,03	2,29	0,11	-8,57	-0,42	-18,34	-0,90	-6,00	-0,30	-8,48	-0,42
LNMC-LV	299,51	0,18	77,29	0,05	104,43	0,06	26,66	0,02	418,00	0,25	357,52	0,22
NML-IE	-60,49	-0,04	117,29	0,08	344,43	0,23	296,66	0,20	238,00	0,16	197,52	0,13
NCM-BG	2,51	0,02	-11,71	-0,08	7,43	0,05	-2,34	-0,02	-5,00	-0,03	-1,48	-0,01
INM-RO	19,51	0,10	-12,71	-0,06	24,43	0,12	-53,34	-0,26	28,00	0,14	27,52	0,14
ZMDM-SR	-32,29	-0,16	-87,51	-0,43	-46,47	-0,23	-65,34	-0,32	-3641,20	-18,05	-8221,48	-40,74
DZM-HR	27,51	0,18	10,29	0,07	65,43	0,43	47,66	0,32	34,00	0,22	22,52	0,14
NSCIM-UA	26,51	0,69	18,29	0,47	21,43	0,55	24,66	0,64	66,00	1,70	89,52	2,30
CMI-CZ	-0,49	-0,02	-2,71	-0,10	-3,57	-0,14	-3,34	-0,13	-7,00	-0,27	-8,48	-0,32
NPL-GB	1,01	0,02	-3,71	-0,06	-2,51	-0,04	-0,86	-0,01	-5,30	-0,09	-2,78	-0,05

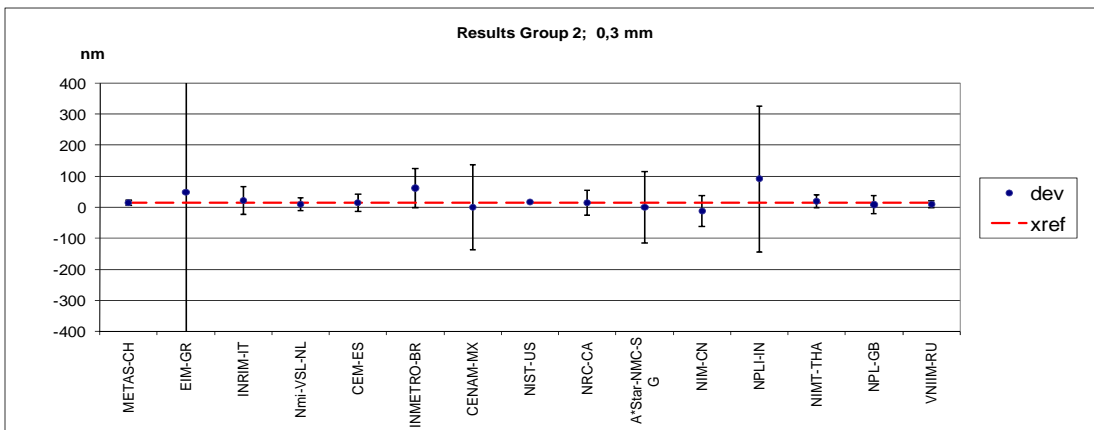
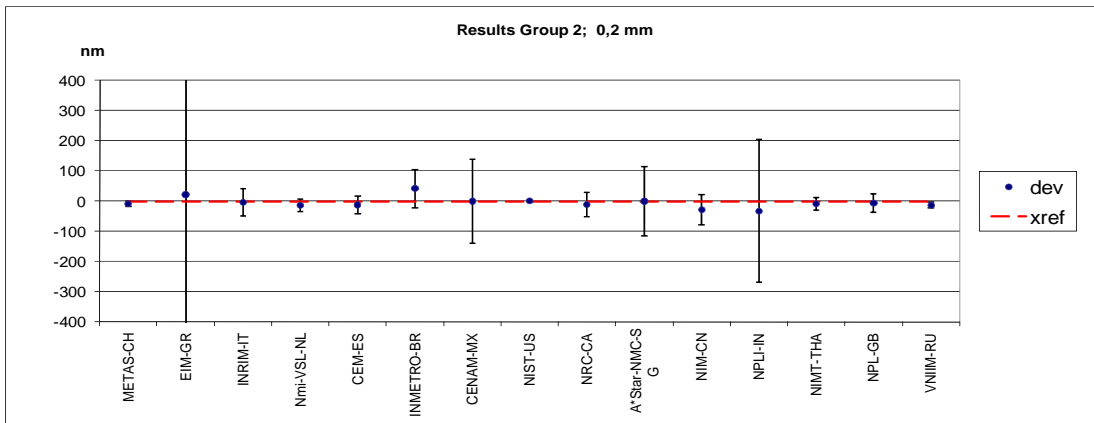
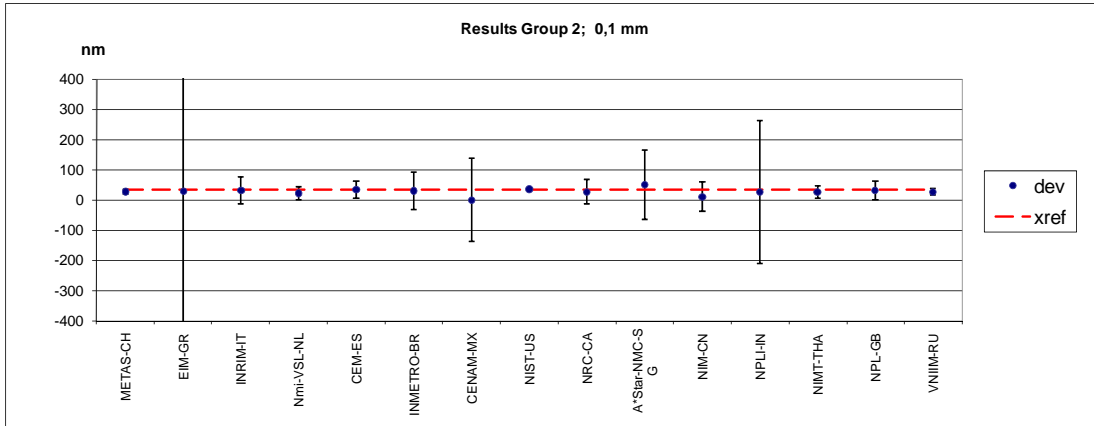
Meas. Point	15.0 mm		20.0 mm		25.0 mm		30.0 mm		35.0 mm		40.0 mm	
X_{ref}	-7.0 nm		-2.7 nm		-147.4 nm		-167.7 nm		-159.2 nm		-159.0 nm	
$u_c(X_{ref})$	5.2 nm		5.2 nm		5.3 nm		5.3 nm		5.4 nm		5.4 nm	
u_{ext}	4.1 nm		2.1 nm		4.4 nm		4.9 nm		4.6 nm		5.0 nm	
No of participants	15		15		15		15		15		15	
R_B	0,78		0,40		0,83		0,92		0,85		0,92	
$R_{B,crit}$	1,33		1,33		1,33		1,33		1,33		1,33	
	X_i-X_{ref}	E_n	X_i-X_{ref}	E_n	X_i-X_{ref}	E_n	X_i-X_{ref}	E_n	X_i-X_{ref}	E_n	X_i-X_{ref}	E_n
MIRS-SI	6,97	0,04	2,71	0,02	7,40	0,04	-12,26	-0,06	-40,75	-0,20	-51,02	-0,23
METAS-CH	-10,03	-0,83	-0,29	-0,02	-6,60	-0,54	-3,26	-0,26	-4,75	-0,38	-3,02	-0,24
OMH-HU	-43,03	-0,22	-25,29	-0,13	-115,60	-0,58	8,74	0,04	70,25	0,35	-163,02	-0,82
BEV-AT	-57,03	-0,26	-45,29	-0,20	-32,60	-0,15	-79,26	-0,36	-95,75	-0,43	-113,02	-0,51
SMU-SK	-14,03	-0,15	-9,29	-0,10	64,40	0,70	80,74	0,88	69,25	0,76	56,98	0,62
PTB-DE	24,57	1,03	8,41	0,35	13,30	0,56	9,24	0,39	9,55	0,40	9,88	0,42
GUM-PL	180,97	0,67	83,71	0,31	81,40	0,30	152,74	0,56	33,25	0,12	113,98	0,41
MIKES-FI	5,97	0,30	-6,29	-0,31	3,40	0,17	-3,26	-0,16	-1,75	-0,09	-0,02	0,00
LNMC-LV	276,97	0,17	512,71	0,31	377,40	0,23	1137,74	0,69	9,25	0,01	478,98	0,29
NML-IE	486,97	0,33	402,71	0,27	907,40	0,61	507,74	0,34	839,25	0,57	1058,98	0,72
NCM-BG	-14,03	-0,09	-10,29	-0,07	-6,60	-0,04	-8,26	-0,05	9,25	0,06	-20,02	-0,13
INM-RO	16,97	0,08	-7,29	-0,04	107,40	0,53	147,74	0,73	139,25	0,69	148,98	0,73
ZMDM-SR	-10830,13	-53,66	-14579,59	-72,22	-18569,50	-91,95	-22325,26	-110,50	-25705,35	-127,16	-29002,22	-143,38
DZM-HR	-0,03	0,00	16,71	0,10	-90,60	-0,52	-108,26	-0,60	-139,75	-0,76	-8,02	-0,04
NSCIM-UA	122,97	3,16	164,71	4,20	209,40	5,30	291,74	7,31	293,25	7,27	320,98	7,86
CMI-CZ	-5,03	-0,19	-0,29	-0,01	-5,60	-0,20	-6,26	-0,22	-1,75	-0,06	-9,02	-0,30
NPL-GB	-4,97	-0,08	8,38	0,14	0,18	0,00	4,52	0,08	3,58	0,06	3,99	0,07

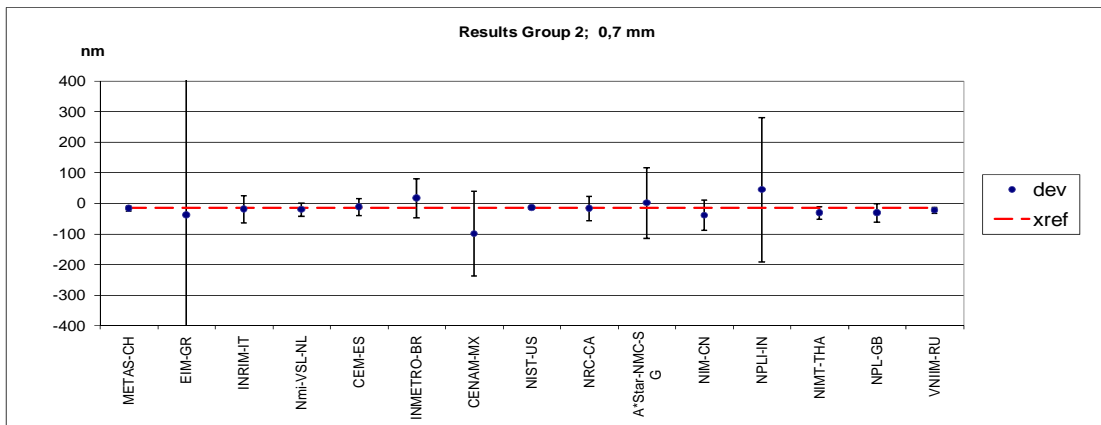
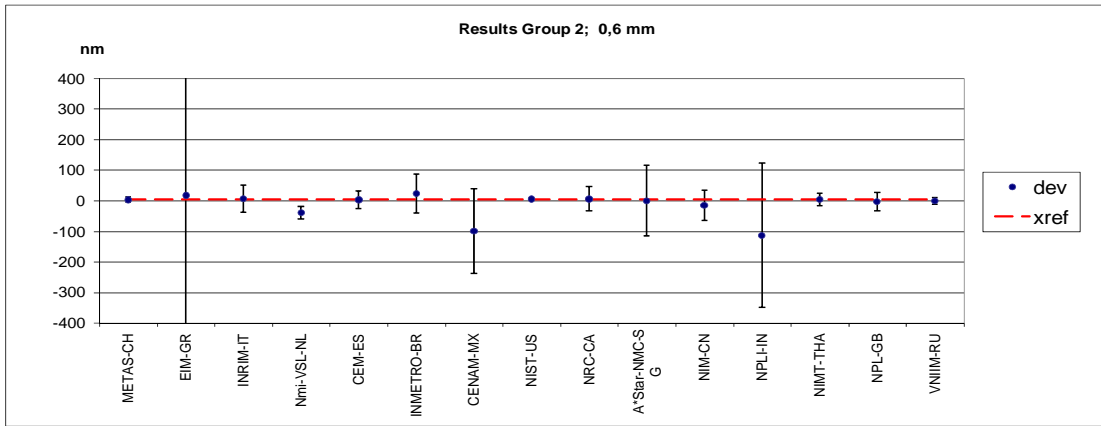
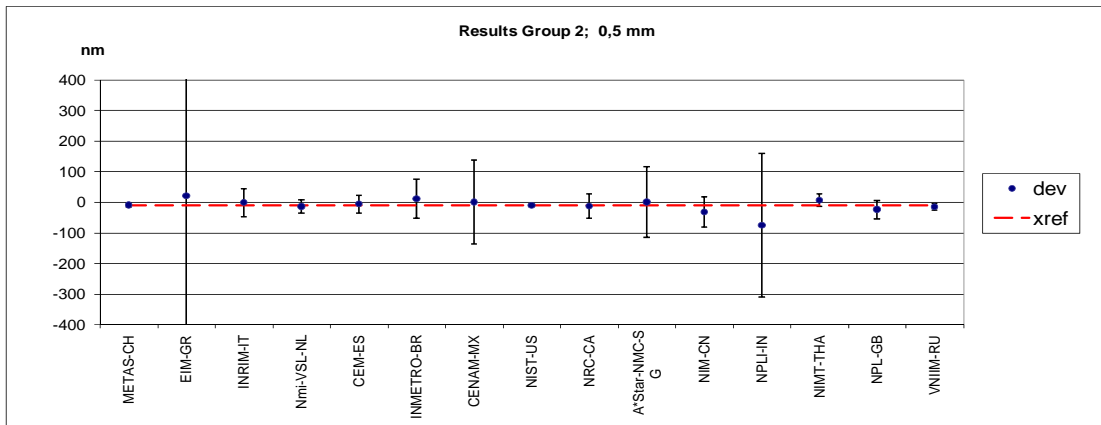
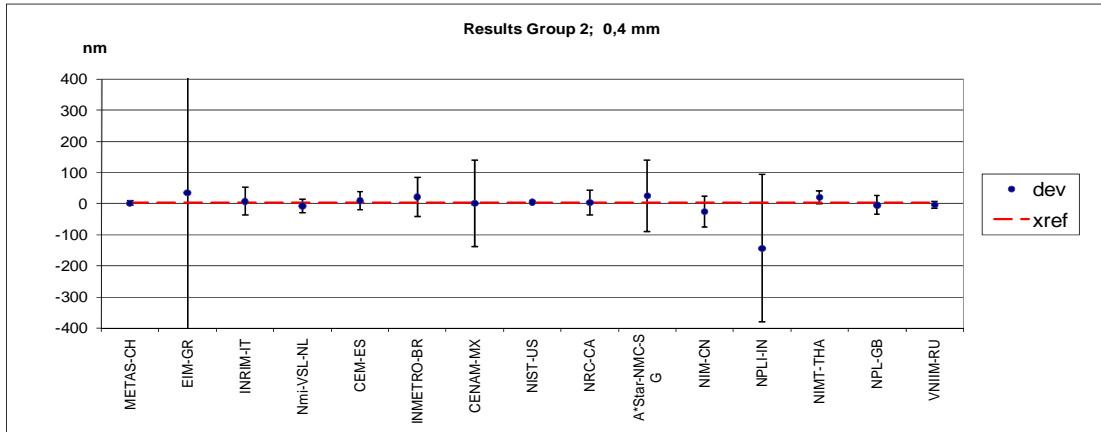
Meas. Point	45.0 mm		50.0 mm		55.0 mm		60.0 mm		65.0 mm		70.0 mm	
X_{ref}	-214.2 nm		-193.4 nm		-211.5 nm		-258.0 nm		-214.8 nm		-245.4 nm	
$u_c(X_{ref})$	5.5 nm		5.5 nm		5.6 nm		5.7 nm		5.8 nm		5.9 nm	
u_{ext}	5.6 nm		5.3 nm		5.2 nm		6.9 nm		6.3 nm		7.1 nm	
No of participants	15		15		14		14		14		14	
R_B	1,01		0,96		0,91		1,21		1,10		1,21	
$R_{B,crit}$	1,33		1,33		1,34		1,34		1,34		1,34	
	X_i-X_{ref}	E_n										
MIRS-SI	-75,81	-0,33	-26,58	-0,11	-59,78	-0,24	-53,67	-0,20	-36,28	-0,13	-35,86	-0,12
METAS-CH	-1,81	-0,14	-2,58	-0,20	-3,78	-0,28	-3,67	-0,27	-6,28	-0,45	-1,86	-0,13
OMH-HU	-67,81	-0,34	-67,58	-0,34	-140,78	-0,70	-61,67	-0,31	-18,28	-0,09	-84,86	-0,42
BEV-AT	-136,81	-0,62	-96,58	-0,44	-131,78	-0,59	-161,67	-0,73	-163,28	-0,74	-199,86	-0,90
SMU-SK	105,19	1,15	86,42	0,94	86,22	0,94	114,33	1,24	69,72	0,76	82,14	0,89
PTB-DE	13,29	0,56	12,82	0,54	8,72	0,37	12,13	0,52	13,32	0,57	7,74	0,33
GUM-PL	-21,81	-0,08	-65,58	-0,23	-101,78	-0,35	-165,67	-0,56	-121,28	-0,41	-234,86	-0,78
MIKES-FI	-5,81	-0,29	-1,58	-0,08	0,22	0,01	-0,67	-0,03	0,72	0,04	-0,86	-0,04
LNMC-LV	354,19	0,22	863,42	0,52	330,22	0,20	836,33	0,51	-6,28	0,00	134,14	0,08
NML-IE	974,19	0,66	1113,42	0,75	1090,22	0,74	1856,33	1,26	2073,72	1,40	2024,14	1,37
NCM-BG	-16,81	-0,11	-31,58	-0,20	-32,78	-0,20	-37,67	-0,23	-35,28	-0,22	-37,86	-0,23
INM-RO	164,19	0,81	143,42	0,70	190,22	0,93	236,33	1,16	173,72	0,85	204,14	0,99
ZMDM-SR	-32941,51	-162,73	-36955,78	-182,42	-40189,78	-198,20	-43648,77	-215,05	-48015,18	-236,32	-50708,46	-249,29
DZM-HR	14,19	0,07	25,42	0,13	-11,78	-0,06	-9,67	-0,05	12,72	0,06	-10,86	-0,05
NSCIM-UA	145,19	3,51	414,42	9,86	424,22	9,93	465,33	10,71	449,72	10,17	474,14	10,52
CMI-CZ	-14,81	-0,48	-19,58	-0,61	-7,78	-0,23	-19,67	-0,57	-10,28	-0,29	-14,86	-0,40
NPL-GB	3,44	0,06	2,84	0,05	-0,25	0,00	-1,12	-0,02	-4,23	-0,07	3,21	0,05

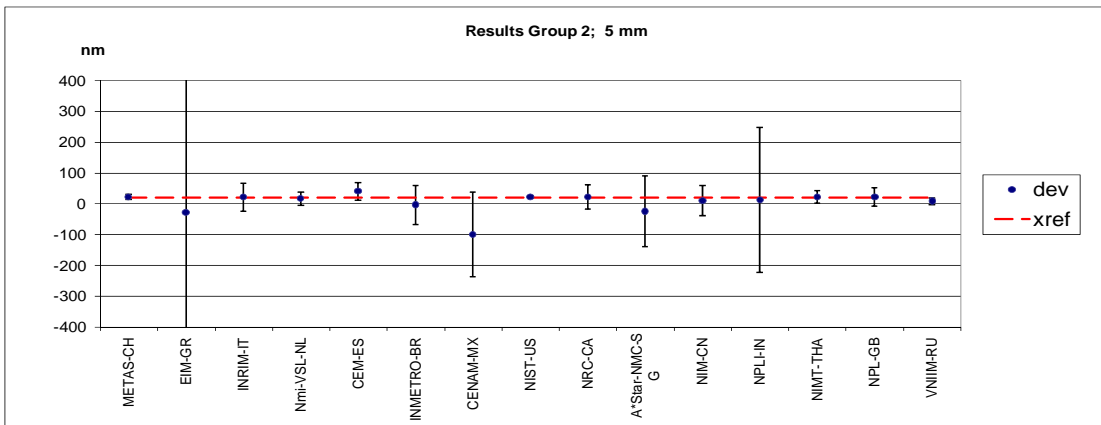
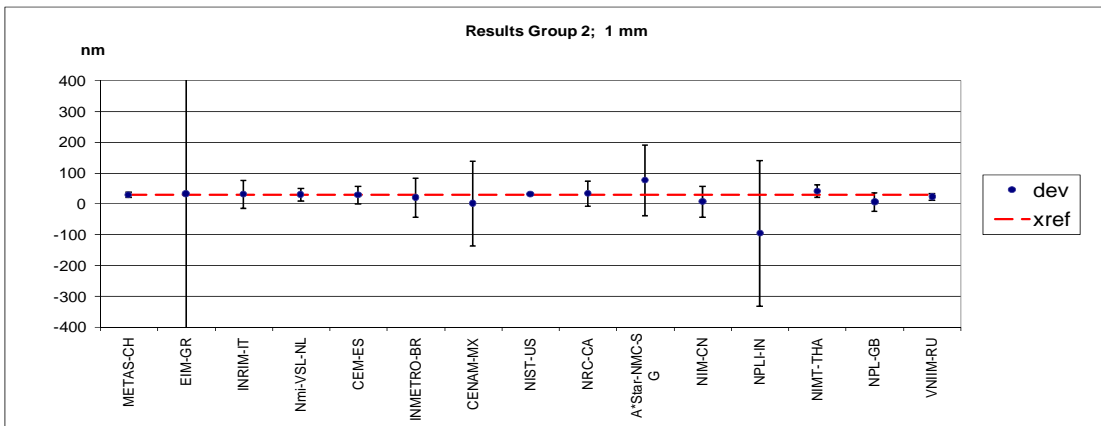
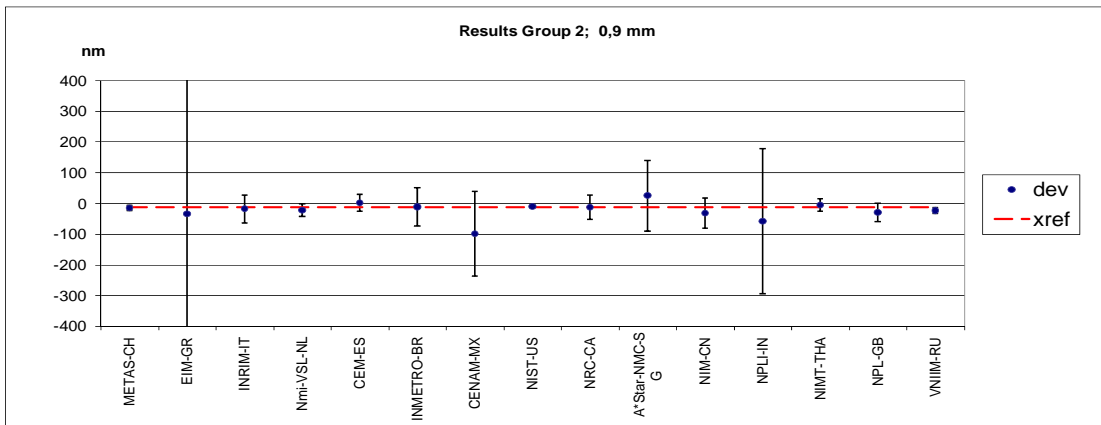
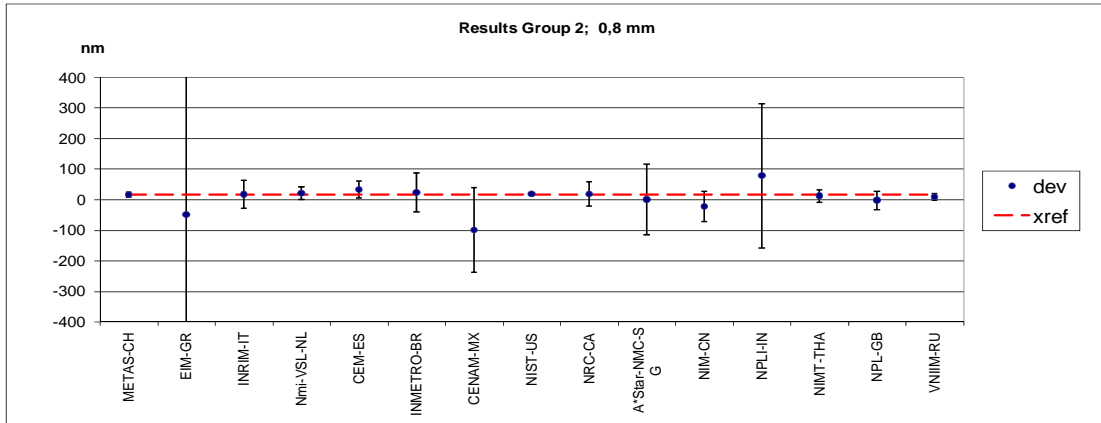
Meas. Point	75.0 mm		80.0 mm		85.0 mm		90.0 mm		95.0 mm		100.0 mm	
X_{ref}	-282.3 nm		-240.8 nm		-269.4 nm		-429.1 nm		-362.0 nm		-391.0 nm	
$u_c(X_{ref})$	5.9 nm		6.0 nm		8.0 nm		6.9 nm		7.0 nm		6.3 nm	
u_{ext}	7.3 nm		7.4 nm		10.4 nm		8.7 nm		9.0 nm		7.4 nm	
No of participants	13		13		11		12		13		12	
R_B	1,23		1,24		1,30		1,27		1,28		1,17	
$R_{B,crit}$	1,35		1,35		1,38		1,36		1,35		1,36	
	X_i-X_{ref}	E_n										
MIRS-SI	-9,20	-0,03	-39,87	-0,13	-52,70	-0,16	-80,93	-0,24	-58,03	-0,17	-49,01	-0,14
METAS-CH	0,80	0,05	-1,87	-0,12	4,30	0,36	-4,93	-0,34	-3,03	-0,20	3,99	0,24
OMH-HU	-278,20	-1,39	-215,87	-1,08	-263,70	-1,32	-209,93	-1,05	-104,03	-0,52	-95,01	-0,47
BEV-AT	-184,20	-0,83	-234,87	-1,06	-248,70	-1,12	-227,93	-1,03	-253,03	-1,14	-318,01	-1,43
SMU-SK	89,80	0,97	39,13	0,42	70,30	0,76	207,07	2,24	150,97	1,63	140,99	1,52
PTB-DE	7,20	0,31	9,03	0,39	36,60	1,77	18,77	0,85	9,17	0,42	3,09	0,14
GUM-PL	-170,20	-0,55	-292,87	-0,94	-294,70	-0,93	-175,93	-0,55	-189,03	-0,58	-197,01	-0,59
MIKES-FI	-3,20	-0,16	5,13	0,25	-24,70	-0,52	30,07	0,63	19,97	0,42	2,99	0,14
LNMC-LV	530,80	0,32	10,13	0,01	-682,70	-0,41	-990,93	-0,60	-848,03	-0,52	-1329,01	-0,81
NML-IE	2780,80	1,88	2260,13	1,53	2327,30	1,57	2769,07	1,87	3201,97	2,16	3230,99	2,18
NCM-BG	-43,20	-0,26	-48,87	-0,30	-45,70	-0,28	-55,93	-0,33	-61,03	-0,36	-52,01	-0,31
INM-RO	230,80	1,12	200,13	0,97	247,30	1,20	399,07	1,92	301,97	1,45	360,99	1,73
ZMDM-SR	-55087,90	-270,49	-58629,17	-287,50	-61980,70	-303,89	-65609,83	-320,97	-68649,43	-335,32	-72887,61	-355,28
DZM-HR	-29,20	-0,13	-21,87	-0,10	-42,70	-0,18	38,07	0,16	40,97	0,17	78,99	0,32
NSCIM-UA	467,80	10,18	475,13	10,13	493,30	10,55	503,07	10,39	543,97	10,99	525,99	10,32
CMI-CZ	-14,20	-0,37	-18,87	-0,47	-12,70	-0,32	-29,93	-0,71	-20,03	-0,46	-21,01	-0,46
NPL-GB	1,47	0,03	0,12	0,00	10,72	0,19	5,33	0,09	-0,47	-0,01	9,37	0,16

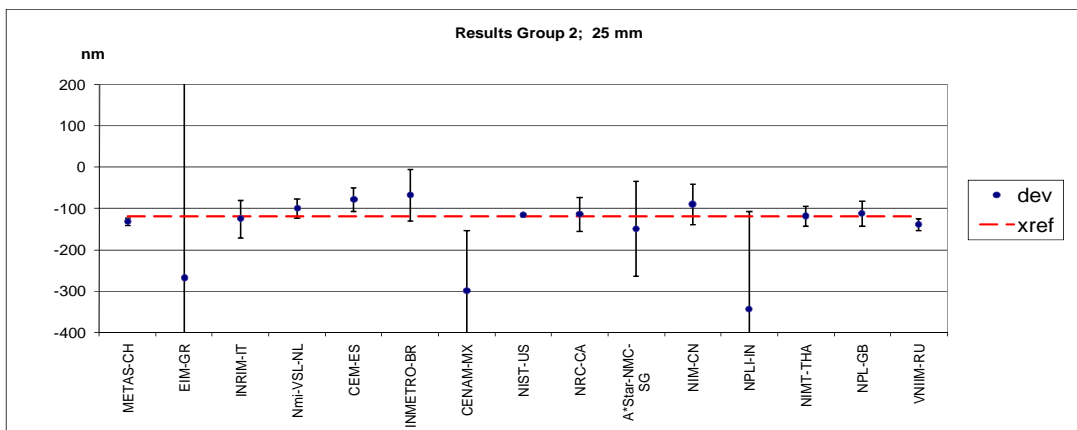
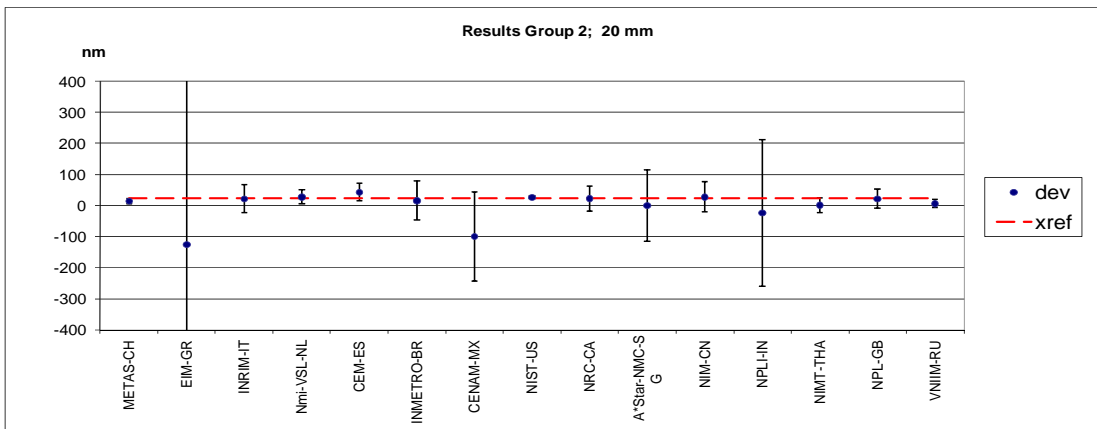
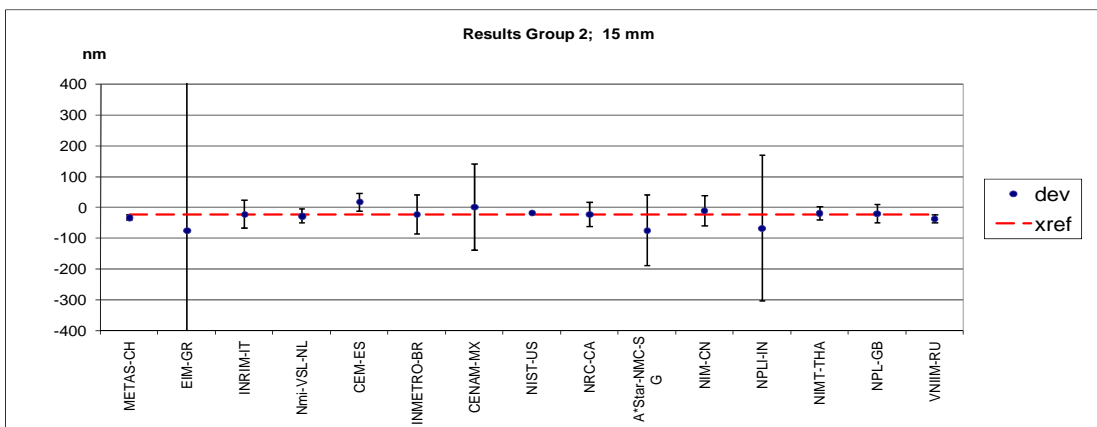
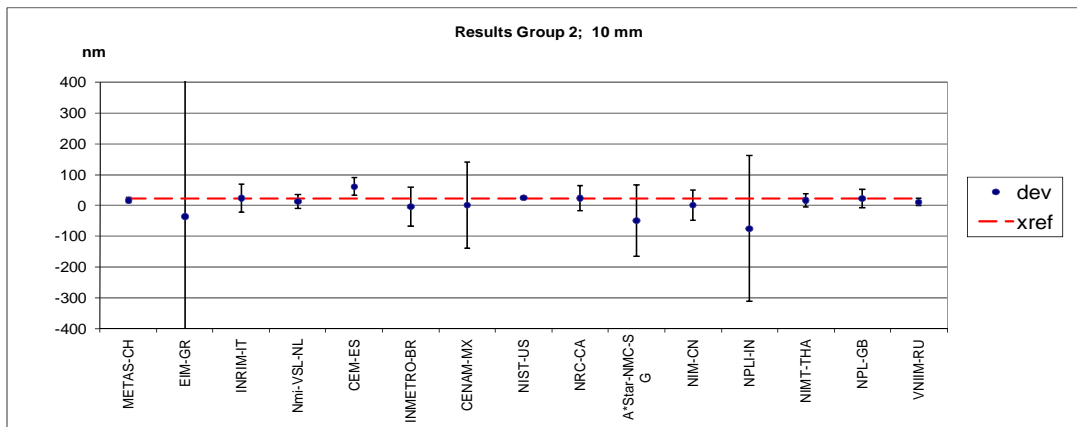
1.3 Group 2 – deviations from reference value

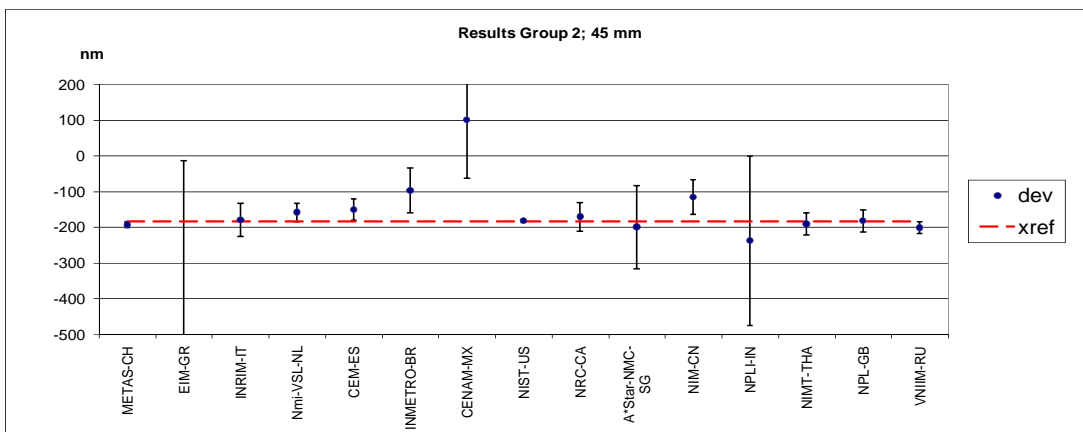
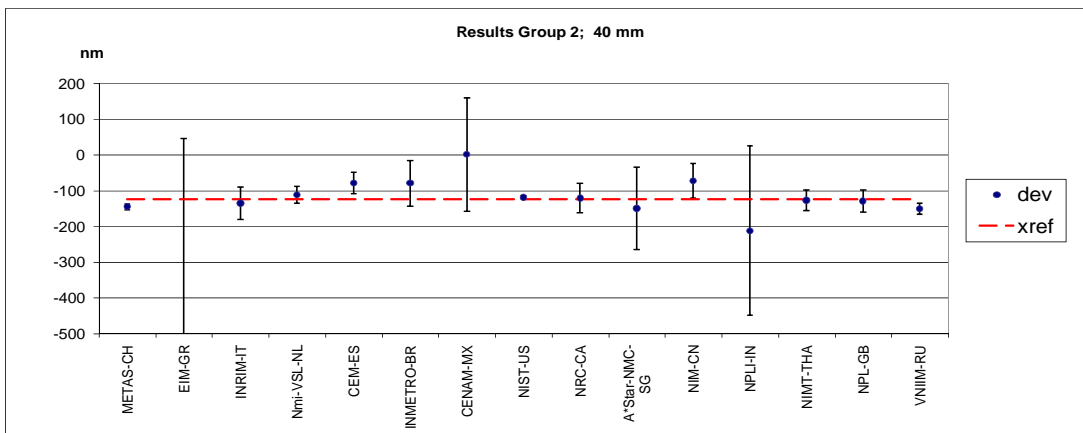
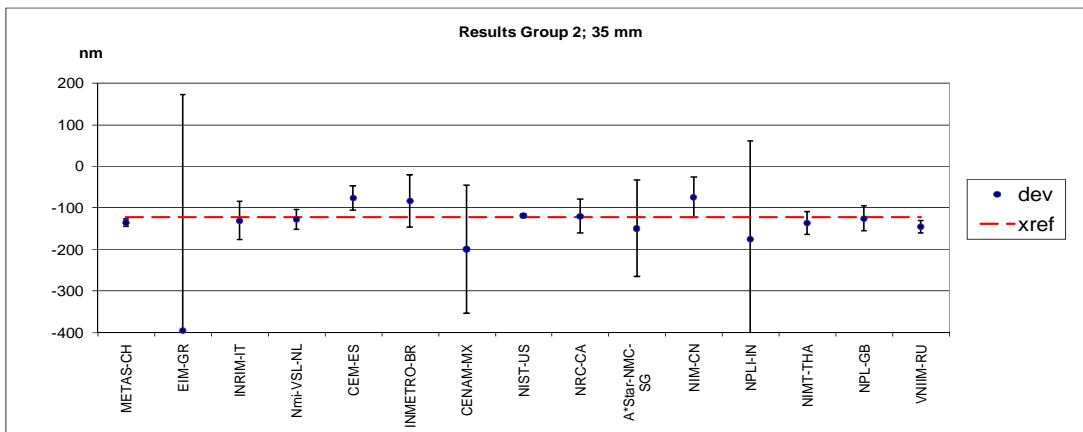
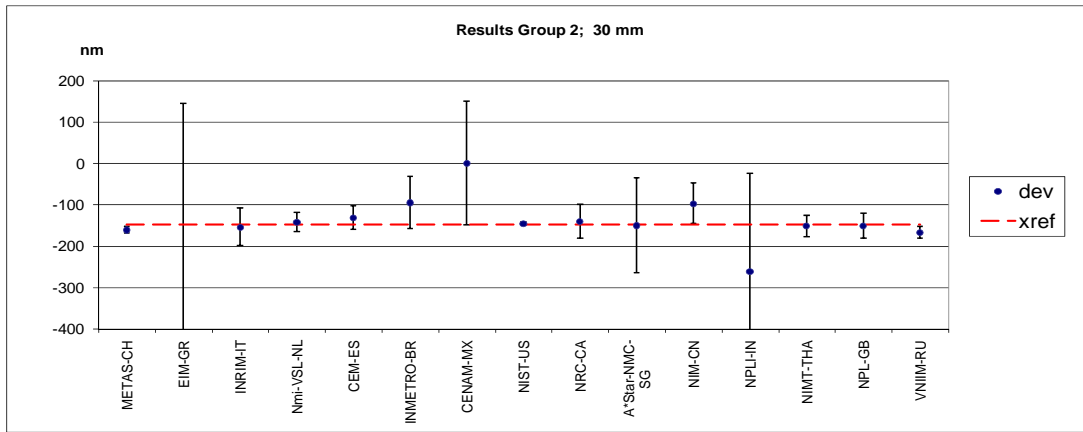
Graphical presentation of measurement results follows in 30 diagrams. Uncertainty bars in the diagrams for single measuring points represent standard uncertainty u ($k = 1$).

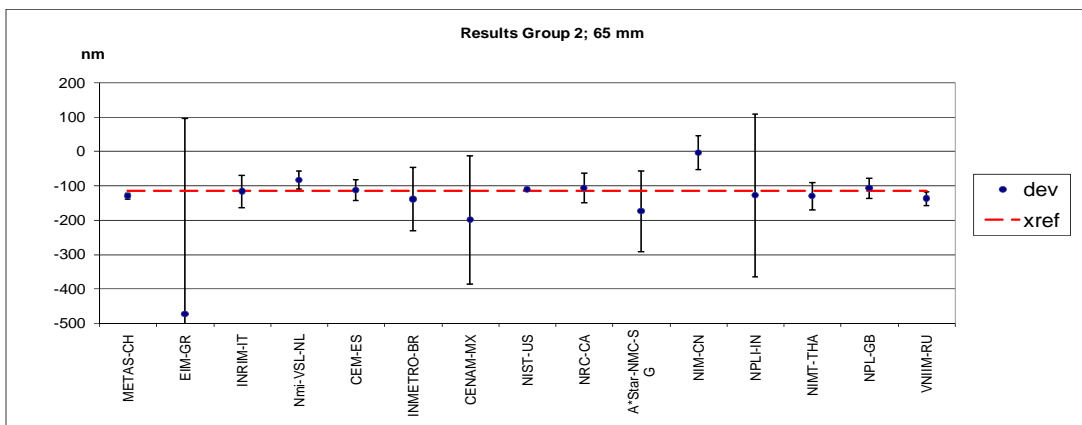
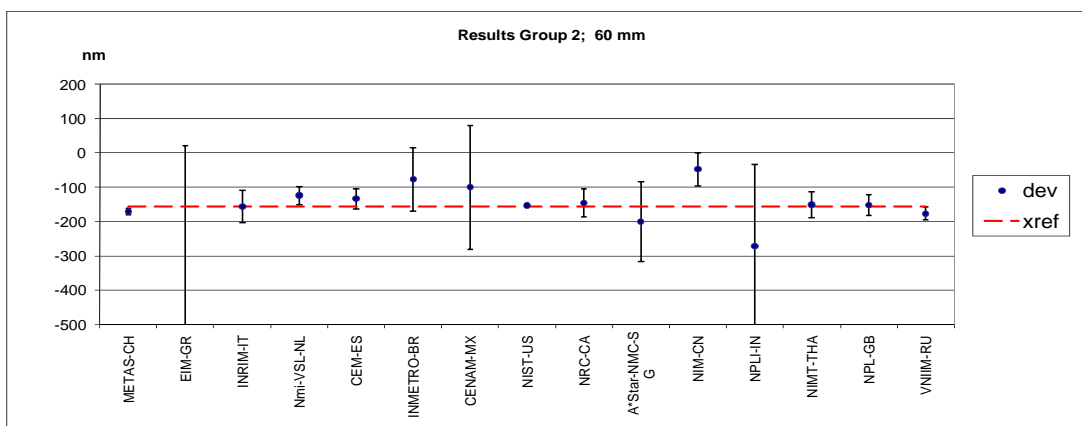
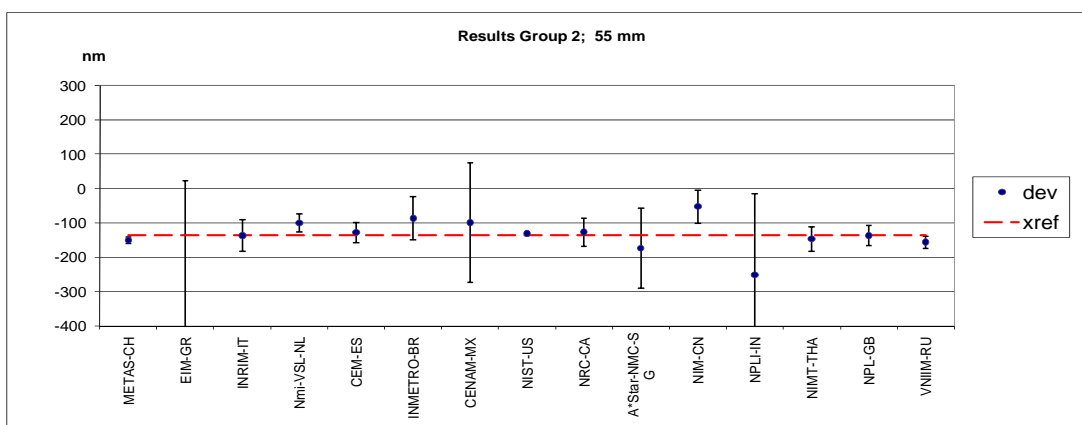
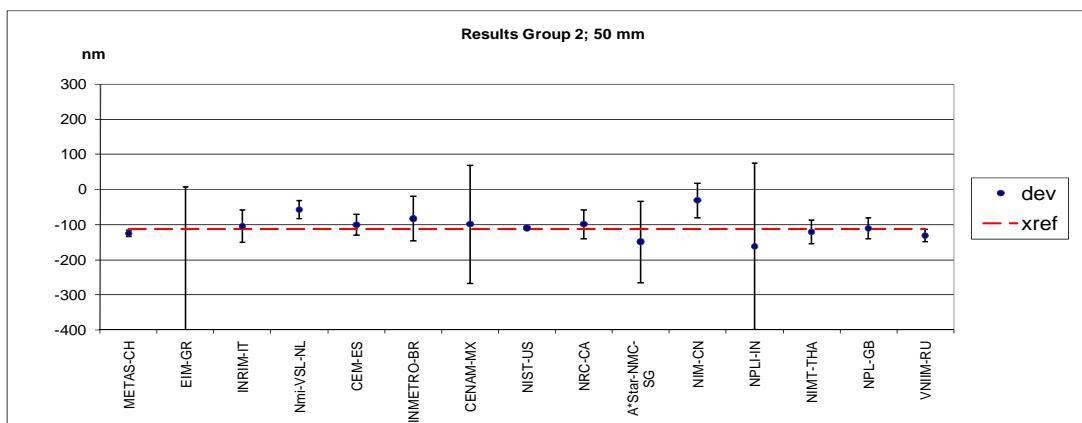


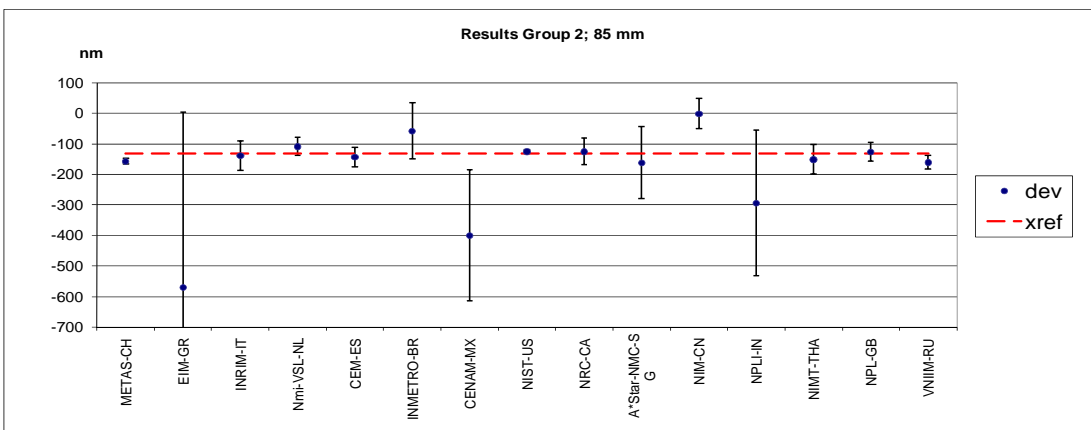
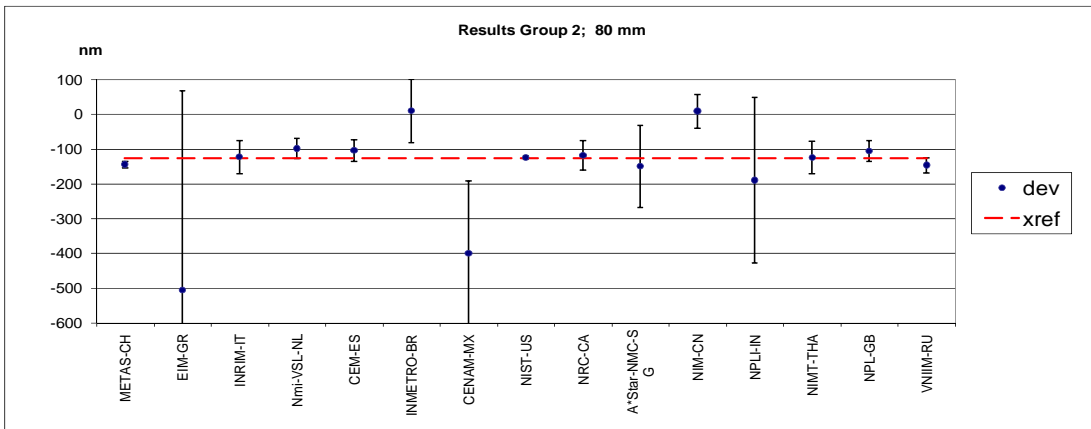
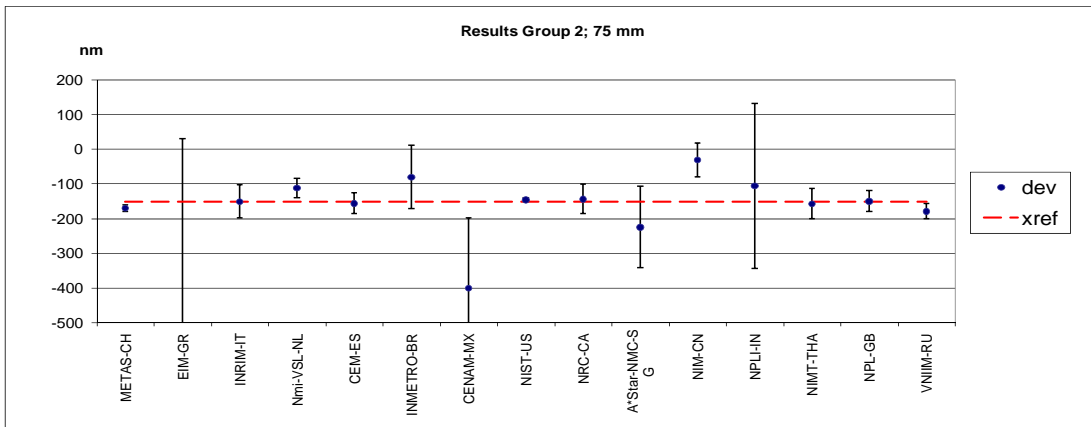
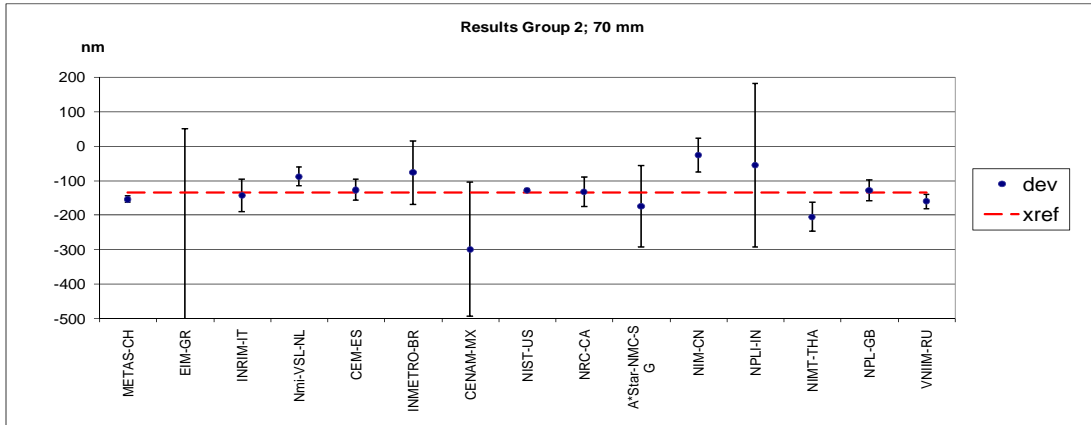


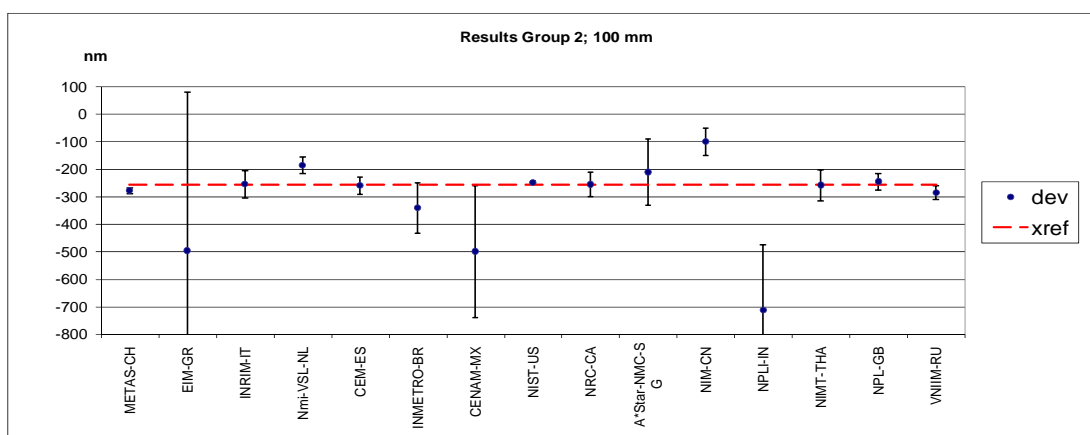
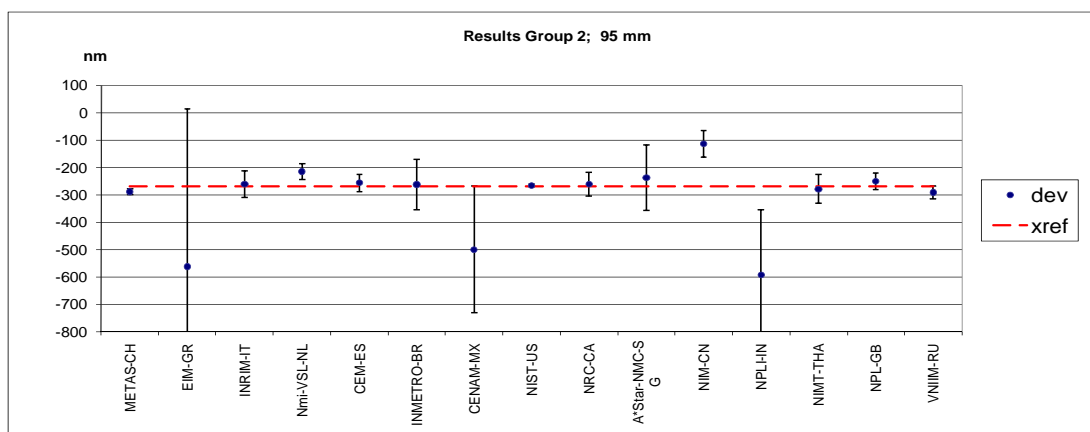
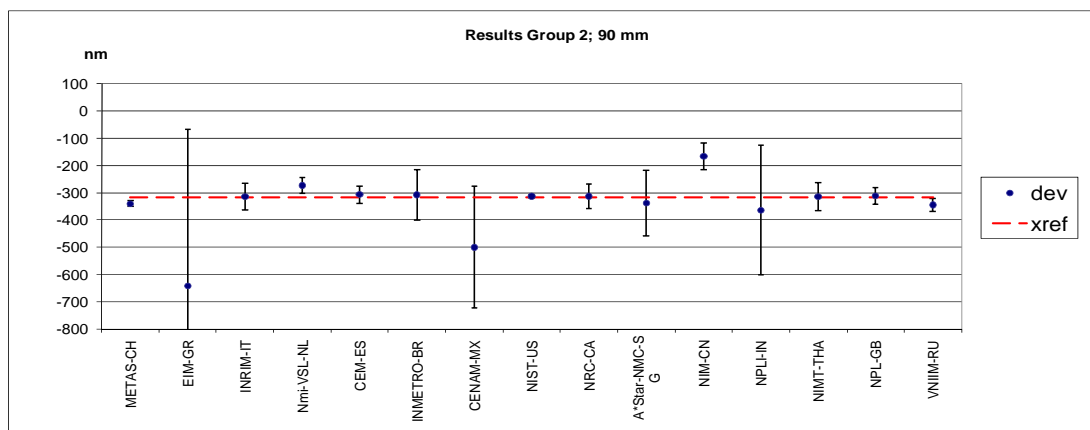












1.4 Group 2 - Calculated values

The results given in Table 1.4 were calculated from the largest consistent subset. This subset was created by eliminating laboratories with the greatest E_n values until the Birge criterion (Ch. 7) was met. E_n values $|E_n| > 1$ are marked with yellow colour. Eliminated laboratories for single measurement points are shown in Table 1.3.

Table 1.3: Laboratories that were excluded from calculation of the reference values:

Measuring point (mm)	No. of excluded laboratories	Excluded laboratories
100	1	NIM-CN

Table 1.4: Results calculated from the given values – Group 2

Meas. Point	0,1 mm		0,2 mm		0,3 mm		0,4 mm		0,5 mm		0,6 mm	
x_{ref}	33,8 nm		-1,5 nm		15,7 nm		3,3 nm		-11,3 nm		3,4 nm	
$u_c(x_{ref})$	2,7 nm											
u_{ext}	1,1 nm		1,5 nm		0,9 nm		1,2 nm		0,9 nm		1,7 nm	
No of participants	15		15		15		15		15		15	
R_B	0,41		0,55		0,34		0,45		0,34		0,64	
$R_{B,crit}$	1,33		1,33		1,33		1,33		1,33		1,33	
	x_i-x_{ref}	E_n										
METAS-CH	-5,8	-0,39	-6,5	-0,43	-1,7	-0,12	-2,3	-0,16	1,3	0,08	-0,4	-0,02
EIM-GR	-4,8	0,00	23,5	0,02	32,3	0,03	30,7	0,03	31,3	0,03	13,6	0,01
INRIM-IT	-2,8	-0,03	-2,5	-0,03	5,3	0,06	3,7	0,04	9,3	0,10	2,6	0,03
Nmi-VSL-NL	-11,8	-0,28	-11,5	-0,27	-5,7	-0,14	-11,3	-0,27	-3,7	-0,09	-43,4	-1,04
CEM-ES	1,2	0,02	-10,5	-0,18	-0,7	-0,01	5,7	0,10	4,3	0,08	-0,4	-0,01
INMETRO-BR	-3,8	-0,03	43,5	0,35	46,3	0,37	17,7	0,14	22,3	0,18	19,6	0,16
CENAM-MX	-33,8	-0,12	1,5	0,01	-15,7	-0,06	-3,3	-0,01	11,3	0,04	-103,4	-0,38
NIST-US	2,2	0,70	2,7	0,88	1,0	0,31	1,1	0,35	0,1	0,02	1,5	0,50
NRC-CA	-7,0	-0,09	-9,7	-0,12	-2,1	-0,03	-1,0	-0,01	-2,5	-0,03	1,9	0,02
A*Star-NMC-SG	16,2	0,07	1,5	0,01	-15,7	-0,07	21,7	0,09	11,3	0,05	-3,4	-0,01
NIM-CN	-22,8	-0,23	-26,5	-0,27	-27,7	-0,28	-29,3	-0,30	-21,7	-0,22	-19,4	-0,20
NPLI-IN	-7,8	-0,02	-30,5	-0,06	76,3	0,16	-147,3	-0,31	-64,7	-0,14	-117,4	-0,25
NIMT-THA	-8,1	-0,20	-7,2	-0,18	2,9	0,07	17,1	0,42	16,3	0,40	0,6	0,02
NPL-GB	-2,9	-0,05	-4,3	-0,07	-7,2	-0,12	-8,4	-0,14	-13,3	-0,22	-6,6	-0,11
VNIIM-RU	-6,8	-0,35	-11,5	-0,59	-5,7	-0,30	-8,3	-0,43	-4,7	-0,24	-4,4	-0,22

Meas. Point	0,7 mm		0,8 mm		0,9 mm		1 mm		5 mm		10 mm	
x_{ref}	-16,7 nm		16,8 nm		-13,0 nm		29,3 nm		19,7 nm		22,1 nm	
$u_c(x_{ref})$	2,7 nm		2,7 nm		2,7 nm		2,7 nm		3,1 nm		3,1 nm	
u_{ext}	1,2 nm		1,3 nm		1,3 nm		1,1 nm		1,4 nm		1,9 nm	
No of participants	15		15		15		15		15		15	
R_B	0,44		0,49		0,48		0,41		0,46		0,61	
$R_{B,crit}$	1,33		1,33		1,33		1,33		1,33		1,33	
	x_i-x_{ref}	E_n										
METAS-CH	-1,3	-0,09	-1,8	-0,12	-3,0	-0,20	-1,3	-0,09	1,3	0,09	-6,1	-0,42
EIM-GR	-22,3	-0,02	-66,8	-0,06	-22,0	-0,02	1,7	0,00	-48,7	-0,04	-59,1	-0,05
INRIM-IT	-3,3	-0,04	0,2	0,00	-6,0	-0,07	0,7	0,01	1,3	0,01	0,9	0,01
Nmi-VSL-NL	-5,3	-0,13	3,2	0,08	-10,0	-0,24	-0,3	-0,01	-3,7	-0,09	-10,1	-0,23
CEM-ES	3,7	0,06	16,2	0,29	14,0	0,25	-2,3	-0,04	20,3	0,36	37,9	0,67
INMETRO-BR	32,7	0,26	6,2	0,05	1,0	0,01	-10,3	-0,08	-23,7	-0,19	-26,1	-0,21
CENAM-MX	-83,3	-0,30	-116,8	-0,42	-87,0	-0,32	-29,3	-0,11	-119,7	-0,43	-22,1	-0,08
NIST-US	1,6	0,50	1,4	0,44	1,7	0,55	1,0	0,33	1,0	0,25	2,8	0,67
NRC-CA	-0,9	-0,01	0,6	0,01	-0,6	-0,01	2,5	0,03	1,8	0,02	0,8	0,01
A*Star-NMC-SG	16,7	0,07	-16,8	-0,07	38,0	0,17	45,7	0,20	-44,7	-0,19	-72,1	-0,31
NIM-CN	-23,3	-0,24	-39,8	-0,41	-19,0	-0,19	-23,3	-0,24	-10,7	-0,11	-21,1	-0,22
NPLI-IN	59,7	0,13	61,2	0,13	-46,0	-0,10	-125,3	-0,27	-7,7	-0,02	-98,1	-0,21
NIMT-THA	-15,6	-0,38	-5,0	-0,12	6,3	0,16	10,7	0,26	1,1	0,03	-6,0	-0,14
NPL-GB	-15,6	-0,26	-19,7	-0,33	-17,7	-0,30	-24,1	-0,40	2,3	0,04	-0,9	-0,02
VNIIM-RU	-7,3	-0,38	-8,8	-0,45	-11,0	-0,56	-7,3	-0,37	-11,7	-0,57	-12,1	-0,55

Meas. Point	15 mm		20 mm		25 mm		30 mm		35 mm		40 mm	
x_{ref}	-22,8 nm		23,5 nm		-119,8 nm		-148,9 nm		-123,3 nm		-124,6 nm	
$u_c(x_{ref})$	3,1 nm		3,2 nm		3,3 nm		3,3 nm		3,4 nm		3,5 nm	
u_{ext}	2,2 nm		2,1 nm		3,0 nm		2,6 nm		2,9 nm		3,7 nm	
No of participants	15		15		15		15		15		15	
R_B	0,69		0,67		0,92		0,77		0,86		1,07	
$R_{B,crit}$	1,33		1,33		1,33		1,33		1,33		1,33	
	x_i-x_{ref}	E_n										
METAS-CH	-11,2	-0,77	-8,5	-0,58	-13,2	-0,89	-12,1	-0,81	-12,7	-0,85	-20,4	-1,34
EIM-GR	-52,2	-0,05	-149,5	-0,13	-149,2	-0,13	-273,1	-0,24	-272,7	-0,24	-397,4	-0,35
INRIM-IT	-0,2	0,00	-1,5	-0,02	-6,2	-0,07	-5,1	-0,06	-7,7	-0,08	-11,4	-0,13
Nmi-VSL-NL	-6,2	-0,14	4,5	0,10	18,8	0,41	6,9	0,15	-4,7	-0,10	12,6	0,26
CEM-ES	38,8	0,68	19,5	0,34	40,8	0,72	17,9	0,31	46,3	0,81	45,6	0,79
INMETRO-BR	-0,2	0,00	-7,5	-0,06	50,8	0,40	53,9	0,43	39,3	0,31	44,6	0,35
CENAM-MX	22,8	0,08	-123,5	-0,43	-180,2	-0,62	148,9	0,50	-76,7	-0,25	124,6	0,39
NIST-US	3,4	0,80	3,8	0,90	3,2	0,74	3,1	0,71	4,0	0,88	5,3	1,13
NRC-CA	-1,5	-0,02	-0,4	-0,01	4,7	0,06	9,1	0,11	2,5	0,03	3,5	0,04
A*Star-NMC-SG	-52,2	-0,23	-23,5	-0,10	-30,2	-0,13	-1,1	0,00	-26,7	-0,12	-25,4	-0,11
NIM-CN	10,8	0,11	4,5	0,05	28,8	0,29	51,9	0,53	48,3	0,49	51,6	0,53
NPLI-IN	-45,2	-0,10	-46,5	-0,10	-224,2	-0,47	-112,1	-0,24	-52,7	-0,11	-87,4	-0,18
NIMT-THA	3,1	0,07	-22,3	-0,49	0,2	0,00	-2,3	-0,05	-13,8	-0,25	-3,3	-0,06
NPL-GB	2,1	0,03	-0,9	-0,01	6,4	0,11	-1,7	-0,03	-2,9	-0,05	-4,9	-0,08
VNIIM-RU	-15,2	-0,64	-17,5	-0,70	-20,2	-0,76	-18,1	-0,64	-22,7	-0,76	-26,4	-0,85

Meas. Point	45 mm		50 mm		55 mm		60 mm		65 mm		70 mm	
x_{ref}	-184,2 nm		-112,9 nm		-135,4 nm		-155,8 nm		-115,2 nm		-134,8 nm	
$u_c(x_{ref})$	3,6 nm		3,7 nm		3,8 nm		3,9 nm		4,0 nm		4,1 nm	
u_{ext}	3,4 nm		3,5 nm		3,4 nm		3,8 nm		3,8 nm		5,0 nm	
No of participants	15		15		15		15		15		15	
R_B	0,94		0,94		0,91		0,97		0,95		1,20	
$R_{B,crit}$	1,33		1,33		1,33		1,33		1,33		1,33	
	x_i-x_{ref}	E_n										
METAS-CH	-9,8	-0,64	-13,1	-0,84	-15,6	-0,99	-15,2	-0,95	-15,8	-0,97	-20,2	-1,22
EIM-GR	-397,8	-0,35	-448,1	-0,39	-411,6	-0,36	-391,2	-0,34	-358,8	-0,31	-385,2	-0,34
INRIM-IT	4,2	0,05	6,9	0,08	-2,6	-0,03	-0,2	0,00	-1,8	-0,02	-8,2	-0,09
Nmi-VSL-NL	25,2	0,51	53,9	1,07	34,4	0,67	31,8	0,61	31,2	0,59	45,8	0,85
CEM-ES	33,2	0,57	11,9	0,20	7,4	0,13	21,8	0,37	2,2	0,04	6,8	0,11
INMETRO-BR	86,2	0,69	28,9	0,23	48,4	0,39	78,8	0,43	-24,8	-0,13	57,8	0,31
CENAM-MX	284,2	0,87	12,9	0,04	35,4	0,10	55,8	0,15	-84,8	-0,23	-165,2	-0,43
NIST-US	1,1	0,23	2,1	0,42	3,7	0,71	2,7	0,49	4,0	0,71	5,8	0,97
NRC-CA	12,7	0,16	13,2	0,16	8,0	0,10	10,2	0,12	8,3	0,10	1,8	0,02
A*Star-NMC-SG	-15,8	-0,07	-37,1	-0,16	-39,6	-0,17	-44,2	-0,19	-59,8	-0,26	-40,2	-0,17
NIM-CN	68,2	0,70	80,9	0,83	82,4	0,84	107,8	1,10	110,2	1,13	107,8	1,10
NPLI-IN	-53,8	-0,11	-50,1	-0,11	-116,6	-0,25	-115,2	-0,24	-13,8	-0,03	78,8	0,17
NIMT-THA	-7,7	-0,13	-8,9	-0,14	-12,3	-0,18	4,9	0,07	-15,9	-0,20	-71,2	-0,86
NPL-GB	1,2	0,02	0,6	0,01	-2,1	-0,03	3,3	0,06	7,4	0,12	6,3	0,11
VNIIM-RU	-17,8	-0,54	-20,1	-0,59	-21,6	-0,60	-21,2	-0,57	-22,8	-0,59	-26,2	-0,65

Meas. Point	75 mm		80 mm		85 mm		90 mm		95 mm		100 mm	
x_{ref}	-151,2 nm		-127,5 nm		-133,1 nm		-317,9 nm		-269,1 nm		-256,7 nm	
$u_c(x_{ref})$	4,3 nm		4,4 nm		4,5 nm		4,6 nm		4,8 nm		4,9 nm	
u_{ext}	4,8 nm		5,0 nm		5,6 nm		5,5 nm		5,9 nm		5,9 nm	
No of participants	15		15		15		15		15		14	
R_B	1,12		1,15		1,23		1,19		1,25		1,20	
$R_{B,crit}$	1,33		1,33		1,33		1,33		1,33		1,34	
	x_i-x_{ref}	E_n										
METAS-CH	-18,8	-1,12	-17,5	-1,02	-24,9	-1,43	-22,1	-1,24	-19,9	-1,10	-22,3	-1,20
EIM-GR	-389,8	-0,34	-377,5	-0,33	-436,9	-0,38	-323,1	-0,28	-292,9	-0,26	-240,3	-0,21
INRIM-IT	0,2	0,00	4,5	0,05	-5,9	-0,06	2,9	0,03	7,1	0,07	1,7	0,02
Nmi-VSL-NL	39,2	0,71	28,5	0,51	24,1	0,43	44,9	0,78	53,1	0,91	69,7	1,18
CEM-ES	-4,8	-0,08	22,5	0,37	-10,9	-0,18	10,9	0,18	12,1	0,19	-4,3	-0,07
INMETRO-BR	71,2	0,39	136,5	0,74	74,1	0,40	9,9	0,05	6,1	0,03	-85,3	-0,46
CENAM-MX	-248,8	-0,62	-272,5	-0,65	-266,9	-0,62	-182,1	-0,41	-230,9	-0,50	-243,3	-0,51
NIST-US	5,0	0,80	2,2	0,34	7,7	1,13	4,5	0,64	2,8	0,38	7,1	0,94
NRC-CA	7,6	0,09	9,4	0,11	7,7	0,09	5,1	0,06	7,2	0,08	-0,1	0,00
A*Star-NMC-SG	-73,8	-0,31	-22,5	-0,10	-28,9	-0,12	-20,1	-0,08	31,1	0,13	44,7	0,19
NIM-CN	120,2	1,23	135,5	1,39	131,1	1,34	150,9	1,55	154,1	1,58	256,7	2,63
NPLI-IN	45,2	0,10	-62,5	-0,13	-160,9	-0,34	-46,1	-0,10	-322,9	-0,68	-456,3	-0,96
NIMT-THA	-6,9	-0,08	3,0	0,03	-18,7	-0,19	3,9	0,04	-10,3	-0,10	-2,6	-0,02
NPL-GB	1,3	0,02	21,2	0,36	6,9	0,12	6,4	0,11	17,9	0,30	10,6	0,18
VNIIM-RU	-27,8	-0,67	-19,5	-0,45	-27,9	-0,63	-27,1	-0,59	-22,9	-0,48	-29,3	-0,60

Appendix 2: Descriptions of measurement setups and methods as reported by the participants

GROUP 1

BEV Austria

SIP 3002 length measuring machine with a standard HP 5529A laser interferometer only (i.e. no internal scale.) A standard linear interferometer, an Agilent 10751D air sensor, and 3 material temperature sensors were used. All systems calibrated by the BEV. The instrument is equipped with an incident light CCD-microscope. A special holder was constructed to ensure that the scale axis and the measurement axis of the laser interferometer coincide to within 0.1 mm.

For these measurements a 100× NA 0.55 objective with LED illumination was used. The image of the scale marks (as seen on a video monitor) were placed between two fixed lines (produced by a line generator) by manually moving the carriage together with the microscope. This visual technique together with residual straightness errors causes the most important uncertainty contribution.

To evaluate this uncertainty contributions measurements were performed by 4 different operators and on 5 diverse locations (orientation) on the machine. The stated results are the mean of this 5 measurements which are themselves the means of the observer-specific values. Because of instrumental boundary conditions the actual measurements were performed in two steps: 1 mm all 0.1 mm and 100 mm all 5 mm, respectively. The uncertainty for this two configurations is significantly different mainly of relocking effects.

Thermal drift was compensated by a time symmetrical measurement scheme. The scale temperature was estimated by measuring the table temperature some 5 cm away from the artefact. The scale support was near the end of the artefact (i.e. not at the Airy points).



CMI Czech republic

CMI uses interferometric comparator IK-1 (CMI design) with static CCD microscope (objective 20x, ~130nm/pixel), transmission illumination by adjustable green or red LED, adjustable moving stage with linescale and interferometer retro-reflector.

Image processing:

line image is parallel to CCD rows: all pixels from selected range of one row are first added, then positions of both edges is found by linear interpolation of row sums, average of this two edge positions is taken as line position.

The stage automatically moves to predefined positions with about $\pm 4\mu\text{m}$ precision (each line always close to the centre of the field of view). The readings of interferometer and CCD residual deviation are taken in synchronization. Resolution, noise and vibrations are bellow 10 nm. The stage returns to reference (zero) line after each movement.

DZM Croatia

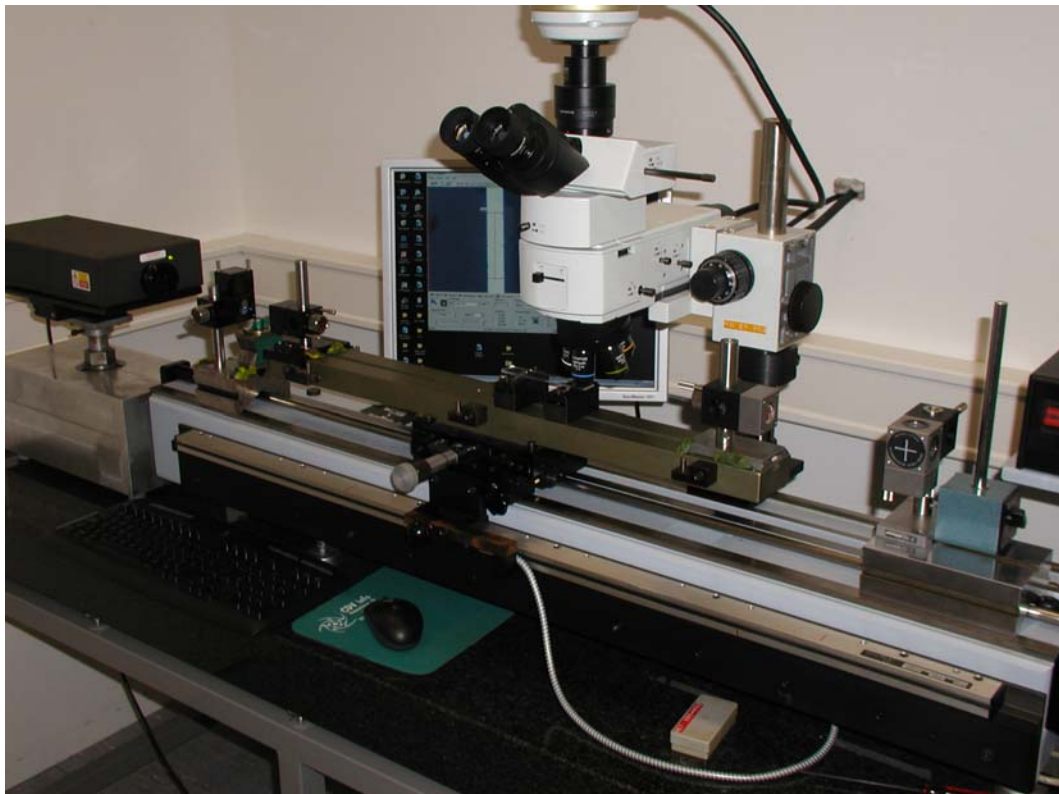
The measuring range of the device is 500 mm and it is primarily intended for the calibration of precise line scales. Device is fully constructed and produced at our Laboratory.

Stage movement is done manually.

The sighting process is done by means of a microscope with a digital CCD camera Olympus DP 70 with 12, 5 Megapixels with objective magnification of 50X.

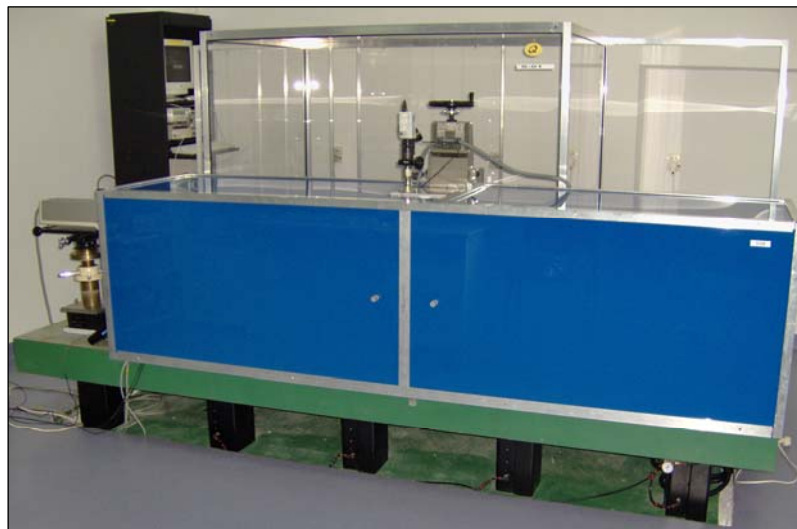
The measuring system used is the laser interferometer (Renishaw ML 10). The basis of the Renishaw Laser Interferometer system is HeNe Laser operating at a wavelength of 0,663 μm . The EC 10 Environmental Compensation unit automatically measures the three critical environmental parameters (temperature, pressure and relative humidity) and passes the data to the CS 10 Control Unit of which will compensate for any resultant change in wavelength.

The image processing is static, which means that it is necessary to process images and not the "live" signal of the display provided by a CCD camera. The software solution functions in such a way that all the pixels of a certain image are transmitted into a black&white combination and then the position of the line centre is calculated by arithmetic algorithms. The software solution provides the exact position of the line centre in pixels. In order to convert the values in pixels into the length values, it is necessary to calibrate the pixels size, i.e. to find out the length amount of every pixel. Calibration of the pixels is done absolutely by taking two images of the same line, which are shifted by the distance read on the laser interferometer.



GUM Poland

The 1-D measuring bench (SIP) with total length of one meter is the base of the line scale measurement set-up. The set-up is located in the air-conditioned lab, housed and mounted on the concrete plate supported by the pneumatic vibroisolation system. The scale lines are detected using the microscope and the CCD-camera, mounted on the fixed column. The lines are observed on the monitor equipped with two parallel lines generated electronically. The distance of the generated lines can be adjusted for the artifact to be measured. The scale lines are aligned between this two lines by eye in a symmetrical manner with precision piezo-electric actuator. The line spacing is measured with the laser interferometer HP-5528A. The line scale was placed on the moving, remote controlled carriage. The linear reflector of the interferometer is mounted on the carriage. The measurement data are collected with PC computer through the HP-IB interface.



The line scale was supported, during the measurement, at the Airy points using gauge blocks. The measurements were carried out in normal and reversed orientation (0° and 180°). There was applied the image window height close to $50\ \mu\text{m}$, the microscope with 20x objective and total magnification of 770x for the analysis of measurements.



The environmental parameters (material and air temperature) were measured by interferometer sensors. Humidity was measured with thermo-hygrometer LB-706. The refractive index of air was calculated from the modified Edlen formula [G. Bönsch and E. Potulski, *Metrologia*, 1998, 35] with sensors corrections.

INM Romania

Instrument:

- longitudinal comparator, equipped with an optical microscope and a laser interferometer with laser source He – Ne stabilized in frequency, having a resolution equal to 0,01 μm .

The longitudinal comparator is based on the cinematic method, according to Abbe principle: the line scale must be aligned on the same longitudinal axis with laser beam on the measurement direction, in the scope to eliminate the first order errors. Because the line scale was short, it was supported with the whole surface on the special carriage of the comparator.

Measurement method:

Method of measurement consists in the displacement of the reference line measure along the measurement direction. Speed of displacement is about maxim 10 mm/min. Marks' viewing of line measure is made using an optical microscope. The line is put on the mobile arm of the interferometer and the distance between marks is directly measured in length units.

The appearance of a fringe in the field of view of interferometer is determined by a deviation of optical path from measurement arm of interferometer equal with $\lambda/2$, where λ is the wavelength in the propagating medium at medium's temperature, pressure and humidity of the laser He-Ne radiation, used as monochromatic source of light.

During one measurement between the beginning and the end of the measurement, difference between the thermometer readings was equal to $\Delta t_g = 0,01$ $^{\circ}\text{C}$. The difference between the temperature of the room and the reference temperature was 0,4 $^{\circ}\text{C}$...0,8 $^{\circ}\text{C}$ during all measurements.

LNMC Latvia

Action principle of horizontal comparator IZA-7 is based on optical viewfinder method.

Comparator IZA-7 design maintains adhering to principle of longitudinal comparison.

Measured item is possible to set up on the bedplate so that its axis could be the longitudinal extension of scale line axis. Scale line axis alignment with line of moving bedplate.

Measurement of length (line) is performed by method of comparison measured item line with comparator line scale using 2 microscopes with steadily span and parallel optical axis.

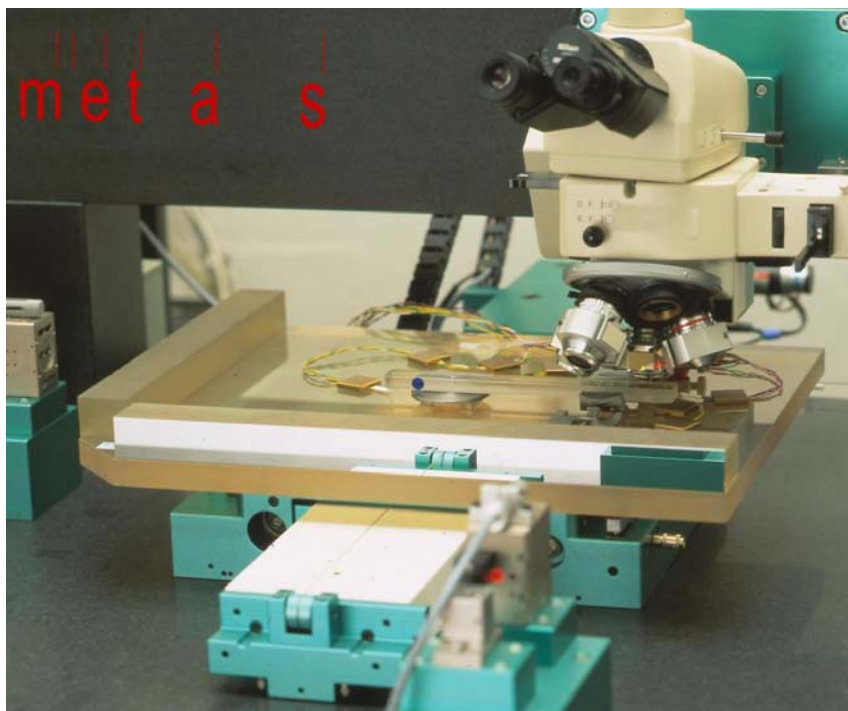
One microscope is used for aiming line, the other for reading on comparator scale.

METAS Switzerland

Measuring system:

The measurements were performed on a 2D photomask measuring system with a measurement range of 400 mm x 300 mm. The system has an xy-stage with unique vacuum air-bearings featuring very small errors of motion. Two speed controlled servo motors move the table by means of fine strings. Once positioned, the stage is clamped to the granite base table by a vacuum brake. A differential two axis plane mirror interferometer (HP) measures the position of the stage. The moving mirrors are attached to a Zerodur base plate and the reference mirrors are fixed to the microscope objectives. Air pressure, temperature, humidity and CO₂ content are on line accessed to determine the refraction index of the air by the Edlen formula. A microscope with a CCD camera and an episcopic illumination is used to localise structure positions. The microscope has a motorised turret and focus. For automatic focussing the image contrast is maximised.

The machine is located in a temperature stabilised clean room cabin of class 100 (US) within the clean room section here at METAS.



Scale mounting:

The line scales were aligned parallel to the x- or y-axis of the 2D photomask measuring system. They were supported at the Airy points, with a distance of 66.4 mm, by 4 spheres, two on a pivot. The scales were aligned using piezoelectric actuators. Vertically to better than 10 $\mu\text{m}/100\text{ mm}$. Additionally, as a 2D measuring system is used, the x-axis of the object coordinate system is placed through the alignment marks by a numerical coordinate transformation to better than 4 $\mu\text{m}/100\text{ mm}$.

Line evaluation:

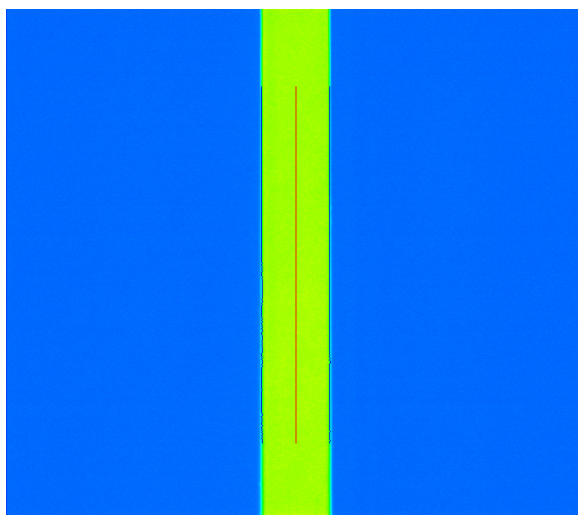
Each vertical line in the video image is analysed within the region of interest (ROI). The centre of a line profile is the average of the left and the right edge. The edge locations are determined

with a moment based edge operator. A line is fitted through all individual profile centres using only points within 2σ . The intersection of the fitted line with the reference line is used as the scale line position. The reference line was determined using the right and left pair of the horizontal alignment marks. Each line was evaluated within a length of $50\ \mu\text{m}$ (height of the ROI).

Table: Image size and evaluation range.

Magnification		20x	50x
		μm	μm
Image size:	x	244	98
	y	182	73
Evaluation range:	x	30	40
	y	50	50

Typical line at 50x magnification with edge and line centre indication:



Measurement strategy:

The 2D photomask measuring system can operate fully automatically, therefore always a complete set of measurements was made lasting for about 2 hours. Such a set consisted of the following measurements:

Scale (mm)	Lines	Repetitions
0, 0.1 .. 1	11	10
0, 5 .. 100	21	10
0 .. 100 (for verification only)	2	10

Both line scales were measured in four orientations 0° , 90° , 180° and 270° with the 20x objective and additionally at 0° and 180° with the 50x objective. For the final result all these measurements were averaged. There was no systematic difference.

Corrections:

For the final results all known corrections were applied. In particular, the thermal expansion was corrected using the given thermal expansion coefficients of $5E-07/K$ for quartz. The temperature deviations from $20^{\circ}C$ were within $\pm 0.1 K$ (average $20.06^{\circ}C$). Furthermore, as the measuring system is located 550 m above sea level, the average barometric pressure during the measurements was only around (945 .. 950) mbar. The results were reduced to the standard pressure of 1013 mbar with the given compressibility coefficient of $-8.90E-07/bar$ for quartz. This correction was $-5.9 nm$ for 100 mm.

Uncertainty contributions:

For the total uncertainty 30 contributions were considered. The largest contributions at 100 mm were for both scales, the repeatability, the air temperature and the scale support. For quartz scales also the material temperature is critical because glass has a low thermal conductivity and a small thermal capacity therefore it is difficult to measure its temperature. The accuracy of the thermistors itself is not the problem.

MIKES Finland



Figure 1. MIKES' line scale interferometer

MIKES' line scale interferometer (fig 1) uses a dynamic method of measurement with a moving microscope for speed, simplicity, and considerations of space requirements. The graduation line distances are measured during continuous motion, which makes the system fast and the interferometer insensitive to minor turbulence in the interferometer beam path. Possible problems with speed fluctuations and time delay in observing the lines are avoided by using an electrically shuttered CCD camera as a line detector and synchronous data sampling.

The interferometer is constructed on a vibration isolated stone table to eliminate mechanical disturbances. The interferometer is situated in a laboratory room with air temperature 20 ± 0.05 °C and humidity $46 \pm 2\%$ RH. The microscope is fixed on one side of a carriage and the CCD camera on the top of the microscope, axis of which is adjusted perpendicularly to the scale plane.

The displacement of the microscope is followed by a Michelson interferometer utilising a calibrated 633 nm Zeeman-stabilised He-Ne laser. The light of laser is coupled via single mode fibre to the interferometer and adjusted parallel with the carriage movement by using a quadrant detector. Abbé error is eliminated with a large cube corner, making it possible to adjust the focus point of the microscope and the apex of the cube corner to the same point. This cube corner is constructed from three separate round mirrors adjusted to angles of 90° with each other. Ideal adjustment of the focus point and the apex of the cube corner nearly completely eliminates the Abbé error. The interference fringes are detected by two detectors with 90° phase difference and counted by a direction-sensitive quadrature counter.

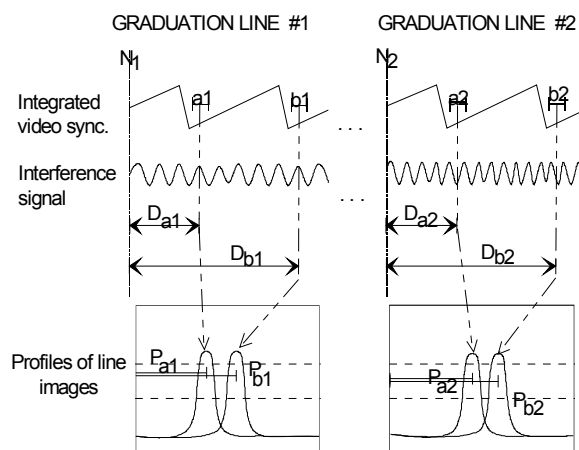


Figure 2. Analysis of the measurement data.

In measurement run, the carriage moves in one direction while the programme continuously monitors the counter reading. When the carriage is approaching a line, the programme slows down the speed of the carriage and just before passing over the line it stores the current counter reading (N_i ; figure 2), starting a synchronized sampling. In the sampling, one interference signal and an integrated video synchronisation signal, for determination of the field forming positions (a_i , b_i), are digitised, the graduation line image is stored, and the refractive index and temperature of the scale are calculated and stored. This set of samples is taken for each line after which a new run is started in the opposite direction. A single measurement of the decimetre lines of a 1 m scale takes approximately 15 minutes. The first approximation for the measured length is calculated as the distance between the positions where the graduation line fields are formed ($N_i - D_{ij}$).

Average profiles of the graduation lines are formed by summing picture element intensities of each row of the CCD. Each image of the CCD camera consists of two fields charged in 1 ms and with time separation of 20 ms. Thereafter, the centre points of the graduation lines (P_{a1} , P_{a2} , P_{b1} , P_{b2}) are determined from the slopes of the line profile and a correction term needed to superimpose the centre points is applied. The refractive index of air is determined by Edlen's formula updated by Bönsch et al. The line scale interferometer is capable of calibrating line separations from 10 μm to 1 m of good quality line standards, having line widths from 2 to 50 μm .

The measurements for comparison were done like for normal customer asking high accuracy calibration of good quality line standard. As specified in the protocol the width of the measuring section was adjusted to $50 \pm 2 \mu\text{m}$ and scale was supported from Airy points. The line spacings were measured in two different positions along the range of the stone rail. In both positions the scale was measured in normal and reversed orientation. Each measurement consisted of 5 runs. The averages of these 4 measurements are the results. Compressibility correction was calculated and applied.

Unfortunately the reference line was noticed to be non-ideal (fig 3). In separate test was studied what is the effect of this non-ideality. In test 10 first lines were measured normally and so that the defected area was excluded from the analysis. The difference was +12 nm with 6 nm STD. This correction was applied to the result.

Also lines 0.1; 0.4; 85; 90 and 95 mm were clearly non-ideal (see receipt confirmation from MIKES). For this reason the value of the uncertainty component "Influence of line detection algorithm with line quality" was raised to 20 nm for these lines. This approximately doubles their uncertainty.



Figure 3. Non-ideality in the reference line (pointed by red arrow).

References:

- A. Lassila, E. Ikonen, and K. Riski, Interferometer for calibration of graduated line scales with a moving ccd camera as a line detector, *Applied Optics* 1994, 33, 3600-3603.
- A. Lassila, Updated performance and uncertainty budget of MIKES' line scale interferometer, *In Proc. of euspen*, Glasgow, Scotland, May 31 – June 2, 2004, p 258-259.

MIRS Slovenia

Measurement setup

The line scale was measured on a Zeiss ULM 01-600 C 1D measurement machine by using laser interferometer HP 5528 A as a measurement system and Opto zoom microscope with CCD camera as a line detection system.

The scale is supported in Airy points by two metal half cylinders. Additional fixture is not necessary due to low movement speed (hand driven table).

The measurement setup is shown in Fig. 1



Fig. 1: Measurement setup

The centre of a line is detected by the video-positioning system consisting of a zoom microscope, CCD camera and a line detecting software, which was developed in the laboratory in the LabView environment.

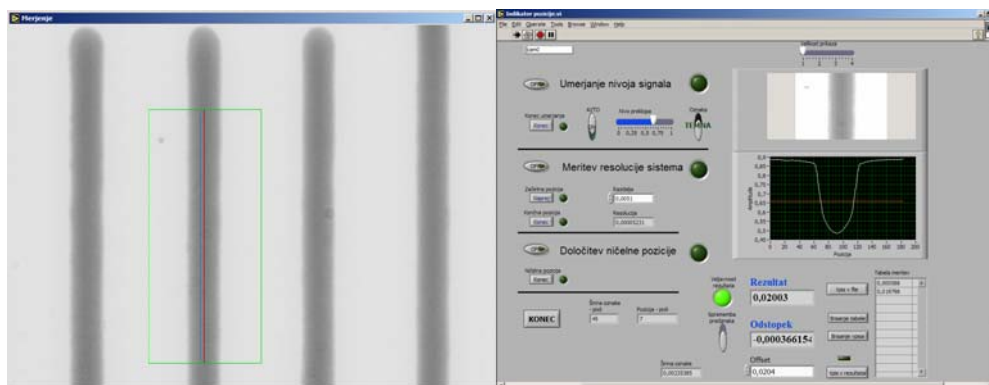


Fig. 2: Line detection software – screen masks

The material temperature is measured with a Zeiss termistor contact sensor (resolution 1 mK, standard uncertainty of calibration 2 mK) on the measuring table, while the air temperature is measured with Agilent temperature sensor with resolution of 10 mK.

Measurement procedure:

Each line position was measured from zero position (the system was positioned in zero point after each measurement). The whole procedure was repeated 10 times in a short time period. Arithmetic mean from those measurement represented measurement result, while the standard

deviation represented the repeatability component of the measuring uncertainty. In order to evaluate reproducibility, the measurement was repeated in 5 different days with two different operators.

NCM Bulgaria

The measuring system consists of a comparator, laser interferometer (with light source He-Ne laser 633 nm, HP5529A), moving carriage with mounting on it reflector and (with light source laser diode) for location of scale marks, temperature measuring system, barometer and hygrometer.

The scale was placed horizontally on two supports at Airy points.

NML Ireland

Equipment Used:

Agilent 5519A Laser and SIP Horizontal Measuring Machine

Procedure:

The HP laser retro reflector is mounted to the end of the main bed of the SIP measuring machine, nearest the laser head. The HP interferometer is fixed to the longitudinal carriage of the SIP.

For line scales of nominal size greater than 10mm a transparent table is placed on the longitudinal carriage of the SIP measuring machine. This table is illuminated from below with a light source.

The glass scale under test is placed on the transparent table and aligned with the main axis (x axis) of the SIP using the adjustment screw on the transparent table.

The vertical microscope of the SIP is then aligned with the glass scale under test. An appropriate eyepiece and magnification is then selected to give optimum clarity to the glass scale under test, taking into account the line width and line quality of the line scale under test.

The central cross wire (the cross wires are imposed on the eyepiece of the SIP microscope) is aligned with the datum line of the glass scale. In this position the HP laser system is zeroed.

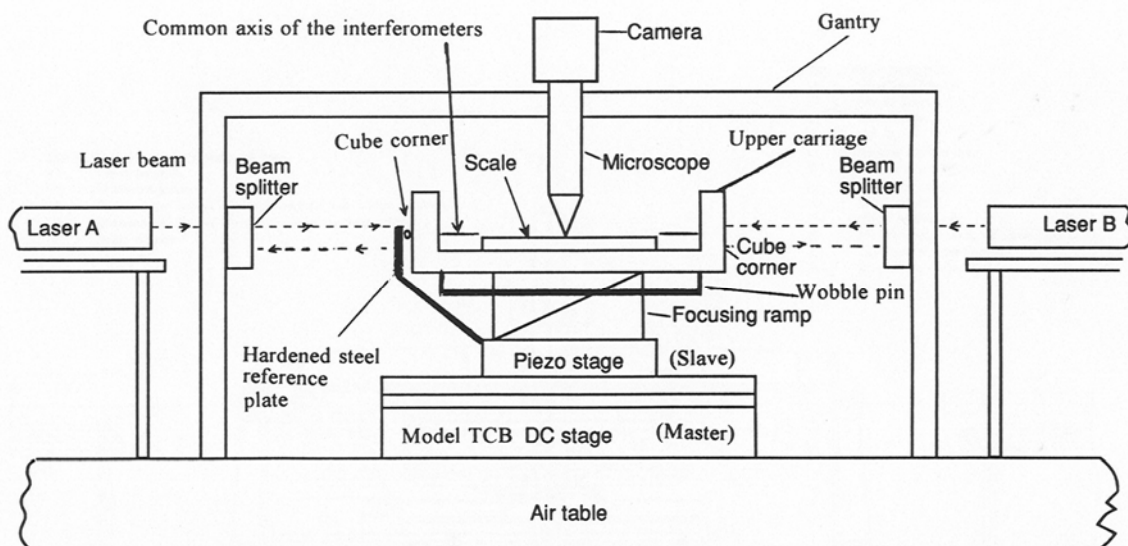
The carriage of the SIP is then moved until the second line of the glass scale is aligned with the cross wires. The distance moved is recorded from the display of the HP laser system.

This exercise is repeated at selected positions over the length of the glass scale. 5 repeat measurements are taken at each selected position along the scale and the average taken.

NPL United Kingdom

The NPL linescale machine consist of a 400mm range, interferometrically monitored, air-bearing stage that moves the scale to be measured under a nominally fixed optical probe. The probe consists of the NPL NanoVision image processing system.

Scale motion is measured by two co-linear independent laser interferometers, one being an NPL differential Jamin type with plane mirror and second being an HP Michelson type with cube-corner reflectors. The measurement is carried out in a laboratory atmosphere and a weather station monitors the refractive index of the air. Following the Abbe principle, the common axis of the interferometers lies in the plane of the scale to be calibrated and is co-linear with the line containing successive measuring points on the scale. Separation of the cube-corner / plane mirror reflectors (one flexure-mounted) is maintained by a fused silica 'wobble-pin'. The two beam splitter units are each flexure-mounted on the frame of the machine, separated from the measuring head by further silica wobble-pins.



A scale under examination is 'Airy point' mounted with the chrome uppermost and with no compression force on the scale. The scale is illuminated with reflected light. A combination of the two measurements obtained greatly reduces the chances of common-cause error in displacement-measurement and the configuration provides an indication of accuracy and repeatability.

The 2006 measurements were taken with the NPL 400mm machine in a temporary laboratory with poor environment conditions. The measurements were made without using an auto focusing routine.

The 2008 measurements were taken with the NPL 400mm machine in a dedicated laboratory in the New NPL building. The environment conditions here are much better. The measurements were made using an auto focusing routine and employing a second-generation version of NPL NanoVision video probe.



NSCIM Ukraine

The measurement of the scale intervals was carried out by the absolute method using the interference setup of the primary standard of the unit of length DETU 01-03-98, which is a horizontal comparator with Michelson dynamic laser interferometer and photoelectric microscope for fixing the centre of the measured scale marks. The photoelectric microscope (PEM) and the corner reflector of the measuring arm of the laser interferometer are rigidly fixed on the movable table of the comparator. The scale under measurement is installed in a special positioner on the stationary table of the comparator.

To create the required measurement conditions the interference setup is placed into a heat chamber with automatically maintained air temperature of (20 ± 0.05) °C.

The length of the scale intervals is determined in the wavelengths of the stabilized He-Ne laser radiation ($\lambda = 0.63 \mu\text{m}$) by means of reversible counting of the fringes kept within two automatic settings of the PEM to the tops of the image of the measuring scale marks. The equation is as follows,

$$L = N\lambda_0 / 16n + \alpha\Delta tL_H,$$

where N is the number of fringes (impulse number) kept within the measured scale interval; λ_0 is the wavelength of the laser source in vacuum; n is the air refractive index; α is the linear expansion factor of the scale material; Δt is the scale temperature deviation from 20 °C; L_H is the nominal length of the scale interval.

The air refractive index is calculated by the Edlen formula using the measured values of pressure, temperature and humidity. The temperature of the gauges and the air is measured with regard to the base of the interference setup using the platinum resistance thermometer, copper constant thermocouples and direct current bridge. The pressure and humidity are measured using standard devices.

The real value of the scale interval length is determined as the average value of the measured scale interval lengths in the direct and reverse motion of the PEM.

OMH Hungary

The measurements were done on the 3 m universal length measuring machine made by Zeiss, with the help of HP 5528 laser interferometer.

The environmental parameters were measured by independent calibrated measuring instruments. For the temperature measurements, 4 wires PT 100 thermoresistors were connected to Keithley type 196 multimeter. The readings were made automatically through HP-IB parallel interface. For the air temperature 2, for the material temperature 5 thermometers were used. The average of the 2 and the 5 values were used as air and material temperature.

The air pressure was measured by Wallace & Tiernan digital barometer Type Diptron 3, the data were taken also via HP-IB interface.

The air humidity was measured by a Digilog 60 capacitive digital humidity measuring instrument.

The correction factor was calculated by the EDLEN formula.

The data from the HP laserinterferometer were taken also via HP-IB interface.

The magnification of 100 X was used and the magnified image was seen on the SONY videomonitor through a videocamera. The image processing system generates digitally movable horizontal and vertical lines that serve to help to set the centre of the lines. The horizontal magnification was 1200 x.

The scale was placed on a steel base as the lines were standing vertically, 2/9L points were used.

The angle error of the carriage movement in vertical and horizontal plane (pitch and jaw) was measured by Agilent laserinterferometer in 0,1 sec resolution.

PTB Germany

The PTB performed the measurements reported here with its Nanometer Comparator. Here only a short description will be provided. Detailed descriptions have been published already elsewhere [1-3]. A schematic of the Nanometer Comparator is shown in Fig. 1.

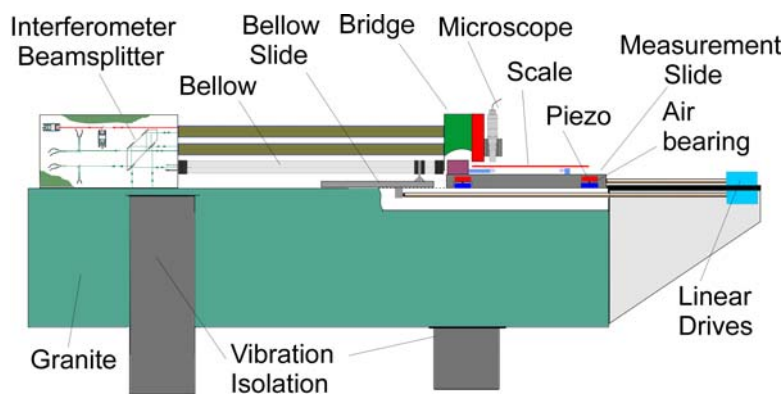


Figure 1: Schematic of the Nanometer Comparator

The Nanometer Comparator is equipped with a vacuum interferometer. An iodine-stabilized, frequency doubled Nd:YAG laser, which is operated according to the recommendations of the BIPM, serves as radiation source. The radiation is fed through polarisation maintaining fibres from the laser, which is located outside the measurement cabin, to the vacuum interferometer. The measurement slide is guided by air bearings and driven by a linear motor. Angular vacuum interferometers and piezo electric actuators integrated in the measurement slide are used in a closed loop to correct for the remaining angular deviations of the measurement slide. The z-axis actuators are also used to perform the z-axis fine motion required to determine the focus position of the sample. The sample is supported at its Airy points with a fixed and a movable roller. The fixed roller is supported by a height adjustable mount directly connected to the housing of the measurement reflector. The loose roller is put on a height stage mounted on the slide. A home-made optical microscope, which is shown schematically in figure 2, is used to detect the graduation lines of the scale. The housing was machined out of invar. The white light illumination is provided by a

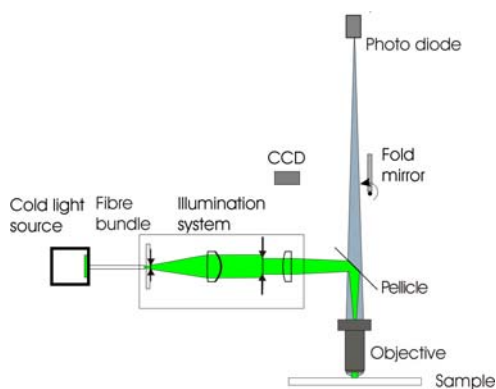


Figure 2: Schematic of the microscope

cold light source and guided to the microscope by an incoherent fibre bundle. The illumination optics has been designed to achieve a Köhler illumination. The light is directed through the objective towards the sample by a pellicle. Here a 50 x Nikon measurement objective with a

numerical aperture of 0.55 and a working distance of 16 mm was used. By means of a fold mirror the image of the line can be observed directly using a CCD camera. This feature is used to align the sample horizontally. During the measurements the light of the image is detected by a photo diode after it passes through a fixed slit. In the object plane the slit has the dimensions of $4\ \mu\text{m} \times 50\ \mu\text{m}$. The intensity profile of the line and the related positions were acquired simultaneously by means of a hardware trigger provided by a function generator. In order to restrict the data acquisition to a region closely located around the line only, a gate signal for the trigger was derived from the digital scales of the measurement slide. The following algorithm was used to determine the position of a line. First the intensity profile of the line was normalized so that all values are between zero and one. Straight lines are then fitted to the intensity displacement dependence in the intensity range between 0.4 and 0.6. From this the positions, where the intensity equals 0.5, are calculated for right and left edge. Finally the average of these two positions is calculated and considered as the position of the line.

The measurements were corrected for the deviation of the air pressure and the temperature from the normal conditions (1013.25 hPa and 20°C) using the linear coefficients of the compressibility and thermal expansion as given in the technical protocol of the comparison. Furthermore the influence of the residual gas in vacuum chamber of the interferometer on the wavelength was corrected for using a simplified Edlen equation.

b.) Measurement conditions and measurement uncertainty

Due to the different spacings between the lines to be measured the measurements were divided in two independent parts. First the lines of the first millimeter and then the lines over the whole scale were measured. The scale was measured in the first and again in the third week of January 2007. The scale was aligned to better than $0.1\ \mu\text{m}$ vertically and within $1\ \mu\text{m}$ laterally the day before the measurements were performed. The whole setup then was left to reach its thermal equilibrium over night. Before the measurements were performed the focus position of the scale was determined and the z-position of the scale was readjusted accordingly. Each day 5 data sets in forward and backward direction were collected for the two independent parts. The measurement speed of the short part was 0.1 mm/sec and that of the long part was 0.2 mm/sec. Then the scale was remounted in the reverse orientation. To obtain the final result the average results of each day were averaged again. The results of the uncertainty estimation are summarised in the table on the following pages.

The pilot laboratory was informed in a separate short report about the influence of the partly contaminated graduation on the measurement results of the PTB (report sent on Feb 8th 2007). The severe contamination of the sample leads in general to a considerable increase of the measurement uncertainty. At several lines (the position relative to the zero line are given in the table) an additional contribution was necessary to account for the experimentally observed scatter and the differences between the PTB mask comparator, which also has measured the scale, and the Nanometer Comparator. We like to mention here that neither the control measurements nor a comparison of these two instruments performed on the quartz scale used in the Nano 3 comparison performed parallel to the comparison showed any disagreements or variations, so that the observed larger variations of the results and differences between the instruments can be solely attributed to the contamination of the sample. In addition, a further comparison between the two instruments on a clean area of the scale also yielded a complete agreement within the observed experimental scatter, which was in the order of a few Nanometer.

References

- [1] J. Flügge, H. Dangschat, A. Spies, J. Tschirnich and H. Pieleles: "Concept of a interferometric length comparator with measurement uncertainties in the nanometer scale", Proceedings of 1st Euspen Conference, Bremen, Mai 1999, p. 227-230
- [2] J. Flügge, R. Köning and H. Bosse: "Status of the nanometer comparator at PTB", Proc. SPIE, Recent Developments in Traceable Dimensional Measurements, Jennifer E. Decker; Nicholas Brown; Eds., 2001, Vol. 4401, 275-283
- [3] J. Flügge, R. Köning and H. Bosse: "Achievement of sub nanometer reproducibility in line scale measurements with the Nanometer Comparator", to be published in the SPIE proceedings of the Advanced Lithography conference, held in San Jose in February 2007

SMU Slovakia

The line scale was calibrated on the setup consisting from the 1-D length measuring machine Abbe Zeiss (measuring range up to 200 mm) and the laser interferometer HP 5529B.

The frequency (vacuum wavelength) of HP HeNe 633 nm laser has been calibrated against the HeNe/I₂ 633 nm primary standard of SMU.

The line scale was laid upon the 150 mm gauge block placed horizontally (height of 9 mm) supported by two semicylindrical supports in the mutual distance corresponding to Bessel points related to 150 mm long artifact of rectangular shape – the reason was possibility to use clamp attaching the Pt resistance thermometer directly to the gauge block onto which the measured glass artifact was resting.

The extrapolated axis of calibrated scale intersected the axis of cube corner and thus the Abbe principle was kept.

The carriage bearing both measured line scale and cube corner was moving under the optical microscope. Due to bending of the artifact over the whole measured range just the limited magnification could be used – objective 10x, eyepiece 12,5x

The position of the line was observed in the area determined by two parallel lines (at the beginning and at the end of the scale) – as those as were not visible during the targeting on the measured lines, the height of observed area in the visual field was based on the subjective estimation.

The temperature of both the glass plate and air in the neighbourhood of the laser beam was measured by two Pt 100 thermometers (1 for scale, 1 for air), the air pressure was measured by the digital barometer DPi 141 and the relative humidity by the ALMEMO tester.

The scale was calibrated in two positions and the final result for each line is given by the arithmetic mean of two values corresponding to both positions of artifact (for every measured line, in each position the number of repeated measurements was equal)

The length values were corrected to 20 °C using the linear thermal expansion coefficient $5 \times 10^{-7} \text{ K}^{-1}$.

The pressure compressibility correction (negligible, cca -1 nm for 100 mm length) to 1013,25 hPa has been applied using the length compressibility factor - $8,9 \times 10^{-7} \text{ bar}^{-1}$.

ZMDM Serbia

The measurements were performed on a 1-D measuring machine (bench) with a total length of three meters (Zeiss type ULM 3000). Scale lines were detected using Zeiss optical microscope, mounted on a moving wagon of the measuring machine. A laser interferometer (HP 5526 A) was used to measure the displacement of the microscope.

Scale support: During measurements the line scale was supported on two roller bearings at Airy points without any clampings. Scale is aligned visually with the displacement axis of translation stage and measuring (laser) axis. Alignment is checked by comparing the focus and position of the end lines while displacing the translation stage from the line “0” up to the line “100”. This procedure is repeated several times.

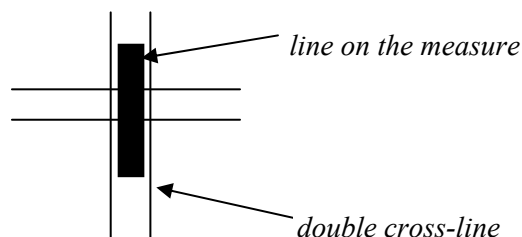
Measuring bench: The translation stage of the measuring bench consists of two parts. The main part is sliding on the bench and is used to coarsely move the microscope into desired position. The second part of the translation stage (which is mounted on the main part) is used for fine-setting the microscope onto the line. Everything is operated manually.

Measurement procedure: The line scale was measured by coarsely move the microscope to each scale line (using the main part of the translation stage) and then fine-tune on the line with second part of the translation stage.

Since the instrument is manually operated, the measurements are time-consuming. In order to control induced drifts, the microscope was moved to the zero-point after every 10 lines measurements for checking.

Line scale was measured in two orientations with overall microscope magnification 50x. In one orientation two repeating measurements – forward and backward - were made as one group for each run. The total number of runs for each orientation were 12 except for total length 100 mm and first 1 mm (20). Then scale were reinstalled in reverse orientation and the alignment is checked as mentioned above. The final result is the average of all these measurements.

The positions of the lines were determined by direct visual positioning of vertical double cross-line of the measuring microscope at the center of each line in reflected white light with green filter. Left and right edge of each line were detected visually as the same (50%) gap light intensity level between microscope double cross-line and left and right edge of the line.



GROUP 2

A*Star – NMC Singapore

The comparison was done using a laser line width measurement system (as shown in Figure 1 & 2) at the National Metrology Centre, Singapore. The system consists of five major parts: a main base with two working stages driven by separate linear motors for sample holding and positioning, a laser interferometer for displacement measurement, a photoelectric microscope for line edge detection, an electronics unit for system control and a PC for data acquisition and recording. The He-Ne laser used in the interferometer is Lamb-dip stabilized and its wavelength is corrected for temperature, humidity and atmospheric pressure.

The scale was placed so that the main inscriptions were uppermost and supported at the Airy points by stainless steel rollers. A lightly pinch was applied at the Airy points to avoid the scale shifting due to the movement of the working stage. The scale was viewed using transmitted light. The length of interval was measured along the longitudinal axis and at approximately mid-position of the scale.

Measurements were taken in two orientations. At each orientation, the scale was properly aligned and two repeated measurements were made.

For each measurement, it covered two independent measuring ranges: one from 0 to 1 mm and the other from 0 to 100 mm, both with a step of 0.1 mm. For the range from 0 to 1 mm, a closed reading was taken at the end of the measurement. For 0 to 100 mm, the measurement was divided into three sections: 0 to 50 mm, 40 to 90 mm and 80 to 100 mm in view of excess data collection. Adjustment factors at the overlapping intervals (40 to 50 mm and 80 to 90 mm) were considered in the calculation.

The average of the four measurements of the two orientations was reported as the final results. All results of measurement are referred to a temperature of 20 °C.

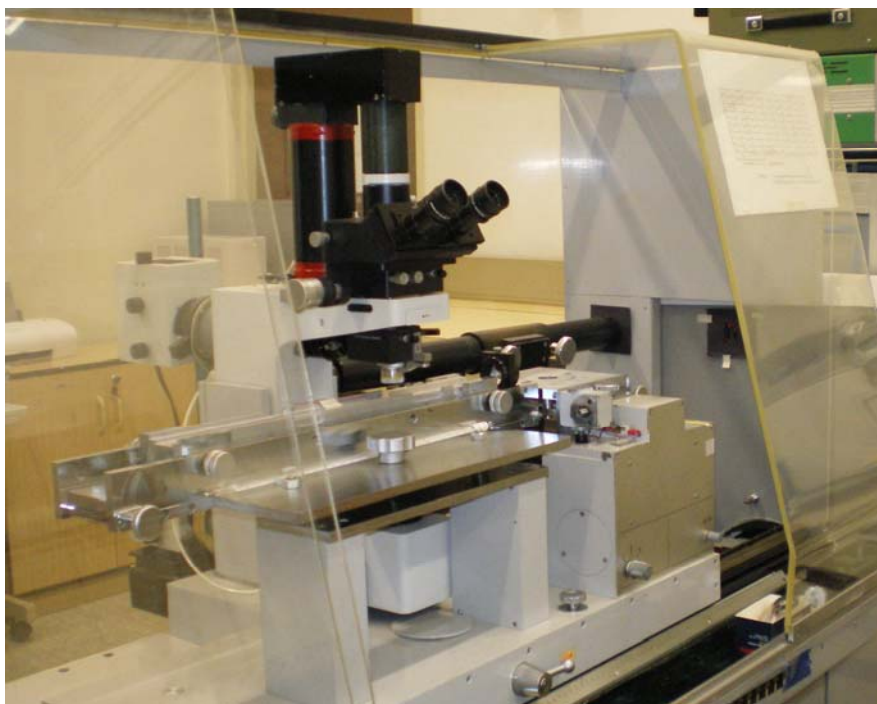


Figure 1: The laser line width measurement system

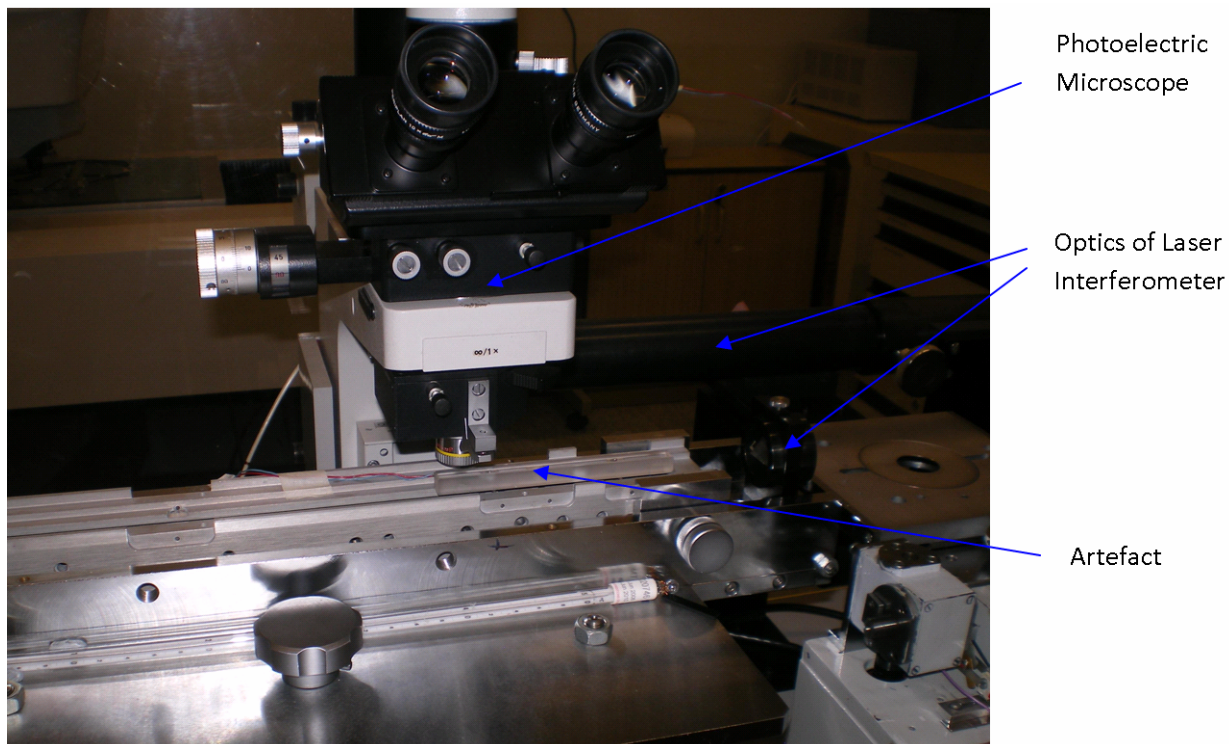


Figure 2: Enlarged view of the line edge detection unit

CEM Spain

Make and type of instrument

Custom-built length comparator CEM-TEK 1200 equipped with, two beams on flat mirrors, laser tracker and pseudo-Abbe measurement principle.

Light sources / wavelengths used or traceability path:

Stabilized Laser Source HP 5517C, $\lambda_0 = 632.991\ 365\ 64\ \text{nm}$, calibrated against He-Ne reference laser CEM-1 (national standard)

Method used to determine the refractive index of the air :

Measuring of ambient conditions and applying of Edlèn's formulae plus laser tracker (relative refractometer) for continuous updating of n value.

The laser is reseted in the first line (reference line position "0") using a reference standard (gauge block) calibrated by interferometry.

Optical system:

The detection of the line is made by automatic recognition by the optical system with the help of home made software.

CENAM México

An optical microscope brand Leitz, model Libra 200, with 200x magnification was used.



The measurement range of the instrument is 150 mm x 100 mm, and the minimal division of the microscope scale is 0,1 μm

The lines edges were detected visually in a monitor connected to a CCD camera.

The distances between line centers were obtained by Micro/Measure Microscope Software and the temperature variation from the standard temperature was $\pm 0,4$ $^{\circ}\text{C}$.

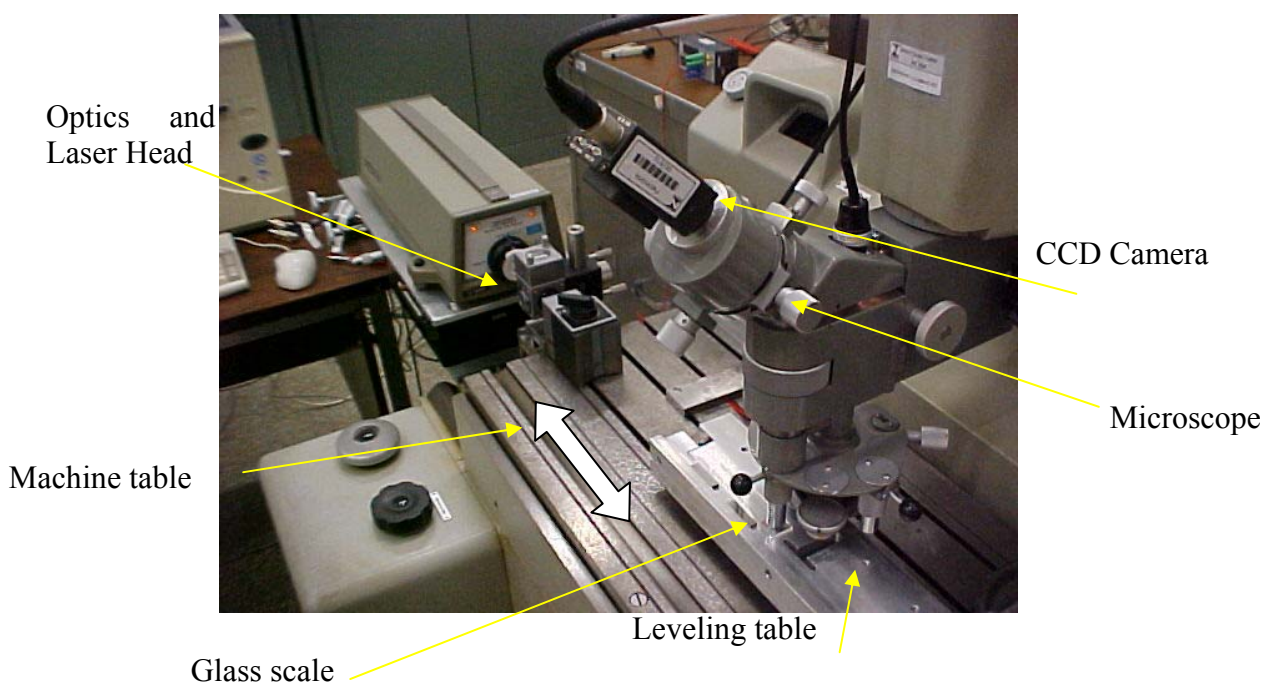
EIM Greece

The measurements were performed with the use of a Leitz universal measuring microscope with x100 total magnification. A Renishaw laser system was used for the measurements of the line scale displacement while the centers of the lines were estimated by the analysis of the digital images of the line scale at each measuring position. The air temperature, humidity and pressure were recorded during the measurement.

INMETRO Brazil

The scale was calibrated in a system composed by a microscope mounted in an optical CMM (Trioptic–SIP) whose table is able to move in one direction. The table movement is detected by an interferometric laser system. The scale was laid over a special table so that it could be leveled aligned to laser beam and focused appropriately. Due to limitations, the scale was not supported in Bessel points as recommended in the Protocol. The measurements were performed in the same points as that ones outlined in the Protocol taking as reference the “0” point. The temperature during the measurements was $(20\pm 0,6)$ °C, with a variation within 0,1 °C.

2 – System configuration



INRIM Italy

The measuring apparatus is based on a Moore Measuring Machine equipped with a laser interferometer and an optical probe. This latter consists of a optical microscope with a CCD-camera.

Tab. 1. Instrument identification.

Instrument	Manufacturer	Model	Ser. No.
Universal Measuring Machine	Moore	n. 3	M245
Laser interferometer	HP	5518	3626A03700
Microscope	Nikon	OPTIPHOT 100S	628562
Objective	Leitz	$\infty/0$ Plan 125X N.A. 0,80	
CCD camera	Basler	FM 60955	

Measurement setup

The optical probe is used for the calibration of line standards. A rectangular window is created via software to simulate a probe; the “contact” is obtained from the image processing tool described below.

The window width corresponds to the ball tip diameter of a “contact” probe, whereas the window height determines the number of pixel rows activated (integration amplitude). By displacing the artefact (relative displacement between artefact and CCD camera), the window “penetrates” in the measurement area and defines the artefact edge position by measuring its distance from the window side (left or right, see Fig.1).

The optical probe is calibrated with reference to the laser interferometer. The pixel-size (about 0.08 $\mu\text{m}/\text{pixel}$, with a magnification of 125X) of the image window is obtained from the displacements measured with the laser interferometer when the window penetrates (of about 6 μm) the edge line from both left- and right-sides. In this way, the measurement runs are driven mostly as for the mechanical probe, except for the probe calibration which is based on the interferometer itself.

From the “contact” readings and the laser interferometer we determine the edge x-positions at the left- and right-sides of the line with an image window of about 32 μm width and 64 μm height. Then, the position of the centre of the line is obtained from the middle of the left- and right-edge positions.

Traceability is given by the wavelength of the laser interferometer.

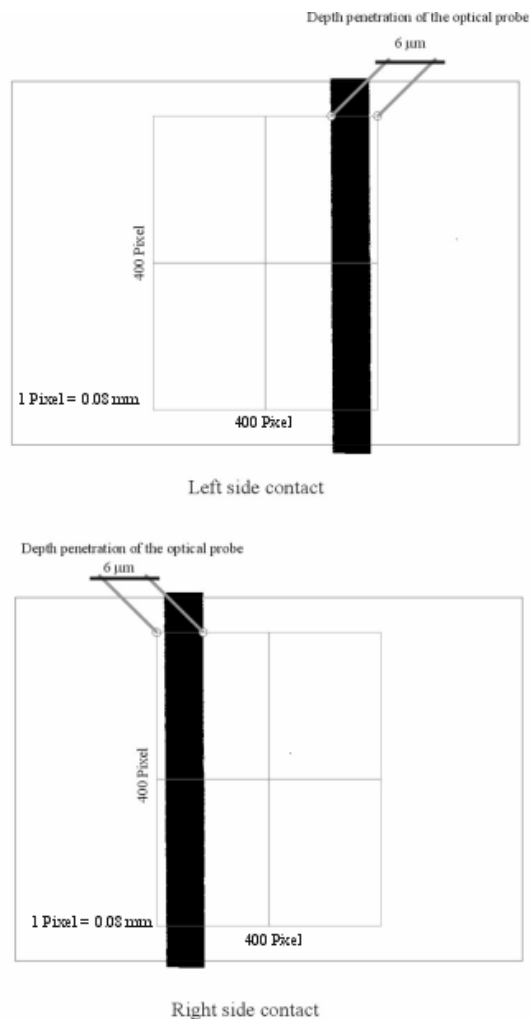


Fig. 1: The figure describes the way the position of the line was deduced from the image (a line of about $5\ \mu\text{m}$ width is shown in the image)

Measurement procedure

The equipment configuration from bottom up was: Moore carriage, vertical stage (height adapter up to Abbe condition in vertical), tilt and rotary stages, base support designed for the Airy support points of the linescale, linescale.

The applied procedure is the following:

The linescale is placed on the base support and is aligned (visually) with the measuring axis. Then, the alignment is improved by checking the focus and position of the line end on the video frame while displacing the artefact from the line „0“ up to the line „100“ and back (to be repeated several times).

With the automatic control of the Moore machine, no manual handling of the linescale is required to reset the equipment between each set of measurements.

The positions of the lines are then measured at the central section of the lines with a CCD image window length of about $80\ \mu\text{m}$.

The adopted measurement strategy is:

1. Every 5 mm line over 100 mm (31 runs);
2. Every 0.1mm line over first 1 mm (16 runs);

About half of the measurement runs have been performed with the linescale in the reversed orientation.

For each run the deviation from the nominal length is obtained from the average of forward and backward measurements of the line positions.

Ambient

Measurements have been carried out in a laboratory with air temperature control ($20 \pm 0.1^\circ\text{C}$). The table below gives the range of the ambient parameters during the measurement runs.

Ambient air temperature	19.96 – 20.08 °C
Pressure	99.7 – 100.8 kPa
Humidity	~ 50%

Air refractive index is calculated using the revised Edlen's formula; the ambient parameters are measured by a precision thermometer, a Rosemount barometer and a Mitchell igrometer. The CO₂ content is assumed to be 400 ppm.

B) Tabular description of the measurement methods and instruments

Line detection

Parameters	Parameters used for the measurement
Microscope type:	Nikon Optiphot 100S / Objective Leitz $\infty/0$ Plan 125X N.A. 0,80
Light source	<i>Halogen lamp - Illuminator Intralux 4000</i>
Wavelength(s)	<i>White light</i>
window length	<i>64 μm</i>
window width	<i>32 μm</i>
Detection mode	<i>Image processing of the 2D CCD image video frame</i>
Detection principle	<i>Left- and right-side line edge detection to determine the centre line position</i>
Sampling frequency (image/interferometer)	<i>15 frames/second; synchronous reading of signal and interferometer</i>
Edge detection criterion	<i>50 % level dark-white light intensity</i>
Edge detection short term repeatability (1s)	<i>4 nm</i>

Interferometric measurement

Parameters	Parameters normally used for the measurement equipment	Achievable measurement uncertainty for measurands
Interferometer light source / wavelength	Stabilized He-Ne laser / 633 nm	$7 \cdot 10^{-9} \cdot L$
Resolution of displac. Interferometer	10 nm	2,9 nm
Interferometer medium	Ambient air	
Refractive index:	calculated from ambient air parameters	$2,3 \cdot 10^{-8} \cdot L$
=> refractometer:		

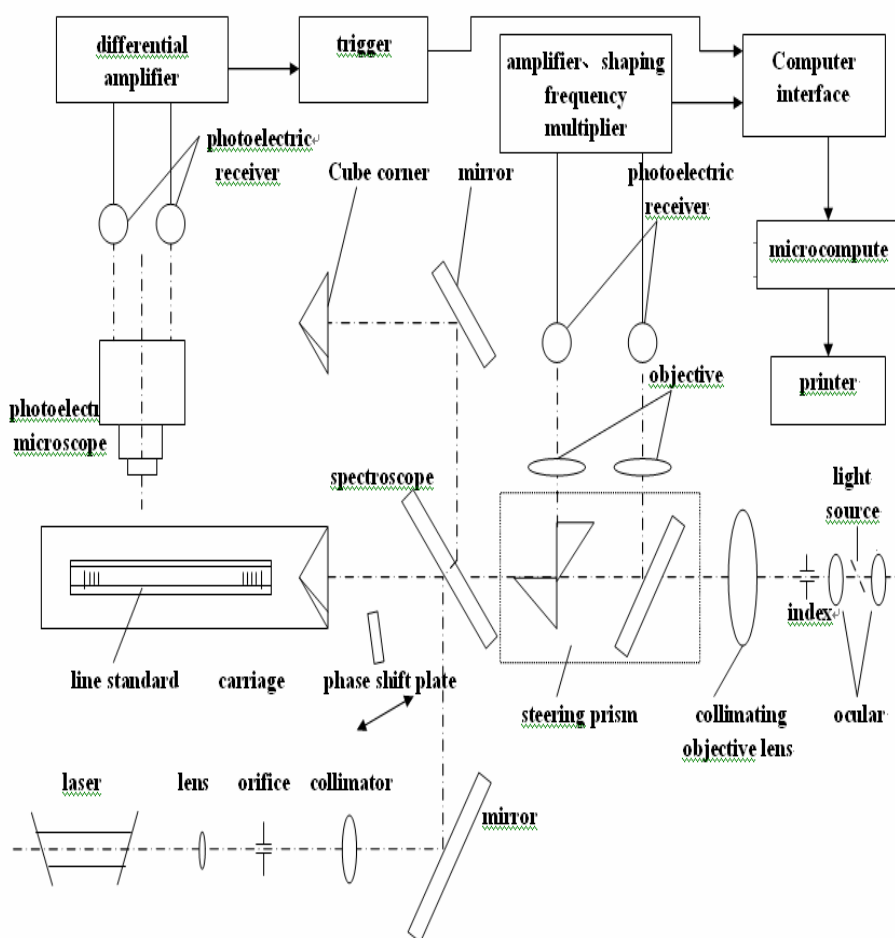
=> Edlen's formula:	revised Edlen's Formula	
Air temperature	20±0,1°C, precision thermometer	
Air pressure	~ 100 kPa, Rosemount barometer	
Air humidity	~ 50%, Mitchell igrometer	
CO ₂ -content	Assumed to be 400 ppm	

Other measurement conditions

Parameters	Parameters normally used for the measurement equipment	
scale orientations	0° and 180°	
kind of support	<i>Airy support base</i>	
clean room class	<i>Not classified – laboratory with filtered air</i>	

NIM China

The line scale standards of No:2 was measured in Gauge Block and Line Scale Laboratory, Length Division, NIM. The comparator used for comparison measurement is made by NIM, which consists of He-Ne Laser with the wavelength 633 nm, main Interferometer, optical-electronic microscope, moving table, driving system, base, temperature measuring system, electronic part, computer and software. The interferometer is Michelson type with resolution of 80 nm. The optical-electronic microscope uses dual slit to detect line position. Because the scale is transparent, the transmission light was used. Measurement starts from first line and continues till last line.



The principle diagram of Line Scale interference comparator

It took two weeks to finish total measurement. The kind of support is line contact. Four supports were used, whose positions were on the Bessel points marked on the scale. The scale was in series with the main beam path of interferometer with Abbe-error free. Scales were measured in two orientations. In one orientation two repeating measurements were made as one group. Then scale was reinstalled in reverse orientation and the instrument was readjusted such as focus and alignment and so on to eliminate possible system error. 48 groups of measurements were made, which means the Number of measurement of each scale is 96. The end result is the average of total measurement.

Measuring environment condition is as following:

Measuring place:	normal laboratory room
Room temperature:	20C±0.1C
Scale temperature:	20C±0.1C
Humidity:	normal
Air pressure:	1015.5Pa±3.0 Pa

NIST USA

The 100 mm scale was measured with the NIST Line Scale Interferometer (LSI). The LSI consists of a scanning electro-optical line detector, a high precision one-axis motion system, and a high accuracy heterodyne interferometer for determining the displacement of the test artifact beneath the line detector. The wavelength of a stabilized helium-neon laser corrected for temperature, humidity, atmospheric pressure and CO₂ is used as the length standard. The instrument is housed in an environmental chamber in which all environmental properties are carefully monitored. The complete description of the design and operation of the NIST LSI is given in the Journal of Research of the National Institute of Standards and Technology Volume 104, Number 3, May-June 1999, .. *The NIST Length Scale Interferometer*. ..

Reflected light was used to obtain line images. The scale was measured in the horizontal position with scale face up and supported at the Airy points. The scale was laid on a flat glass surface, supported at left in the center at a single point with a 6 mm diameter, 0.1 mm thick paper pad and the scale was supported at the right at two points, at the edges of the scale with similar pads. This support was used to avoid slippage of the scale, due to inertia during measurement, and the three point support prevents a twisting force on the scale as well as allowing free expansion and contraction of the scale.

On the 100 mm scale there were two independent measurements. From zero to 1 mm with 0.1 mm steps and from zero to 100 mm with 5 mm steps.

Measurements were made from line center to line center using a graduation line segment of 50 μm long, in the center of the two horizontal alignment lines as indicated on page 11 fig.3 of the Technical Protocol document. Data was recorded by averaging 400 interferometer readings when the scale was stopped and servo-locked at each measured graduation line.

The environmental chamber and scale temperatures were held within ±0.005 °C of 20 °C during the measurements. The air temperature was measured close to the path of the interferometer laser beam and scale temperature was measured at three locations along the scale and the mean temperature was used for scale length corrections. The lengths are reported at a temperature of 20 °C (68 °F). A coefficient of linear thermal expansion of $5.1 \times 10^{-7} / ^\circ\text{C}$ for the quartz scale were used in normalizing the lengths to 20 °C. During measurements the average atmospheric pressure was 99825 Pa and the average relative humidity was 50 %.

Tabular description of the measurement methods and instrumentsLine detection

Parameters	Parameters used for the measurement
Microscope type:	Scanning photoelectric microscope (See Ref. #1 p. 230)
Light source	White light
Wavelength(s)	$\approx .7$ to $.4 \mu m$
Slit length (mask)	0.08 mm
Slit width	0.1 mm
Polarization	none
Coherence	NA
Aperture/magnification	100
Detection mode	Line image detected by photo multiplier
Detection principle	The left and right line edges are simultaneously detected and the line center derived by the servoing line detector circuit. (See Ref. #1 p. 230-231)
Detection velocity	0
Sampling frequency (image / interferometer)	400 readings / sample
Edge detection criterion	Edges are detected at the 50 % intensity level. (See Ref. #1 p. 232)
Edge detection short term repeatability (1s)	1 nm or less

Displacement measurement

Parameters	Parameters normally used for the measurement equipment	Achievable measurement uncertainty for measurands
Interferometer light source / wavelength	0.6329913311 μm	1.2×10^{-8}
Resolution of displacement Interferometer	1 nm	
Interferometer medium	Air	
Refractive index:		
=> refractometer:	NA	
=> Edlen's formula:	Revised 1994	2×10^{-8}
Air temperature	20.000 °C \pm 0.005 °C	0.001°C
Air pressure	99000 to 101000 Pa	4 Pa
Air humidity	20 to 50 %R.H.	1.2 %
CO ₂ -content	400 ppm	25 ppm
Guide error	1.5 arc sec / m	0.1 arc sec
Abbe offset	Negligible	0.2 mm
Alignment error:	0.06 arc sec	
Interferometer	H.P. 10565 interferometer	1 nm
Scale	1 m length	100 nm / m

Other measurement conditions

Parameters	Parameters normally used for the measurement equipment	Achievable measurement uncertainty for measurands
Scale temperature	20.000 °C ± 0.005 °C	0.001 °C
Number of repeat measurements in one scale position	4 measurements	
Number of scale orientations	2 orientations	
Kind of support	The scale is supported at the Airy points, on a wedge at one point and on a (one point supported) roller at the other point.	
Clean room class	Class 10000	

NMi-VSL Netherlands

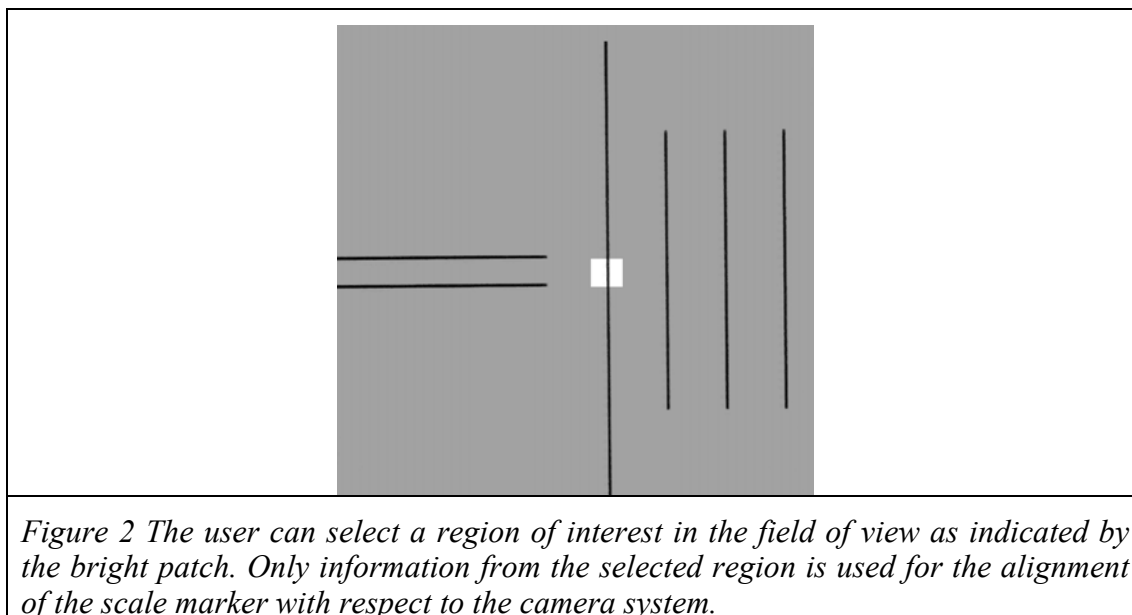
Measurement set-up.

The line scale has been measured with the set-up shown in figure 1. The set-up consists of a SIP 400 measuring machine of which only the 400 mm travel of one of the axis is used for line scale calibrations. The alignment procedure and actual measurement is performed by manually adjusting the positions.



Figure 1 Overview of the line scale calibration set-up. The line scale is positioned on a specially designed translation stage (1b) of a SIP 400 length measuring machine (1a). The structures on the scale are visualized using a video camera (2a) and a video monitor (2b). After data processing of the video signal (2c) several control signals are displayed (2d) and used for alignment of the scale with respect to the camera. The position of the scale relative to the camera is measured using a laser interferometer (3a,3b) and stored on a computer (3c). Ambient conditions are constantly monitored and up to 10 sensors can be using to record (4a,4b) the temperature of critical components.

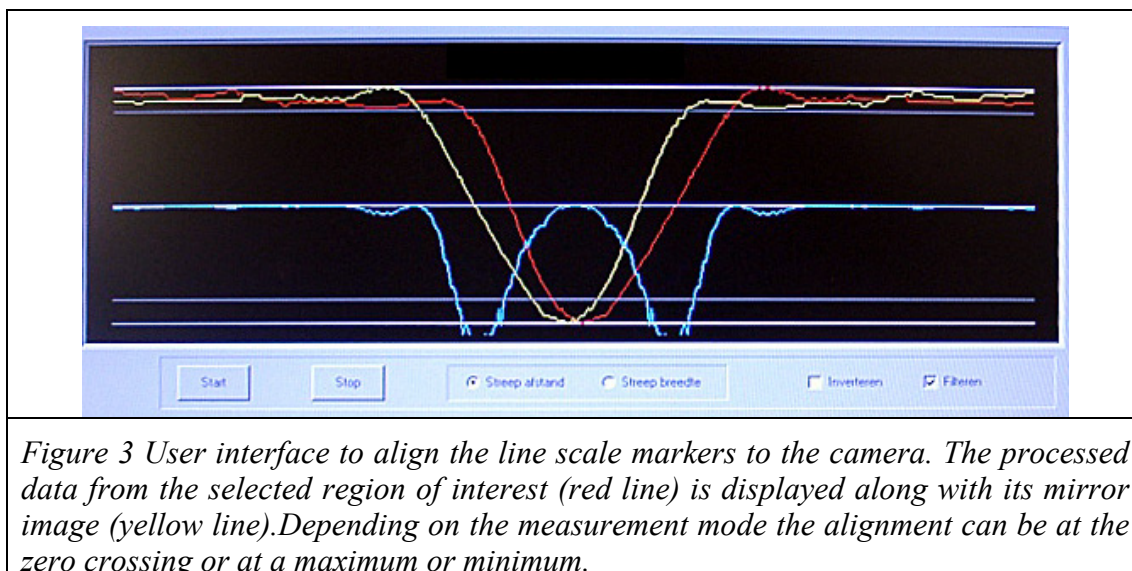
The original translation platform of the SIP 400 is replaced by a temperature controlled stage. The line scale and the retro mirror of the measurement arm are positioned onto an invar plate that is attached to the temperature controlled stage. The L-K7 line scale was supported on its Airy points.



The markers on the line scale are imaged using a CCD camera and a video monitor. A 1000 x magnification is used to image the L-K7 scale structures. In order to obtain a picture of sufficient quality additional illumination is required that is provided by optical fiber along the camera mount. To minimize heating of the scale, the amount of light is controlled to a minimum.

The SIP table with the line scale is translated manually while the movement of the table is measured by a laser interferometer.

The alignment of the scale markers to the video camera is performed by processing the camera signal with a frame grabber and a computer. In the field of view the user can select a region that will be used for the measurement, see fig. 2. The image in the selected region is processed by averaging all image lines, normalizing the result and displaying this averaged information and its mirror image on a computer screen. Accurate alignment on a line scale marker is performed by maximizing the overlap of the averaged information and its mirror image, see figure 3.



The alignment can be optimized by maximizing the overlap of the two signals. When the operator has adjusted the position of the scale to optimized alignment the data from the laser interferometer is transferred to a second computer.

The temperature of the air, line scale and SIP are continuously monitored during the calibration with a separate temperature measurement set-up. This set-up allows sequential recording of up to 10 temperature sensors. The temperature of the scale has been measured by positioning two thermistors on the scale surface above the Airy points. The thermistors were held by gravity without additional clamping. In order to keep the scale as clean as possible no thermally conductive paste was used to improve the thermal contact.

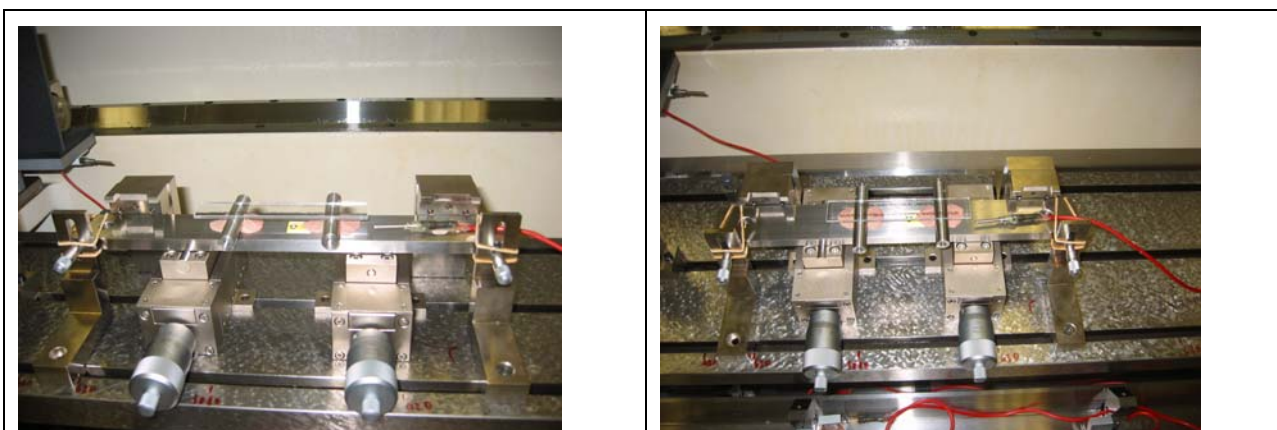
The alignment of the scale to the SIP is performed using the horizontal line structures at the left and right of the L-K7 scale. The alignment of the scale to the camera is optimized by matching the direction of the horizontal and vertical scale structures to software generated horizontal and vertical reference lines on the computer monitor. Final adjustments are optimized by rotating the line scale and/or camera and minimizing the vertical shift of the left and right horizontal lines while the scale is translated along its length.

Measurement procedure

The scale is measured both in the forward direction (0 mm to 100 mm) and in the backward direction. The center line position of the reference line (0 mm) is measured before each of the center line position of the line to be measured. During the acquisition the temperature of the air and of the scale, the air pressure and humidity are constantly monitored. These values are periodically updated when necessary (as judged by the operator) in the acquisition program for the laser interferometer. For this comparison the entire measurement has been repeated three times.

Analysis:

The analysis of the measurement data from the laser interferometer consists of averaging the values from the forward and backward series. The repeatability for a single measurement (forward and backward) is based on calculating the variance with respect to the average value for each position. The uncertainty due to the repeatability has been calculated from the square root of the averaged variances for three measurements.



Alignment:

With horizontal and vertical micrometers, by observing the two main lines of the scale (at the beginning and the end) and the central one, trying to maintain in focus. For those less-in-focus lines, the optical system possesses autofocus.

NPLI India

The glass scale is fixed on sliding platform of universal measuring machine (UMM) Model – MUL -214 B (Make SIP- Switzerland). It is aligned along the 50 μ m wide parallel lines looking into locating microscope of UMM. A heterodyne laser interferometer (LI), Model - Universal calibrator 5529A, (Make Agilent-USA), is set on the sliding platform of UMM to obtain measurements of graduations of glass scale.

The edges of the desired nominal graduation are detected by looking into locating microscope. Repeatedly, laser Interferometer is initialized at zero mark on the glass scale, then the platform of UMM is moved to locate nominal graduation of the glass scale under the locating microscope of UMM. The corresponding readings are measured by the LI and evaluated to determine the deviation (dL) from each nominal length.

NRC Canada

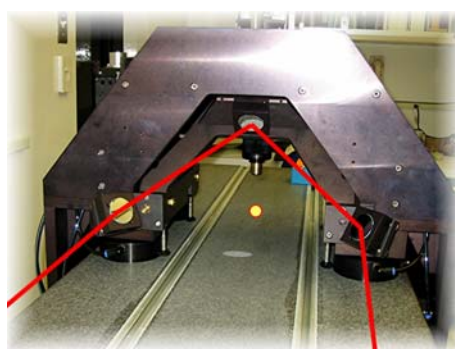
The scale was measured on the **NRC 4-metre Line Scale Comparator**. This instrument has a granite bed (L,W,H = 4500,500,800 mm) with top and side surfaces lapped flat & straight. The aluminum carriage rides the length of the bed on air bearing pucks and is constrained by opposing air pucks that press against both sides of the bed. An HP heterodyne laser interferometer measures the displacement of the carriage, and a motor drive can position the carriage to within 1 μm of a requested position from the host computer.



Line Scale Set-up & Viewing: A fixed CCD camera/microscope is mounted on the carriage looking vertically down to a focus point 100 mm above the bed. Line scales to be measured are supported at this elevation above the bed, and are fine adjusted to be level and in focus during set-up by manual elevating jack/tilting screws. The line scales are also moved sideways with respect to the focus point, to centre the linescale measurand axis to the focus-point trajectory made as the carriage moves along the bed. Special jigs with these adjustment motions hold a long scale comprised of a rigid beam at the Airy support points, whereas short scales on thin substrates, such as microscope micrometer scales, are placed flat on an elevated glass-plate platform that allows either transmitted or reflective illumination.



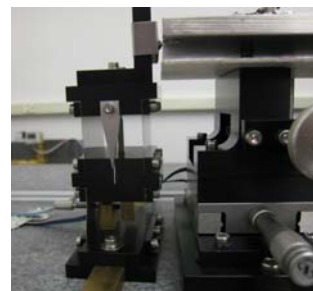
For K7, the NRC Airy-point fixtures were not suited to directly support the 100 mm scale on its Airy points, and so it was simply laid flat on the invar platform support and fixed with plastic putty at its sides.



Displacement Interferometer: The carriage displacement interferometer uses an 'open cube-corner' design that allows the interferometer measuring point to coincide with the microscope viewing point, and thereby minimize Abbe error due to carriage motion error. On the front of the carriage are 3 small plane mirrors arranged to form the open cube-corner retroreflector, with its vertex made to coincide to with the microscope focus point. The HP interferometer optics are organized at one end of the granite bed. The displacement-measuring beam is directed along one side of the bed to the carriage, where it makes the succession of

reflections off the 3 mirrors and retro-reflects back down the bed along the opposite side: the coming & going beam paths are separated by 200 mm, so that large line scale objects up to 4 metres long can be laid between them. At the interferometer end of the bed is a small stationary cube-corner prism that reverses the path of the measuring laser beam, sending it back to the

carriage, traversing the 3 mirrors, and then back into the interferometer optics where it mixes with the reference laser beam to form the interferometer displacement signal. Thus the measuring beam makes a double-pass to measure the carriage displacement along the bed. The interferometer reference beam is also turned by a retro prism, but it also makes a double pass up-and-down the bed, this time up the middle to a plane mirror on a flexure anchored to the bed and contacting the end of the line scale to be measured: in this way the interferometer reference (zero) is coupled to the zero of the line scale with the smallest material 'deadpath' between them, and automatically compensates for any mechanical shift of the scale during measurement.



For the K7 scale mounted to the invar plate, the interferometer reference-arm retro-reflector was made to spring-contact the end of the invar plate.

Displacement Corrections: Sensors measure the air temperature, pressure and humidity to correct the laser wavelength in air, and also measure the line scale and the granite bed temperature to correct for material thermal dilatation. An autocollimator monitors the carriage motion error (pitch and yaw) so that residual Abbe corrections can be applied to the carriage displacement measurements.

Data Collection: The host computer executes a script of positions to visit along the scale, via the carriage motor drive. At each position the carriage is stopped and allowed to settle, then the CCD microscope image is recorded (actually, an average of 10 successive video images), along with the interferometer reading of the actual carriage position (actually, an average of 30 or more readings taken during the video capture) as well as all the sensor and autocollimator readings, plus a time/date stamp. This allows fast collection of data to minimize drift, and then processor-intensive offline analysis of recorded data runs can be done repeatedly and at leisure, allowing exploration of changes to analysis model parameters.

Line Center Algorithm: The CCD camera captures the microscope image at high magnification (typically 250 nm/pixel), and so the 50 μm ROI (region-of-interest) 'slit height' for K7 corresponded to 200 CCD lines in the image. The NRC target-center algorithm is based on the mean of left and right edge detection. The left and right edge of the intensity profile along each CCD line in the ROI was determined using a dynamic 50% threshold criterion, and the mid-position is calculated. A straight line, with outlier rejection, was fitted through the 200 mid-position points that spanned the height of the ROI (rejecting edge roughness or contamination artifacts better than a simple average), and the mid-height position of the fitted line was reported as the effective line centre.

Camera as Null Detector: As much as possible, line centres were always determined at same central location in the CCD image for every scale line, so that measured location of each line on the line scale depended only on the carriage displacement measurement by laser interferometer, and not the magnification scale factor of the CCD image. This was accomplished by moving the carriage in five small (3 μm) successive steps about the expected carriage position that put the desired scale line in the nominal centre of the CCD image: the carriage position was measured at each step (via the laser interferometer) and the image recorded. In offline analysis, the line image center was determined for each step, expressed in camera pixel coordinates, and a trend line fitted through line-image position (in pixels) vs. carriage position (in millimetres), to calculate the effective carriage position corresponding to that line imaged at the exact center of the camera field (pixel 320.00 in a 640 pixel field). This was done for every scale line in the same way, so that most residual systematic errors would be common-mode constants that cancel when all line positions are expressed relative to the zero-line. The residuals about the 5-point line fit were

typically less than 2 nm, suggesting that the fitted line centre location was consistent and repeatable to better than 2 nm.

Data Run Design: The script, or list of required measurement positions, is created offline in MS Excel. For the K7 scale, the list consisted the 30 prescribed lines plus the zero line. After the 100 mm line measurement, the carriage was driven 5 mm further, before reversing direction and measuring the 31 lines in reverse order. After returning to measure the zero line, the carriage was driven an additional 2 mm backwards, and then driven forwards to re-measure the zero line a final time in the data run, taken in the same direction as the first measurement, so as to reveal the closing error under hysteresis conditions. Thus, a K7 data run consisted of $31 + 1 + 31 + 1 + 1 = 65$ lines. This describes data runs in the normal orientation of the scale (from 0 to the 100 mm line). A script was also designed for measuring the same lines when the scale was oriented in the reverse sense, starting a run at the 100 mm line and sequencing to the 0 line position, and then back to the 100 mm line (with the additional turn-around points as in the normal-orientation case.) Within a given data run, the forward-back repeatability of a given scale line location was the order of 20 nm, suggesting some drift problems, but differences the order of 100 nm were observed between normal and reversed orientation runs, as discussed below.

Data Runs for Reported Results: The results in the Table are the simple average of a normal-scale run, a reversed scale run and a 2nd normal scale run.

Observed Problems and Uncertainty: The NRC 4-metre Line Scale Comparator is still under development and has not yet achieved its expanded uncertainty performance goal of $U = Q[20 \text{ nm}, 0.2 \text{ ppm L}]$, where $Q[a,b]$ is the quadrature sum of a & b, and L is the distance between two scale lines (95% confidence interval). This uncertainty goal is the value expected when one applies a GUM model analysis to the customary influence factors for this type of comparator instrument, evaluated at the performance level of the modeled NRC instrument constituents.

However, during K7 data runs it was observed that after all corrections for environment, set-up and motion errors, there were still large differences between successive data runs and even larger between the normal and reverse data runs, calling for an increase in uncertainty to $U = Q[80 \text{ nm}, 0.4 \text{ ppm L}]$ to account for the variations in the data runs. The source of the run-to-run and of the normal-to-reverse variations has not been identified yet, but may be due to failure to support the scale on the Airy points (causing unmodeled irregular bending distortions) and/or unmodeled thermal drift in the way the quartz scale is supported and fixed on the invar carrier, subject to illumination heating, and shifts/drifts in the coupling of the scale zero-line and the reference retro-reflector. NRC is investigating this aspect. Meanwhile, for the purpose of the K7 Report, NRC is not submitting a detailed GUM uncertainty model analysis while there exists such large rogue factors that dominate the performance.

NIMT Thailand

Principle of measurement:

Graduated scales of the glass scale are measured using line scale interferometer. The light source is, wavelength 633 nm passes through the vacuum chamber and bellow.

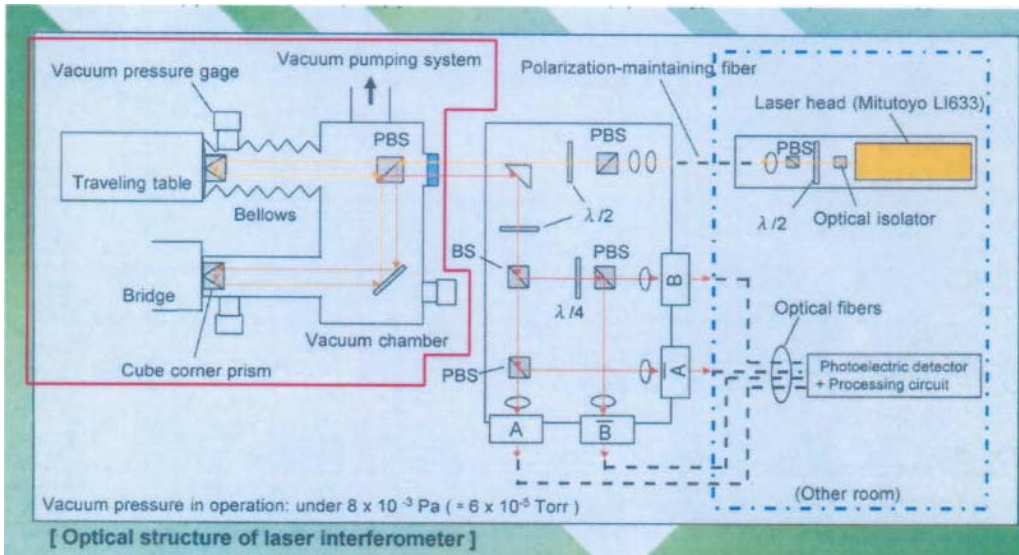


Fig I. Diagram of vacuum laser interferometer system

Resolution of the laser interferometer is approximately 0.8 nm (Referred to the manufacturer), which was calculated from $(633 \text{ nm} \times 1/2 \text{ (optical part)} \times 1/400 \text{ (electronic part)}) \cong 0.8 \text{ nm}$

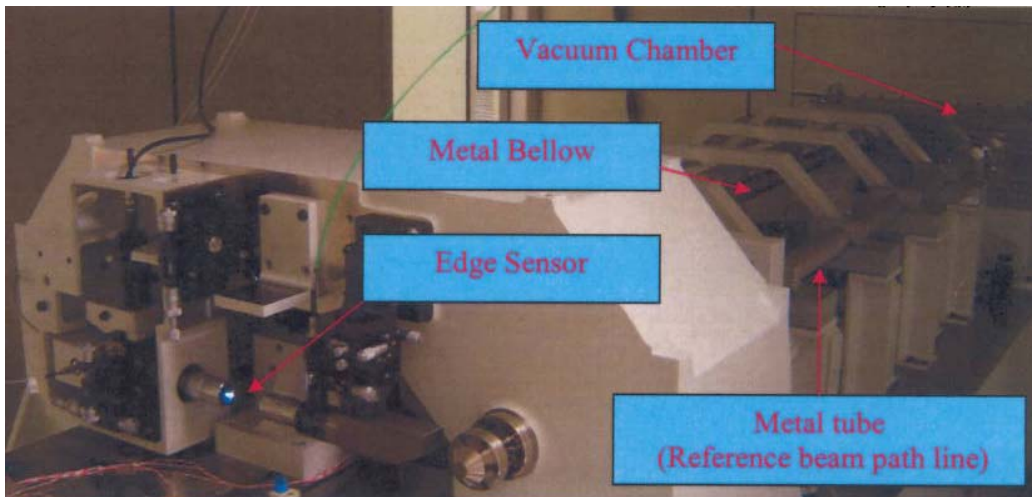


Fig2. The system of the laser interferometer

Graduated scales are detected by Edge sensor. Using triple slits system as show in Fig3.

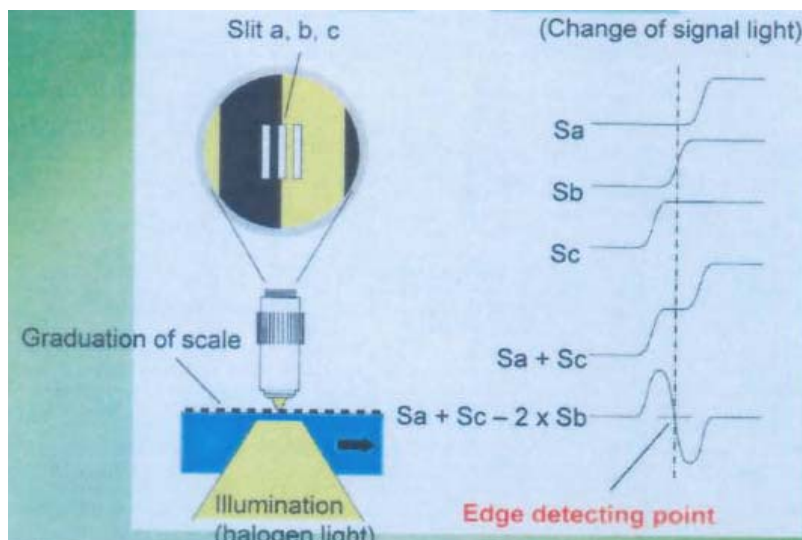


Fig3. Principle of Edge sensor

Resolution of Edge sensor is approximately 0.64 nm (Referred to the manufacturer).



Fig4. Edge sensor detection

Measurement setup:

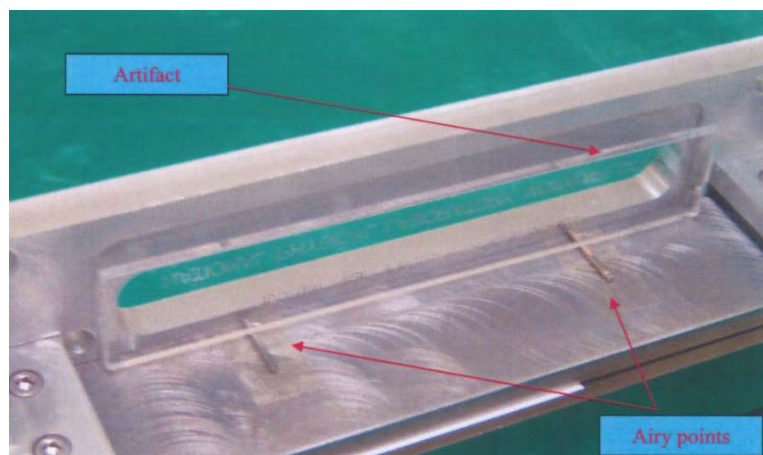


Fig5. Support and setting

Temperature measurement:

Due to artifact is small, the temperature is measured at the standard scale instead.

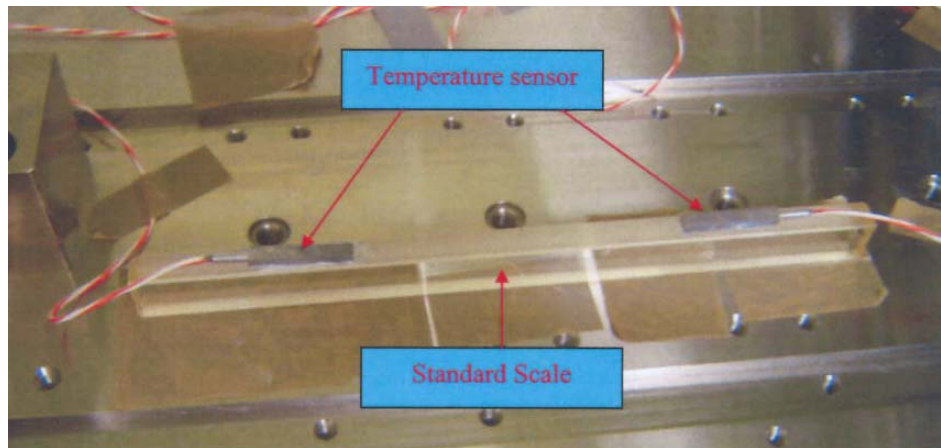


Fig6. Temperature measurement

Temperature measurement by:
Precision Thermometry Bridge with probe
Mfr: ASL, Model: F 300, Serial number: 00780303

VNIIM Rusia

An optical scheme of the comparator (Fig.1) consists of a laser polarization interferometer, a refractometer and a microscope. Parts of the laser interferometer and refractometer are fixed on a granite base. A carriage is moved over teflon supports at a distance of 1 m. As the carriage moves its rotation is not greater than $5 \mu\text{rad}$. Two reflectors of the interferometer and the confocal microscope are mounted on the carriage. The microscope focus is located on the measurement axis of the interferometer.

In the microscope there are a laser diode with a wave length of 540 nm and an objective with an aperture of 0.9. An illuminator of the microscope forms an illuminated strip with a width of $1 \mu\text{m}$. Light is reflected and forms the image in a photodiode. The length of the slot corresponds to $50 \mu\text{m}$ in the plane of a scale.

One of the two modes ($\Delta = 640 \text{ MHz}$) of the stabilized He/Ne laser is used in the interferometer, the second one is applied in the refractometer. A refractive index is measured in the process of pumping out a chamber of 1 m in length with air. Both the refractometer and interferometer have two photo diodes providing to shape the signals with a phase shift of 90° .

The scale is located on two piezo-supports. Focusing is controlled by a signal from the microscope. The measurement zone is closed by a thermal screen. Alongside the scale a platinum thermometer (10 Ohm) is located. The difference between the temperature of the scale and that of the platinum thermometer is measured with a set of differential thermocouples. The temperature inside a room is kept at a level of $20 \pm 0.1^\circ \text{C}$.

Output signals of the photo-detectors of the laser interferometer, refractometer and microscope enter the computer that is equipped with an analogue-to-digital converter with a multiplexing unit at its input.

A phase of the interference signal is calculated as *arctg* of the ratio of the signals of two photo-detectors. Parameters of the input signals are corrected. The coordinates of the scale graduation line centers are calculated at the time of joint processing of the microscope and interferometer signals. A center of gravity is calculated for that part of the graduation line profile, which is situated between the levels of 25 and 40 % of a maximum level of the signal.

Measurements are done in a dynamic mode. When the microscope is moving over the graduation line the speed of the carriage is decreased (0.05 mm/s).

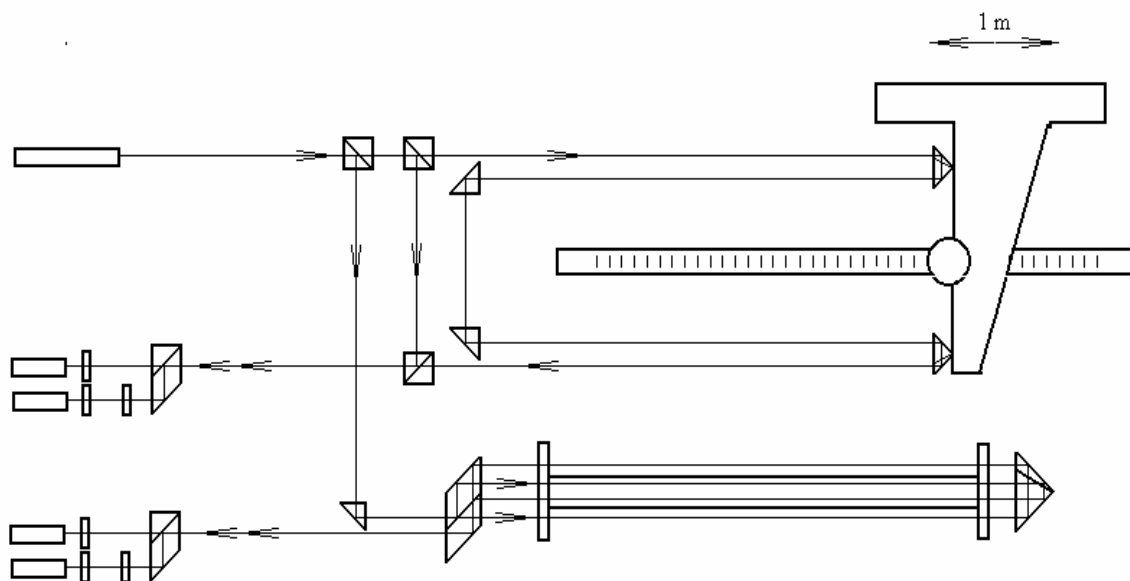


Fig.1 Optical scheme of the comparator.

Appendix 3: Reported uncertainty budgets

GROUP 1

BEV Austria

Input quantity x_i	Distrib.	$u(x_i)$ unit	ν_i	$c_i = \partial dL / \partial x_i$	u_i (dL)
p_{air}	N	15 Pa	∞	$2.7 \cdot 10^{-9} \text{ Pa}^{-1} L$	$0.04 \cdot 10^{-6} L$
t_{air}	N	0.15 °C	∞	$0.96 \cdot 10^{-6} \text{ °C}^{-1} L$	$0.14 \cdot 10^{-6} L$
c_{CO_2}	N	300 ppm	∞	$0.14 \cdot 10^{-9} \text{ ppm}^{-1} L$	$0.04 \cdot 10^{-6} L$
n_{air}	N	$5 \cdot 10^{-8}$	∞	1	$0.05 \cdot 10^{-6} L$
t_{S}	N	0.1 °C	∞	$0.5 \cdot 10^{-6} \text{ °C}^{-1} L$	$0.05 \cdot 10^{-6} L$
barometric compression δL_{κ}	N	$0.026 \cdot 10^{-6} L$	∞	1	$0.026 \cdot 10^{-6} L$
residual contributions δL_{res}	N	5 nm	∞	1	5 nm
line pos. & Abbe & orient.	N	22 nm / 109 nm	4	1	22 nm / 109 nm
<p>These errors can not easily be separated in our scheme. We use the standard deviation of 5 different calibrations (maximum of all lines) as explained on page 1 of this report.</p> <p>Values are for the 1 mm and 100 mm range, respectively.</p>					

Since all contributions except the last one amount to only $Q[5 \text{ nm}, 0.17 \cdot 10^{-6} L]$ it is tempting to assume a constant, length independent measurement uncertainty. Since the calibration procedure is somewhat different for short range ($< 8 \text{ mm}$, mainly stage micrometers) and long range scales ($> 8 \text{ mm}$) we use two constant uncertainties. The smaller one is valid up to 1 mm, the second one from 5 mm to 100 mm.

Combined standard uncertainty: $u_c(L) = 23 \text{ nm} / 111 \text{ nm}$ (@ 1 mm / @ 100 mm)

Effective degree of freedom: $\nu_{\text{eff}}(dL) = 4 / 4$

Expanded uncertainty: $U_{95}(dL) = 65 \text{ nm} / 320 \text{ nm}$

CMi Czech republic

<i>Input quantity x_i</i>	<i>Distrib</i>	$u(x_i)$	v_i	$c_i = \partial dL / \partial x_i$	$u_i (dL) / \text{nm}$
Resolution of edge detection	N	1.5 nm	1000	1	2 nm
Repeatability of edge detection	N	5 nm	30	1	5 nm
Interferometer resolution	N	0.1 nm	1000	1	0 nm
Interferometer nonlinearity	N	1.0 nm	100	1	1 nm
Interferometer dead path influences	N	0.8 nm	1000	1	1 nm
Drift influence	N	0.8 nm	100	1	1 nm
Influence of adjustment of measurement line + Nonlinearities of position sensing	N	10 nm	20	0.577	6 nm
Microscope axis - illumination alignment + defocusing	N	5 nm	10	1 nm/um	5 nm
Influence of line edge detection algorithm, possible asymmetry of line profiles and shape	N	10 nm	20	1	10 nm
Microscope magnification (or other position deviation sensing device)	N	0.1 nm	20	138.0 nm/pix	7 nm
repeatability of scale preparation (bending by fixing, cleaning, ...)	N	12 nm	3	0.577	7 nm
δl_{win} Influence of adjustment of measurement window or slit length	N	5 nm	5	0.707	4 nm
Errors due to Abbe offsets and pitch and yaw of translation stages at one position)	N	1 nm	1000	1	1 nm
total constant part of u					17 nm
v_{eff}			58		

Possible contributions from interferometric displacement measurement technique:					
λ_0 vacuum wavelength of light source used for displacement measurement	N	5.0E-11	1000	1	5.0E-11
n_{air} Index of refraction of air2	N	1.0E-08	1000		
t_{air} Air temperature	N	1.0E-02	20	9E-7 /K	9.0E-09
p_{air} Air pressure	N	5E-2 hPa	1000	2E-7 /hPa	1.2E-08
RH_{air} Air humidity	N	1.0E-02	1000	1E-8 /%	1.0E-10
c_{CO2} Air CO2 concentration	N	100 ppm	1000	1.5E-10/ppm	1.5E-08
δl_{Ai} Errors due to Abbe offsets and pitch and yaw of translation stages	N	1.7E-07	1000	1	1.7E-07
δl_{Si} Errors of scale alignment	N	2.5E-09	1000	1	2.5E-09
δl_{Ii} Cosine errors of interferometer alignment	N	5.6E-09	1000	1	5.6E-09
systematic distortion of measurement frame with movement	N	5.0E-09	1000	1	5.0E-09
Possible contributions from scale properties:					
α_Z, Cr Linear coefficient of thermal expansion of scale material	N	0.0750 K	1000	1E-6/K	7.5E-08
κ_Z, Cr Linear coefficient of compressibility of scale material	N	750 Pa	1000	9.0E-12 /Pa	6.8E-09
δ_{supp} Influence of support conditions	N	2.3E-08	1000	1	2.3E-08
total relative part of u					1.92E-07
v_{eff}			1683		

Combined constant part of standard uncertainty for one line position: $u_c=17$ nm
Combined constant part of standard uncertainty for one line distance from zero line, for three independent measurement (including removal and re-alignment) $u_c=14$ nm

Combined standard uncertainty $u_c(L)=Q[14;192*L]nm, L$ in m

Effective degree of freedom: $\nu_{eff} = 58 ; 1683$

Expanded uncertainty: $U_{95}(L) = Q[28;377*L]nm, L$ in m

DZM Croatia

Input quantity x_i	Distrib.	$u(x_i)$ unit	ν_i	$c_i = \partial dL / \partial x_i$	$u_i (dL) / \text{nm}, L \text{ in mm}$
Stage:					
Error due to Abbe offset in z ($a_p < 0.5 \text{ mm}$) and pitch, δl_{Ap}	R	10	100	1	10
Error due to Abbe offset in x, y ($a_y < 1 \text{ mm}$) and yaw, δl_{Ay}	R	15	100	1	15
Interferometer:					
Interferometer wavelength, $\delta \lambda$	R	0,03	100	L	$0,03 \cdot L$
Air temperature, t_{air}	R	$0,12 \text{ }^\circ\text{C}$	100	$9,5 \cdot 10^{-7} L / ^\circ\text{C}$	$0,112 \cdot L$
Air pressure, p_{air}	R	13 Pa	100	$2,7 \cdot 10^{-7} L / \text{Pa}$	$0,035 \cdot L$
Relative Humidity, RH_{air}	R	0,06	100	$8,5 \cdot 10^{-7} L$	$0,050 \cdot L$
Edlen equation uncertainty, δn_{air}	N	$2 \cdot 10^{-8}$	100	L	$0,020 \cdot L$
Interf. cosine error δl_{li}	R	$0,8L$	100	1	$0,80 \cdot L$
Scale:					
Scale temperature difference from $20 \text{ }^\circ\text{C}$, Δt_s	R	$0,036 \text{ }^\circ\text{C}$	100	$5 \cdot 10^{-7} L / \text{K}$	$0,018 \cdot L$
Errors of scale alignment, δl_{si}	R	$0,55L$	27	1	$0,55 \cdot L$
Movement of scale due to bending, δl_{ai}	R	$0,2L$	100	1	$0,2 \cdot L$
Influence of line edge quality δE_{alg}	R	10	49	1	10
Measurement:					
Overall reproducibility, R	N	55	27	1	55
Interferometer resolution, δl_{res}	R	6	100	1	6
Reproducibility of line detection, S_E	N	35	27	1	35
Interferometer dead path influences, δl_{DP}	R	30	100	1	30

Combined standard uncertainty:

$$u_c(L) = (75 + 0,5 \cdot L) \text{ nm}, L \text{ in mm}$$

Effective degree of freedom:

$$\nu_{\text{eff}}(dl) = 211, \quad L = 100 \text{ mm}$$

Expanded uncertainty:

$$U_{95}(dl) = (150 + 1 \cdot L) \text{ nm}, L \text{ in mm}$$

GUM Poland

Input quantity x_i	Distrib.	$u(x_i)$ unit	ν_i	$c_i = \delta dL / \delta x_i$	$u_i(dL) / \text{nm}$
Line position sensing					
Repeatability of edge detection S_E	N	130,0 nm	7	1	130,0
Reproduceability S_R	N	1	7	L	L
Influence of adjustment of measurement line δ_{lpos}	N	30,0 nm	9	1	30,0
Interferometric displacement measurement					
Vacuum wavelength of light source used for displacement measurement λ_o	N	$2,45 \cdot \lambda_o$ nm	100	L/λ_o	$0,00245L$
Index of refraction of air n_{air}	N	$1 \cdot 10^{-8}$	100	L	$0,010L$
Air temperature t_{air}	N	51,6 mK	100	$9,57 \cdot 10^{-7} \cdot L/K$	$0,0494L$
Air pressure p_{air}	N	6,3 Pa	100	$2,68 \cdot 10^{-9} \cdot L/\text{Pa}$	$0,0169L$
Air humidity RH_{air}	N	0,462 %	100	$8,67 \cdot 10^{-9} \cdot L/RH\%$	$0,004L$
Air CO ₂ concentration c_{CO2}	R	57,7 ppm	100	$1,45 \cdot 10^{-10} \cdot L/\text{ppm}$	$0,0084L$
Interferometer resolution δ_{Res}	R	2,9 nm	100	1	2,9
Interferometer nonlinearity δ_{NL}	R	2,3 nm	100	1	2,3
Interferometer dead path influences δ_{DP}	R	8,1 nm	100	1	8,1
Errors due to Abbe offsets and pitch and yaw of translation stages δ_{Ai}	R	7,8 nm	100	1	7,8
Errors of scale alignment δ_{Si}	R	1,2 nm	100	L	$0,0012L$
Cosine errors of interferometer alignment δ_{Ii}	R	18 nm	100	L	$0,018L$
Scale properties					
Linear coefficient of thermal expansion of scale material α	R	$2,89 \cdot 10^{-8} / K$	100	$L \cdot 0,14 K$	$0,004L$
The difference of the scale temperature t_s in °C during the measurement from the reference temperature of 20 °C Δt_s	N	0,0173 K	100	$5 \cdot 10^{-7} \cdot L/K$	$0,0087L$
Linear coefficient of compressibility of scale material κ	N	$5,14 \cdot 10^{-13} / \text{Pa}$	100	$L \cdot 1170 \text{ Pa}$	$0,0006L$

Variations of air pressure during measurement	Δp_s	N	6,29 Pa	100	$8,9 \cdot 10^{-12} \cdot L / \text{Pa}$	$0,0001L$
Influence of support conditions	δ_{supp}	R	0,6 nm	100	1	0,6

Combined standard uncertainty: $u_c(L) = Q [134 ; 1,00 \cdot L]$ nm, L in mm

Effective degree of freedom: $\nu_{eff}(dl) = 181$ $L = 100$ mm

Expanded uncertainty: $U_{95}(dl) = Q [268 ; 2,00 \cdot L]$ nm; L in mm

INM Romania

Input quantity x_i	Distrib.	$u(x_i)$ unit	ν_i	$c_i = \partial dL / \partial x_i$	$u_i (dL) / \text{nm}$
repeatability of the measurement	normal type A	0.05 μm	19	1	50
thermal coefficient of expansion	rectangular	$0.5 \cdot 10^{-6} \text{K}^{-1}$	50	$L \cdot \Delta t$ $\Delta t = 0,5 \text{ } ^\circ\text{C}$	250L
temperature: -calibration of thermometer - reading error	normal type B trapezoidal	0.025 $^\circ\text{C}$ 0.003 $^\circ\text{C}$	8	αL	25L
comparator certificate	normal type B	0.05+0.1L, μm	10	1	50+100L
wavelength correction due to the environmental parameters	normal type B	0.022L, μm	50	1	22L
deviation of the flatness of the mirrors of retro-reflectors	rectangular	0.08 μm	50	1	46
cosines angle	rectangular	0.002L, μm	50	1	2L
time of data acquisition	rectangular	0.012 μm	50	1	12
Line scale alignment	rectangular	0.02 μm	50	1	20
Rotation of the carriage	rectangular	0.05	50	1	50

Combined standard uncertainty: $u_c(L) = [101,272L] \text{ nm}$;

Effective degree of freedom: $\nu_{\text{eff}}(dl) = 100$

Expanded uncertainty: $U_{95}(dl) = [202,544L] \text{ nm}$

LNMC Latvia

Input quantity x_i	Distrib.	$U(x_i)$ μm	ν_i	$c_i = \partial dL / \partial x_i$	$u_i (dL) / \mu\text{m}$
Reference scale $(0,03+2 \cdot 10^{-7}L)$ δl_s	N	0,030	>100	1	0,009
Repeatability l_R	R	0,7	>100	1	0,7
Scale resolution δl_X	R	0,2	>100	1	0,12
Influence of focal length variation $\delta_{E_{\text{foc}}}$	R	0,3	>100	1	0,17
Eccentricity coil of helical grid δl_u	R	0,2	>100	1	0,12
Difference in T between reference scale and comparator $T = \pm 0,3^\circ\text{C}$ $\alpha = (10,4 \cdot 10^{-6}) \delta t$	R	0,3	>100	$10,4 \cdot 10^{-6} L$	0,36
Deviation of the laboratory T from the reference scale $T = (20 \pm 2)^\circ\text{C}$ $\pm 0,1 \cdot 10^{-6} \Delta t$	R	2	>100	$0,1 \cdot 10^{-6} L$	0,012
Deviation of the laboratory T from the comparator $T = (20 \pm 2)^\circ\text{C}$ $\pm 0,1 \cdot 10^{-6} \Delta t$	R	2	>100	$0,1 \cdot 10^{-6} L$	0,012

Combined standard uncertainty: $u_c(L) = 0,823 \mu\text{m}$

Effective degree of freedom: $\nu_{\text{eff}}(dl) =$

Expanded uncertainty: $U_{95}(dl) = 1,647 \mu\text{m}$

METAS Switzerland

Name and symbol x_i (unit)	distrib.	$u(x_i)$	ν_i	for 100 mm		const	rel. to L
				$c_i = dl/dx_i$	$u_i(dl) / \text{nm}$	$u_i(dl) / \text{nm}$	$u_i(dl) / L$
Translation stage:							
Yaw of x-axis δ_{yaw} (μrad)	R	3.36	100	5.77E-07	1.12	1.12	
Pitch of x-axis δ_{pitch} (μrad)	R	3.36	100	2.89E-07	0.56	0.56	
Parameter: Abbe offset z δ_{Az} (mm)	R	0.5					
Parameter: Abbe offset x δ_{Ax} (mm)	R	1					
Interferometer:							
Vacuum wavelength λ_0 (nm)	N	5E-06	10	1.58E-01	0.79		7.9E-09
Air temperature t_{air} ($^{\circ}\text{C}$)	N	0.05	8	9.02E-05	4.51		-4.5E-08
Air pressure p_{air} (mbar)	N	0.05	4	2.68E-05	1.34		1.3E-08
Air humidity RH_{air} (%rel.)	N	0.75	4	8.50E-07	0.64		-6.4E-09
Air CO2 concentration c_{CO2} (ppm)	R	60	4	1.38E-08	0.48		4.8E-09
Edlen equation n_{air} (rel.)	N	1E-08	100	1.00E+02	1.00		1.0E-08
Interf. Deadpath δ_{DP} (mm)	N	10	10	1.55E-07	1.55	1.55	
Parameter: Change of n (1)	R	3E-07					
Interf. nonlinearity δ_{NL} (nm)	N	3	10	1.00E-06	3.00	3.00	
Interf. cosine error δ_b (μrad)	R	130	10	6.50E-09	0.49		4.9E-09
Imaging:							
Microscope magnification Mag (%)	R	0.2	10	1.15E+01	1.33	1.33	
CCD orientation $\delta \alpha_{CCD}$ ($^{\circ}$)	R	0.01	10	3.49E+01	0.20	0.20	
Parameter: x-positioning d_{pos} (μm)	R	2					
Image distortion δ_{Emm} (%)	R	0.05	10	6.00E+01	1.73	1.73	
Parameter: half linewidth HLW (μm)	N	6					
Microscope focus stage:							
Focal length variation $\delta_{E_{foc}}$ (μm)	R	0.2	10	1.00E-06	0.12	0.12	
Microscope alignment xz $\delta_{E_{align}}$ ($^{\circ}$)	R	0.12	10	3.49E-06	0.24	0.24	
Ref. mirror alignment xz $\delta_{R_{Malign}}$ ($^{\circ}$)	R	0.03	10	6.98E-05	1.21	1.21	
Pitch of z-axis zx $\delta_{E_{pitch}}$ ($\mu\text{rad}/\mu\text{m}$)	R	0.015	10	7.62E-05	0.67	0.67	
Roll of z-axis δE_{roll} ($\mu\text{rad}/\mu\text{m}$)	R	0.01	10	4.00E-06	0.02	0.02	
Parameter: focus-range dF (μm)	R	4					
Param.: Int. ref. beam offset (mm)	R	19.05					

Name and symbol x_i (unit)	distrib.	$u(x_i)$	ν_i	for 100 mm		const	rel. to L
				$c_i = dl/dx_i$	$u_i(dl) / \text{nm}$		
Scale properties:							
Scale alignment horiz. δ_{sh} (μrad)	R	40	10	2.00E-09	0.05		4.6E-10
Scale alignment vert. δ_{sv} (μrad)	R	100	10	5.00E-09	0.29		2.9E-09
Temperature deviation Δt_s (K)	N	0.05	10	5.00E-05	2.50		2.5E-08
Thermal exp. coef. α_s (1/K)	R	1E-07	10	7.00E+00	0.40		4.0E-09
Pressure variation s_{air} (mbar)	R	0.1	10	8.90E-08	0.01		-5.1E-11
Compressibility κ_s (1/bar)	R	2E-07	10	6.50E+00	0.75		7.5E-09
Scale support δ_{supp} (nm/100mm)	N	4	10	1.00E-06	4.00		4.0E-08
Measurement line def. δ_{pos} (μm)	R	5	10	6.05E-07	1.75	1.75	
Parameter: Line parallelity ($^\circ$)	R	0.06					
Line quality and evaluation δ_{eval} (nm)	R	3	8	1.00E-06	1.73	1.73	
Illumination inhomogeneity δ_{illum} (nm)	R	2	4	1.00E-06	1.15	1.15	
Measurement:							
Repeatability of line det. s_E (nm)	N	6	16	1.00E-06	6.00	6.00	
Total U_c (1S)					10.5	7.9	6.9E-08
Total U_{95}					21.0	15.9	1.4E-07
General expression:				$U_{95} = Q(16 \text{ nm} ; 1.4\text{E-}07 \cdot x)$			

In general for any length L :

$$u_c = Q(7.9 \text{ nm} , 6.9\text{E-}08 \cdot L)$$

$$U_{95} = Q(16 \text{ nm} , 1.4\text{E-}07 \cdot L)$$

with $Q(a,b) = (a^2 + b^2)^{1/2}$

For 100 mm:

Combined standard uncertainty: $u_c(L) = 10.5 \text{ nm}$

Effective degree of freedom: $\nu_{\text{eff}}(dl) = 70 \rightarrow k=1.99$

Expanded uncertainty: $U_{95}(dl) = 21.0 \text{ nm}$

MIKES Finland

Input quantity x_i	Distrib.	$u(x_i)$ unit	ν_i	$c_i = \partial dL / \partial x_i$	$u_i (dL) / \text{nm}$
Repeatability(all components of type A n=20)	Std.	20.0 nm	19	0.23	4.6
Influence of line detection algorithm with line quality, δE_{alg}	Std.	9 nm	4	1	9.0
Vacuum wavelength of laser, λ_0	Std.	4×10^{-9}	100	1 L m	4.0 L
Index of refraction of air, effect of equation, n_{air}	Std.	10×10^{-9}	100	1 L m	10 L
Air temperature, t_{air}	Std.	0.015 K	4	960 L nm/K	14 L
Dew point of air, DP	Std.	0.200 K	4	30 L nm/K	6.0 L
Air pressure, p_{air}	Std.	5.0 Pa	4	2.7 L nm/Pa	14 L
Air CO ₂ concentration, c_{co2}	Std.	50 ppm	4	0.2 L nm/ppm	7.5 L
Linear coeff. of thermal expansion, α	Std.	500 nm/m/K	1	0.020 L Km	10 L
Scale temp. difference from 20 °C, Δt_s	Std.	0.010 K	2	500 L nm/K	5.0 L
Error due to Abbé offsets; pitch and yaw, δl_A	Std.	3.0 nm/0.1m	4	1 L	30 L
Effect of diffraction of laser beam,	Std.	8 nm	2	1 L	8.0 L
Errors of scale alignment, δl_s	Std.	1 nm	10	1 L	1.0 L
Effect of compressibility, K	Rect.	0.020 bar	4	900 L nm/bar	18 L
Effect of flatness dev. of the scale & microscope alignm., δh	Std.	5 nm	3	1	5.0

Combined standard uncertainty: $u_c(L) = Q[11.3; 45 L]$ nm, L in meters

Effective degree of freedom: $\nu_{\text{eff}}(L) = 12 \Rightarrow k=2.2$

Expanded uncertainty: $U_{95}(L) = Q[25; 99 L]$ nm, L in meters

For lines 0.1; 0.4; 85; 90 and 95 mm the uncertainty due to line quality is higher than in the above budget based on non-idealities seen in the visual inspection (see receipt confirmation report from MIKES). The estimated expanded uncertainties for these lines are 54; 54; 55; 55 and 55 nm respectively.

MIRS Slovenia

Input quantity x_i	Distrib.	$u(x_i)$	ν_i	$c_i = \partial dL / \partial x_i$	$u_i(dL)$, nm, L in mm
wavelength drift, ΔL	R	$2,4 \cdot 10^{-9} \cdot L$	4	1	$2,4 \cdot 10^{-9} \cdot L$
Counting system	R	$5 \text{ nm} + 2,5 \cdot 10^{-8} \cdot L$	3	1	$5 \text{ nm} + 2,5 \cdot 10^{-8} \cdot L$
Correction factor	R	$2,5 \cdot 10^{-8} \cdot L$	3	1	$2,5 \cdot 10^{-8} \cdot L$
Wavelength correction for environmental influences, λ_{cor}	R	$2,8 \cdot 10^{-7} \cdot L$	3	1	$2,8 \cdot 10^{-7} \cdot L$
uncertainty of determination of the scale mark center, s	R	26 nm	100	1	26
distance between the measurement and reference position in the video window, L_v	N	25 nm	100	1	25
LI indication in reference position, $L_{L\text{ref}}$	N	25 nm	100	1	25
linear temperature expansion coefficient, α_m	R	$1,15 \cdot 10^{-6} \text{ }^\circ\text{C}^{-1}$	100	$1 \text{ }^\circ\text{C}^{-1} \cdot L$	$1,15 \cdot 10^{-6} \cdot L$
temperature deviation, θ_m	N	$0,1 \text{ }^\circ\text{C}$	100	$0,2 \cdot 10^{-6} \text{ }^\circ\text{C}^{-1} \cdot L$	$0,2 \cdot 10^{-7} \cdot L$
cosine error, e_{cos}	N	0	100	1	0
random error caused by uncontrolled mechanical changes, e_{ems}	N	29 nm	100	1	29
measuring table inclination, e_a	R	30 nm	100	1	30

Combined standard uncertainty:

$$u_c(L) = (61 + 1,2 \cdot L) \text{ nm}, L \text{ in mm}$$

Effective degree of freedom:

$$\nu_{\text{eff}}(dl) = 520; L = 100 \text{ mm}$$

Expanded uncertainty:

$$U_{95}(dl) = (122 + 2,4 \cdot L) \text{ nm}, L \text{ in mm}$$

NCM Bulgaria

Input quantity x_i	Distrib.	$u(x_i)/$ unit	ν_i	$c_i = \partial dL/\partial x_i$	$u_i (dL)/$ nm
Vacuum wavelength λ_0	N	$8 \cdot 10^{-6}$ nm	100	L/λ	$13 \cdot L$
Index of refraction of air n_{air}	-	$16 \cdot 10^{-8}$	-	L/n	$160 \cdot L$
Scale temperature Δt_s	-	0,02 K	-	$\alpha \cdot L$	$10 \cdot L$
Linear coefficient of thermal expansion α_z	-	$4 \cdot 10^{-8}$ 1/K	-	$(t-20) \cdot L$	$3 \cdot L$
Cosine error δl_{li}	R	230 μ rad	5	$0,4 \cdot L$ nm/ μ rad	$92 \cdot L$
Error of scale alignment δl_{si}	R	405 μ rad	6	$0,7 \cdot L$ nm/ μ rad	$284 \cdot L$
Edge geometry influence δ_{Edef}	R	23 nm	4	1	23
Influence of line edge detection algorithm δ_{Ealg}	R	17 nm	8	1	17
Error due to Abbe offset δl_{Ai}	R	40 nm	5	1	40
Influence of detection light wavelength $\delta l_{E\lambda}$	N	14 nm	10	1	14
Influence of focal length variation δ_{Efoc}	R	35 nm	6	1	35
Influence of measurement in reversed orientation δl_{Rev}	R	38 nm	5	1	38
Interferometer nonlinearity δl_{NL}	R	15 nm	5	1	15
Repeatability of edge detection s_E	N	24 nm	20	1	24

Combined standard uncertainty: $u_c(L) = Q[78; 340 \cdot L]$ nm, L in m

Effective degree of freedom: $\nu_{\text{eff}}(d_i) =$ from 29 to 37

Expanded uncertainty: $U_{95}(dL) = Q[158; 690 \cdot L]$ nm, L in m ($k=2,03$)

NML Ireland

Input quantity x_i	Distrib.	$u(x_i)$ unit	ν_i	$c_i = \partial dL / \partial x_i$	$u_i (dL) / \text{nm}$
Calibration uncertainty of Laser	N	20	∞	1	20
Performance of Laser (1.7ppm)	R	98.15	∞	1	98.15
Laser System Resolution	R	5.77	∞	1	5.77
Temperature Corrections	R	0.029	∞	750nm/°C	216.51
Cosine Error	R	3.87	∞	1	3.87
Line Scale Pitch & Yaw Error	R	11.55	∞	1	11.55
Repeatability	N	700nm	4	1	700

Combined standard uncertainty: $u_c(L) = 739.58 \text{ nm}$

Effective degree of freedom: $\nu_{\text{eff}}(dl) = 5$

Expanded uncertainty: $U_{95}(dl) = 1479.16 \text{ nm}$

NPL United Kingdom

TYPE A UNCERTAINTIES	Magnitude	Magnitude assuming a Rectangular Distribution
Thermal Expansion Of Microscope	1.25 parts in 10 ⁸	3.61 parts in 10 ⁸
Vibration	Contributes to St Dev	Contributes to St Dev
Positioning / Setting Repeatability	Contributes to St Dev	Contributes to St Dev
Focusing	Contributes to St Dev	Contributes to St Dev

TYPE B UNCERTAINTIES	Magnitude	Magnitude assuming a Rectangular Distribution
Laser Frequency	1.3 parts in 10 ⁸	3.67 parts in 10 ⁹
Refractive Index (Air Refractometer Value)	8.8 parts in 10 ⁸ (or 2.0 parts in 10 ⁸)	2.54 parts in 10 ⁸ (or 5.77 parts in 10 ⁹)
Angular Stability Of Stage	1.5 parts in 10 ⁸	4.52 parts in 10 ⁹
Thermal Expansion Of Scale	1.5 parts in 10 ⁷	2.05 parts in 10 ⁷
Alignment Of Lasers	1.25 parts in 10 ⁷	3.61 parts in 10 ⁸
Alignment Of Scale	2.83/ L ²	0.817/ L ²

The Standard Uncertainty may now be expressed as:

$$\text{Standard Uncertainty} = \sqrt{\left((6.57 \times 10^{-8})^2 + \left(\frac{0.817}{L^2} \right)^2 \right) \times L^2 + (3.61 \times 10^{-9})^2 + \left(\frac{1.32}{\sqrt{3}} SD \right)^2}$$

hence;

$$\text{Standard Uncertainty} = \sqrt{\left(4.32 \times 10^{-15} + \frac{0.667}{L^4} \right) \times L^2 + 1.3 \times 10^{-17} + \left(\frac{1.32}{\sqrt{3}} SD \right)^2}$$

Therefore;

$$\text{Standard Uncertainty} = \sqrt{\left(4.32 \times 10^{-15} \times L^2 \right) + \frac{0.667}{L^2} + 1.3 \times 10^{-17} + \left(\frac{1.32}{\sqrt{3}} SD \right)^2}$$

Where L is the length of the scale or graticule in μm, and SD is the standard deviation of the measurements in μm.

NSCIM Ukraine

Input quantity x_i	Distrib	$u(x_i)$	ν_i	$c_i = \partial dL / \partial x_i$	$u_i = c_i u_{x_i}$, nm
Inaccuracy of measuring the order of interference	N	14 nm	10	1	14
Wavelength reproduction error	R	$1.8 \cdot 10^{-9}$	100	L	$0.002 \cdot 10^{-6} L$
Inaccuracy of measuring the air parameters:	R				
pressure		0.1 mm Hg	100	$0.357 \cdot 10^{-6} L$	$0.036 \cdot 10^{-6} L$
temperature		0.005 °C	100	$0.927 \cdot 10^{-6} L$	$0.005 \cdot 10^{-6} L$
humidity		0.1 mm Hg	100	$0.056 \cdot 10^{-6} L$	$0.006 \cdot 10^{-6} L$
Inaccuracy of measuring the scale temperature	R	0.005 °C	100	αL $\alpha = 5 \cdot 10^{-7} 1/^\circ\text{C}$	$0.003 \cdot 10^{-6} L$
Inaccuracy of measuring the linear expansion factor of the scale	R	$5 \cdot 10^{-8} 1/^\circ\text{C}$	100	$\Delta t L$ $\Delta t = 0.1 ^\circ\text{C}$	$0.005 \cdot 10^{-6} L$
Inaccuracy of the scale adjusting	R	$5.8 \cdot 10^{-4}$ rad	100	L	$0.17 \cdot 10^{-6} L$
Abbe error	R	$9.6 \cdot 10^{-7}$ rad	100	1	10
Inaccuracy of determining the mark's centre	R	10 nm	100	1	10

Combined standard uncertainty: $u_c(L) = \sqrt{(20\text{nm})^2 + (0.17 \cdot 10^{-6} L)^2}$

Effective degree of freedom: $\nu_{\text{eff}}(dL) = 29$

Expanded uncertainty: $U_{0.95} = 2\sqrt{(20\text{nm})^2 + (0.17 \cdot 10^{-6} L)^2}$

OMH Hungary

	Input quantity x_i	Distributio n	$u(x_i)$ unit	ν_i	$c_i = \partial dL / \partial x_i$	$u_i(dL)$ [nm]
1	λ_0 vacuum wavelength of HP 5528 laserinterfero	Normal	6,0E-08*L		1	6,0E-08*L
2	Index of refraction of air n_{air}	Rectang.	1,0E-08*L	∞	1	1,0E-08*L
3	Air temperature t_{air}	Rectang.	0,020	∞	1E-06*L	2,0E-08*L
4	Air pressure P_{air}	Rectang.	0,108	∞	-3E-08*L	-3,23E-08*L
5	Air humidity RH_{air} (U=1,25%)	Normal	0,169	∞	1E-08*L	1,69E-10*L
6	Compensation factor of laserinterferometer	Rectang.	0,058	∞	1E-08*L	5,77E-08*L
7	Interferometer resolution δL_{Res}	Rectang.	6	∞	1	6
8	Interferometer dead path influences δL_{DP}	Rectang.	11	∞	1	11
9	Drift influence	Rectang.	17	∞	1	17
10	ABBE error in the xy plane	Rectang.	23	∞	1	23
11	ABBE error in the xz plane	Rectang.	3	∞	1	3
12	Cosine error of scale alignment in the xy plane	Rectang.	3E-11	∞	L	3,32E-11*L
13	Cosine error of scale alignment in the xz plane	Rectang.	6E-11	∞	L	5,89E-11*L
14	Cosine error of interferometer alignment	Rectang.	3E-09	∞	L	3,12E-09*L
15	Linear expansion coefficient of the scale materia	Rectang.	5,77E-07	∞	-0,054*L	1,8E-08*L
16	Difference of the scale temperature from the refe	Rectang.	0,11	∞	-5E-07*L	-5,53E-09*L
17	Length difference of scale position (standing or l	Rectang.	5,00	∞	1	5
18	Standard deviation max (*)	Normal	94	19	1	94

*Note: In the line of 18: the maximum standard deviation is used (94 nm)

Combined standard uncertainty: $u_c(L) = Q[100; 9.4E-08 L]$ nm $L=[\text{nm}]$

Effective degree of freedom: $\nu_{\text{eff}}(dl) = 25 (L=100 \text{ mm})$ $k=2.11$

Expanded uncertainty: $U_{95}(dl) = Q[211; 2E-07 L]$ nm $L=[\text{nm}]$

PTB Germany

name and symbol x_i (unit)	Dist.	x_i	for 100 mm		const $u_i(dl)$ /nm	rel. to L $u_i(dl)*E9$ /L
			$c_i = du(x_i)/dx_i$	$u_i(dl)$ /nm		
Translation stage:						
Abbe offset $y, z, A_y, A_z = 1\text{mm}, 2\text{mm}$, Yaw and Pitch of x-axis $\delta_{yaw} (\mu\text{rad}) = 0.1$ and $\delta_{pitch} (\mu\text{rad}) = 0.1$	R	0.1	1 nm/urad	0.06	0.14	
	R		2 nm/urad	0.12		
Interferometer:						
Refractive Index (due to rest gas, in hPa)	R	0.005	270 nm L/(m hPa)	0.078		0.78
Vacuum Pressure (hPa)	R	0.001	270 nm L/(m hPa)	0.016		0.16
Interf. Deadpath L_{DP} (20 mm), pressure stab. during measurement 0.001 mbar	R	20	270 nm L_{DP} /(m hPa)	0.003	0.003	
Interf. cosine error forw. beam δ_{θ_i} (μrad) back. beam	R	15.2	-		0.0003	0.003
		30.54	-			
Beam diffraction, $w_{\text{beam}} = 11\text{ mm}$	R	11	-	0.004		0.04
Vacuum wavelength λ_0 ($\Delta\lambda/\lambda = 1.4 \times 10^{-11}$)	R	1.4×10^{-11}	L	0.001		0.01
Wavefront deformation	N	1×10^{-9}	L	0.1		1
Nonlinearities (nm)	R	0.1	1	0.06	0.06	
Microscope:						
Defocus (observed dependence): 27 nm / $3\mu\text{m}$, $\Delta x = 3 \times \Delta z^2 \text{ nm}/\mu\text{m}^2$, $\Delta z_{\text{max}} = 0.5 \mu\text{m}$	R	0.5	-	0.45	0.45	
Microscope mode dependence	R	15	1		8.7	
Reference line	R	15	1		8.7	
Scale properties:						
Scale alignment horiz. $\Delta y = 0.5 \mu\text{m}$, vert. $\Delta z = 0.5 \mu\text{m}$	R	0.5	-	0.0004		0.004
		0.5		0.0009		0.009
Scale alignment, position of support points, 1 mm interval	R	1	-		3.9	
Unc. thermal exp. coef. $u_\alpha = 5 \times 10^{-8}/\text{K}$, $T_{\text{max}} - 20 \text{ C} < 0.06 \text{ K}$	R	5×10^{-8}	$0.06\text{L} \times \text{K}$	0.173		1.73
Temperature measurement, 10mK $\alpha = 5 \times 10^{-7}/\text{K}$	R	10	$0.5 \times \text{L nm}/(\text{m K})$	0.29		2.9
Pressure measurement $u_{\text{pres}} = 0.6 \text{ hPa}$, $\chi = -8.9 \times 10^{-10}/\text{hPa}$	N	0.60	$-0.89 \times \text{L nm}/(\text{m hPa})$	0.06		0.6
Unc. Compressibility $u_\kappa = 8.9 \times 10^{-11} /\text{hPa}$ ($\Delta p = 40 \text{ hPa}$)	R	8.9×10^{-11}	40hPa L	0.21		2.1

name and symbol x_i (unit)	Dist.	x_i	for 100 mm		const $u_i(dl)$ /nm	rel. to L $u_i(dl)*E9$ /L
			$c_i = du(x_i)/dx_i$	$u_i(dl)$ /nm		
Measurement:						
Reproducibility (4 nm, n=9)	N	1.33	1	1.33	1.33	
Contamination at lines (0.2,0.4,0.5,0.7)	R	60			29	
Total $u_c(1\sigma)$			13 (31.8) nm			
Total U_{95}			30.8 (75.4)			
General Expression	$U_{95} = 2.37 \times Q[13(32); 4.1E-9 \times L]$					

Effective degrees of freedom: 8

SMU Slovakia

Input quantity x_i	Distrib.	$u(x_i)$ unit	ν_i	$c_i = \partial dL / \partial x_i$	$u_i (dL) / \text{nm}$
s_E repeatability of edge detection	N	28 nm	15	1	28
$\delta_{E,def}$ edge geometry influence	R	10 nm	> 100	1	10
$\delta_{E,adj}$ influence of a djustment of measurement line	N	10 nm	> 100	1	10
$\delta_{E,foc}$ influence of focal length variation	N	20 nm	> 100	1	20
$\delta_{E,align}$ microscope axis align.	R	15 nm	> 100	1	15
$\delta_{E,rev}$ influence of measurement in reversed orientation	R	22 nm	> 100	1	22
λ_0 vacuum wavelength	N	10^{-9}	> 1000	L	$10^{-9} L$
n_{air} refractive index of air ¹ incl correction to HP software error	N	$4 \cdot 10^{-5}$	> 1000	L	$4 \cdot 10^{-5} L$
t_{air} air temperature incl. gradient and drift	R	50 mK	> 100	$-9,5 \cdot 10^{-7} \text{K}^{-1} L$	$4,8 \cdot 10^{-5} L$
p_{air} air pressure incl. drift	R	10 Pa	> 100	$2,7 \cdot 10^{-9} \text{Pa}^{-1} L$	$2,7 \cdot 10^{-5} L$
RH_{air} air humidity incl. gradient and drift	R	3%	> 100	$8,5 \cdot 10^{-9} \%^{-1} L$	$2,6 \cdot 10^{-5} L$
c_{CO_2} air CO ₂ concentration incl. drift	R	0,02% (estimated, not measured)	-	$4,5 \cdot 10^{-7} \%^{-1} L$	$9 \cdot 10^{-9} L$
δ_{Res} interferometer resolution	R	10 nm	> 1000	$0,5/\sqrt{3}$	3
δ_{NL} interferometer nonlinear.	N	6 nm	> 1000	1	6
δ_{Ai} errors due to Abbe offsets and pitch and yaw of translation stages	R	100 μrad	> 100	-	$4 \cdot 10^{-9} L$
δ_{Si} errors of scale alignment	R	100 μrad	10	$(\gamma_i^2 / 2\Lambda_i) \cdot L$	$4 \cdot 10^{-9} L$
δ_{Ii} cosine errors of interferometer alignment	R	250 μrad	10	$(\gamma_i^2 / 2\Lambda_i) \cdot L$	$2,5 \cdot 10^{-5} L$
$\alpha_{z,C}$ linear coefficient of thermal expansion	R	$2 \cdot 10^{-7} \text{K}^{-1}$	-	$ 20 - T_m \cdot L$	$2,8 \cdot 10^{-5} L$
$\Delta t_i = (t_i - 20)$ incl. gradient and drift	R	100 mK	> 100	$\alpha_z \cdot L$	$5 \cdot 10^{-5} L$
$\kappa_{z,C}$ linear coefficient of compressibility	R	10^{-7}bar^{-1}	-	$u_p \cdot L$	$4,5 \cdot 10^{-12} L$
δ_{supp} influence of support conditions	R	0,5 mm	10	-	1

Combined standard uncertainty: $u_c(L) = \sqrt{46^2 + (0,094^2) \cdot L^2}$ nm (L in mm)

Effective degree of freedom: $\nu_{\text{eff}}(dl) \approx 500$

Expanded uncertainty: $U_{95}(dl) = \sqrt{92^2 + (0,19^2) \cdot L^2}$ nm (L in mm)

ZMDM Serbia

Input quantity x_i	Distrib.	$u(x_i)$ unit	ν_i	$c_i = \partial dL / \partial x_i$	$u_i (dL) / \text{nm}$
Vaccum wavelength of laser, λ_0	R	$4 \cdot 10^{-9}$	100	1 L	$4 \cdot 10^{-9} L$
Interferometer resolution, δ_{Res}	R	3 nm	100	1	3
Index of refraction of air, n_{air}	N	$1 \cdot 10^{-8}$	100	2 L	$1 \cdot 10^{-8} L$
Air temperature, t_{air}	R	0.1 °C	8	$9.5 \cdot 10^{-7} L$	$9.5 \cdot 10^{-8} L$
Air pressure, p_{air}	R	30 Pa	8	$2.7 \cdot 10^{-9} L$	$8.1 \cdot 10^{-8} L$
Air humidity, RH_{air}	R	3%	5	$1 \cdot 10^{-8} L$	$3 \cdot 10^{-8} L$
Air CO ₂ concentration, c_{CO_2}	R	120 ppm	5	$1.5 \cdot 10^{-10} L$	$2 \cdot 10^{-8} L$
Linear coefficient of thermal expansion, α	N	$5 \cdot 10^{-7} \text{ °C}^{-1}$	10	$0.2 L$	$1 \cdot 10^{-7} L$
Scale temperature difference, Δt_s	N	0.1 °C	8	$5 \cdot 10^{-7} L$	$5 \cdot 10^{-8} L$
Interferometer alignment, δ_{Ii}	R	200 μrad	15	$x_i^2/2 L$	$4 \cdot 10^{-8} L$
Scale alignment, δ_{Si}	R	200 μrad	10	$x_i^2/2 L$	$4 \cdot 10^{-8} L$
Errors due to Abbe offsets and pitch and yaw, δ_{Ai}	R	20 nm	10	1	20
Microscope axis alignment, δ_{Ealig}	R	30 nm	10	1	30
Repeatability of center line detection	N	80 nm	20	1	80
Drift influence (incl. deadpath)	R	50 nm	20	1	50

Combined standard uncertainty: $u_c(L) = Q[101; 0.19L]$ nm, L in mm

Effective degree of freedom: $\nu_{\text{eff}}(dl) = [42, 48L]$ L in m

Expanded uncertainty: $U_{95}(dl) = Q[202; 0.38L]$ nm, L in mm

GROUP 2**A*Star – NMC Singapore**

Input quantity x_i	Distrib	$u(x_i)$ unit	ν_i	$c_i = \partial dL / \partial x_i$	$u_i (dL) / \text{nm}$
Vacuum wavelength, λ_o	R	$3 \times 10^{-8} \lambda_o$	50	L/λ_o	$0.03L$
Interferometer resolution, δ_{Res}	R	24 nm	100	1	24
Cosine errors of interferometer alignment, δ_{Ii}	R	230 μrad	50	$400 \times 10^{-6} L/\text{rad}$	$0.1L$
Air temperature, t_{air}	R	0.21 $^{\circ}\text{C}$	10	$9.2 \times 10^{-7} L/^{\circ}\text{C}$	$0.19L$
Air pressure, p_{air}	R	21 Pa	10	$2.9 \times 10^{-9} L/\text{Pa}$	$0.061L$
Air humidity, RH_{air}	R	2.3 %rh	10	$8.9 \times 10^{-9} L/\%rh$	$0.02L$
Index of refraction of air, n_{air}	R	2.4×10^{-7}	10	L	$0.24L$
Edlen equation, n_{Edl}	R	1×10^{-8}	100	L	$0.01L$
Air CO ₂ concentration, c_{CO2}	R	1×10^{-4}	10	$1.5 \times 10^{-4} L$	$0.015L$
Errors due to horizontal Abbe offsets ($\alpha_h \leq 1\text{mm}$), δ_{Aih}	R	60 μrad	50	α_h	60
Errors due to vertical Abbe offsets ($\alpha_v \leq 0.5\text{mm}$), δ_{Aiv}	R	60 μrad	50	α_v	30
Errors of scale alignment, δ_{Si}	R	50 μrad	100	$50 \times 10^{-6} L/\text{rad}$	$0.003L$
Interferometer dead path, δ_{DP}	R	32 nm	50	1	32
Thermal expansion coefficient of scale, $\alpha_{z, Cr}$	R	$3 \times 10^{-8} \text{ }^{\circ}\text{C}^{-1}$	50	$0.5L/^{\circ}\text{C}^{-1}$	$0.015L$
Temperature difference of the scale from 20 $^{\circ}\text{C}$, Δt_s	R	0.2 $^{\circ}\text{C}$	10	$5 \times 10^{-7} L/^{\circ}\text{C}$	$0.10L$
Repeatability of edge detection, s_E	N	50 nm	13	1	50
Standard deviation of four repeat measurements, L_m	N	65.5 nm	3	1	65.5

Combined standard uncertainty: $u_c(dL) = [(115)^2 + (0.35L)^2]^{1/2}$, L in mm

Effective degree of freedom: $\nu_{\text{eff}}(dL) = 30$ at L = 100 mm

Expanded uncertainty: $U_{95}(dL) = [(230)^2 + (0.70L)^2]^{1/2}$ (k=2)

CEM Spain

Input quantity x_i	Distrib.	$u(x_i)$ unit	ν_i	$c_i = \partial dL / \partial x_i$	$u_i(dL) / \text{nm}$
Laser indication on reference line i	N	22,2 nm	9	1	22,2
Laser indication on reference line 0	R	1,44	>100	1	1,44
Laser wavelength	N	1,50e-09	>100	1,58e+03 L	2,37e-06 L
Index of refraction of air (initial reading of TRACKER)	N	3,52e-08 nm	>100	1,00e+06 L	0,035 L
Thermal coefficient of line scale	R	5,77e-08 °C ⁻¹	>100	1,00e+05 L °C	5,77e-03 L
Temperature deviation of line scale from 20 °C	R	0,116 °C	>100	0,5 L °C ⁻¹	0,058 L
TRACKER Accuracy (1)	R	8,08e-08 L	>100	1	0,081 L
Optics (2)	R	3,7 nm	>100	1	3,7 nm
Dead path	R	8,1 nm	>100	1	8,1 nm
Comparator misalignment (maximum for flat mirrors) (2)	R	2,89e-08 L	>100	1	2,89e-02 L
Misalignment of the line scale	R	1,02e-07 nm	>100	1	1,02e-01 L
Optic set of line position	N	15,3 nm	49	1	15,3 nm

(1) "Achieving Maximum Accuracy and Repeatability with the Agilent 5527A/B Laser Position Transducer System", Product Note.

(2) Optics and Laser Heads for Laser-Interferometer Positioning Systems, Product Overview, Agilent Technologies.

Combined standard uncertainty: $u_c(L) = Q [28.43; 0.15 \text{ L/mm}] \text{ nm}$

Effective degrees of freedom: $\nu_{\text{eff}}(dl) = 42$

Expanded uncertainty: $U_{95}(dl) = Q [60; 0.3 \text{ L/mm}] \text{ nm}$

CENAM México

Input quantity, x_i	Distribution	$u(x_i)$	ν_i	$c_i = \frac{\partial dL}{\partial x_i}$	$u_i^2(dL)$ nm	
					Independent	$*L^2$
Repeatability of edge detection	N	120	11	$(1 + \alpha_{\text{scale}} * \Delta T)$	14 293	
Microscope magnification	R	52	12	1	2 700	
Microscope axis alignment	R	$4,4^{-7}$	100	L		0,19
Line edge detection	R	29	100	1	833	
Microscope calibration	R	$5,77$	100	$(1 + \alpha_{\text{micro}} * \Delta T)$	1 168	
Linear coefficient of thermal expansion of microscope scale	R	$4,62^{-7}$	100	$\Delta T * L$		0,034
Difference of the microscope temperature	R	0,29	100	$\alpha_{\text{micro}} * L$		3,4
Linear coefficient of thermal expansion of scale	R	4^{-8}	100	$\Delta T * L$		0,00026
Difference of the scale temperature	R	0,29	24	$\alpha_{\text{scale}} * \Delta T$		0,026

Combined Standard Uncertainty: $u_c(L) = \sqrt{18994 + 3,8 * L^2}$

$u_c(L)$ in nm

L in mm

EIM Greece

Input quantity x_i	Distrib.	$u(x_i)$ unit	ν_i	$c_i = \partial dL / \partial x_i$	$u_i (dL) / \text{nm}$
Displacement Measurement	R	1ppm	50	1	l
Artifact Temperature	R	0.15 °C	50	$a * l$	$0.075 * l$
Zero Line center estimate	R	0.200 μm	50	1	200
Line center estimate	R	0.200 μm	50	1	200
Scale alignment	R	$1.25 \cdot 10^{-9} * l$	50	1	$0.001 * l$

L in mm

Combined standard uncertainty: $u_c(L) = \sqrt{283^2 + L^2}$ (nm), L in mm

Effective degree of freedom: $\nu_{\text{eff}}(dl) = 123$ for $dl=100$ mm

Expanded uncertainty: $U_{95}(dl) = 2 * u_c(L)$

INMETRO Brazil1. L from 0 mm to 55 mm

Input Quantity x_i	Distrib.	$U(x_i)$ unit	ν_i	$c_i = \partial dL / \partial x_i$	$u_i (dL) / \text{nm}$
Repeatability	N	19 nm	9	1	19 nm
Resolution	R	1 nm		1	0,577 nm
Variation in indication	R	2 nm		1	1,155 nm
Laser alignment	R	0,0001 nm		1	0,00005 nm
Dead length	R	1 nm		1	0,788 nm
Errors of scale alignment	R	0,02 nm		1	0,012 nm
Edge detection	T	130 nm		1	53,072 nm
focal length variation	R	50 nm		1	46,189 nm
Air temperature	N	0,017 °C		9,28E-07 (1/°C)	0,434 nm
Air pressure	N	10,9 (Pa)		2,68E-09 (1/Pa)	0,806 nm
Escale temperature	N	0,010 °C		5,00E-07 (1/°C)	0,137 nm
Thermal expansion coefficient	N	0,000001 (1/°C)		5,46E-01 (°C)	15,015 nm
Partial vapor pressure	N	16,374 (Pa)		3,71E-10 (1/Pa)	0,167 nm
-----	-----	-----		-----	-----

Combined standard uncertainty: $u_c(dl) = 63 \text{ nm} ; 0\text{mm} \leq L \leq 55\text{mm}$

Effective degree of freedom: $\nu_{\text{eff}}(dl) = \infty$

Expanded uncertainty: $U_{95}(dl) = 126 \text{ nm}$

2. L above 55 mm mm to 100 mm

Input quantity x_i	Distrib.	$u(x_i)$ unit	ν_i	$c_i = \partial dL / \partial x_i$	$u_i(dL) / \text{nm}$
Repeatability	N	10 nm	9	1	10 nm
Resolution	R	1 nm		1	0,577 nm
Variation in indication	R	20 nm		1	11,547 nm
Laser alignment	R	0,0001 nm		1	0,00005 nm
Dead length	R	1nm		1	0,788 nm
Errors of scale alignment	R	0,02 nm		1	0,012 nm
edge detection	T	200 nm		1	81,650 nm
focal length variation	R	50 nm		1	28,868 nm
Air temperature	N	0,017 °C		9,28E-07 (1/°C)	0,789 nm
Air pressure	N	10,9 (Pa)		2,68E-09 (1/Pa)	1,465 nm
Escale temperature	N	0,010 °C		5,00E-07 (1/°C)	0,250 nm
Thermal expansion coefficient	N	0,000001 (1/°C)		5,46E-01 (°C)	27,30 nm
Partial vapor pressure	N	16,374 (Pa)		3,71E-10 (1/Pa)	0,303 nm
-----	-----	-----		-----	-----

Combined standard uncertainty: $u_c(dl) = 92 \text{ nm}; 55\text{mm} < L \leq 100\text{mm}$

Effective degree of freedom: $\nu_{\text{eff}}(dl) = \infty$

Expanded uncertainty: $U_{95}(dl) = 184 \text{ nm}$

INRIM Italy

name and symbol x_i	distrib.	$u(x_i)$ unit	ν_i	$c_i = \partial dl / \partial x_i$	$u_i(dl) / nm$ <i>L in mm</i>
edge detection repeatability between series	N	40 nm	30	1	40
interferometer digital resolution	R	2,9 nm	100	1	2,9
vacuum wavelength	N	5 fm	100	L	$7 \cdot 10^{-3} \cdot L$
air refractive index	N	$2,3 \cdot 10^{-8}$	100	L	$23 \cdot 10^{-3} \cdot L$
interferometer non-linearity	R	1 nm	50	1	1
interferometer deadpath	R	2,4 nm	100	1	2,4
linear coefficient of thermal expansion (α) of scale	N	$2 \cdot 10^{-8} K^{-1}$	50	$(t_s - 20) \cdot L$	$1 \cdot 10^{-3} \cdot L$
difference of the scale temperature from the reference temperature during measurement	N	0,013 K	50	$\alpha \cdot L$	$6,5 \cdot 10^{-3} \cdot L$
linear coefficient of compressibility (k) of the scale material	N	$1 \cdot 10^{-12} Pa^{-1}$	50	$(101325 - p) L$	$1 \cdot 10^{-3} \cdot L$
variations of air pressure during measurement	N	0,3 kPa	50	$k \cdot L$	$2,7 \cdot 10^{-3} \cdot L$
Abbe offsets and pitch and yaw of translation stages	R		100		7
Imperfect alignment of scale (laser) with respect to meas. direction	R		100		$50 \cdot 10^{-3} \cdot L$
imperfect alignment in direction and height of the linescale	R		15		$26 \cdot 10^{-3} \cdot L$
Microscope axis alignment and straightness of translation stage	R		10		$15 + 0,18 \cdot L$

Formula or expression of uncertainty shall be given in the same way as for MRA C:

Combined standard uncertainty: $u_c(dl) = 48 \text{ nm } (L=100 \text{ mm})$

Effective degree of freedom: $\nu_{\text{eff}}(dl) = 50$

Expanded uncertainty: $U_{95}(dl)/nm = Q[90, 0.4 L] ; L \text{ in mm}$
 $= 98 \text{ nm } (L=100 \text{ mm})$

NIM China

Input quantity x_i	Distrib	$u(x_i)$ unit	i_i	$c_i = \partial dL / \partial x_i$	$u_i (dL) / \text{nm}$
\ddot{e}_0	R	$1.73 \times 10^{-8} \ddot{e}_0$	50	dL / \ddot{e}_0	$1.73 \times 10^{-8} dL$
n_{air}	N	1×10^{-8}	12.5	dL	$1.00 \times 10^{-8} dL$
t_{air}	R	$0.0115 \text{ } ^\circ\text{C}$	12.5	$0.930 \times 10^{-6} dL \text{ } ^\circ\text{C}^{-1}$	$1.07 \times 10^{-8} dL$
RH_{air}	R	23.09 Pa	12.5	$0.371 \times 10^{-9} dL \text{ Pa}^{-1}$	$0.86 \times 10^{-8} dL$
C_{CO_2}	N	60×10^{-6}	6500	$1.45 \times 10^{-4} dL$	$0.87 \times 10^{-8} dL$
P_{air}	R	15 Pa	12.5	$2.683 \times 10^{-9} dL \text{ Pa}^{-1}$	$4.03 \times 10^{-8} dL$
S_E	N	0.48	39	$\ddot{e}_0 / 8$	38
$\ddot{A}t_s$	R	$0.0058 \text{ } ^\circ\text{C}$	12.5	$5.0 \times 10^{-7} dL \text{ } ^\circ\text{C}^{-1}$	$0.29 \times 10^{-8} dL$
$\dot{a}z, cr$	N	$1.17 \times 10^{-8} \text{ } ^\circ\text{C}^{-1}$	50	$0.026 \text{ } ^\circ\text{C} \times dL$	$0.03 \times 10^{-8} dL$
$\ddot{a}l_{\text{DP}}$	R	0.8nm	2	1	1
$\ddot{a}l_{\text{Res}}$	R	3nm	∞	1	3
$\ddot{a}E_{\text{alig}}$	R	12nm	12.5	1	12
$\ddot{a}E_{\text{res}}$	R	0.289	∞	$\ddot{e}_0 / 8$	23
$\ddot{a}l_{\text{Ai}}$	R	6nm	12.5	1	6
$\ddot{a}l_{\text{NL}}$	R	12nm	12.5	1	12
$\ddot{a}l_{\text{li}}$	R	$3.6 \times 10^{-10} dL$	12.5	1	$0.04 \times 10^{-8} dL$
$\ddot{a}l_{\text{Si}}$	R	$2.4 \times 10^{-10} dL$	12.5	1	$0.03 \times 10^{-8} dL$
D	R	0.0116mm	50	$1 \times 10^{-7} dL \text{ mm}^{-1}$	$0.12 \times 10^{-8} dL$

D -Diameter of diaphragm for incidence light

Combined standard uncertainty: $u_c = \sqrt{(48 \text{ nm})^2 + (4.80 \times 10^{-8} dL)^2} = 48.3 \text{ nm} \approx 49 \text{ nm}$

Effective degree of freedom: $i_{\text{eff}}(dL) = 95$

Expanded uncertainty: $U_{95}(dL) = 98 \text{ nm}$

NIST USA

Description of the measurement uncertainty

Results of the measurements are given on the following pages of this report. The length values are the mean of eight measurements and the expanded uncertainty is

$$U_{95} = k u_c$$

and the combined standard uncertainty is

$$u_c = \sqrt{(u_i^2 + u_j^2)}$$

where u_i is the type-A standard uncertainty and u_j is the type-B standard uncertainty. A coverage factor $k=2.36$ was used which gives for the reported value a level of confidence of 95 percent.

The u_i uncertainty was derived from the measurement result and includes several input quantities which cannot be separated. These uncertainties include those contributed by laser interferometer polarization mixing, scale surface and graduation lines quality, measurement repeatability, line edge detection and line center derivation, measured length difference between normal and reverse scale orientation, measured length deviation due to sudden pressure changes during interferometer readings, and vibrational noise in the measurement system, just to mention a few.

The u_i standard uncertainty is one standard deviation of the mean value and is computed from the formula

$$u_i = \frac{\sqrt{\sum \frac{d^2}{N-1}}}{\sqrt{N}}$$

where d is the deviation of a single measurement from the mean, $N-1$ is the number of degrees of freedom (7) and N is the number measurements (8).

We measured the scale in two interval groups. In group one we measured from 0 to 1 mm at each 0.1 mm interval. In group two we measured from 0 to 100 mm at each 5 mm interval. In each interval group the u_i values are reported as the RMS values of all u_i values within that group.

The u_j standard uncertainty was derived from the sum of several estimated systematic uncertainties present in the measurement system:

$$u_j = \sqrt{(u_{\lambda_0}^2 + u_{n_{ref}}^2 + u_{t_s}^2 + u_{t_r}^2 + u_p^2 + u_{rh}^2 + u_{co_2}^2 + u_{align}^2 + u_{\alpha}^2)}$$

Description of the measurement uncertainty (cont.)

where the estimated systematic uncertainties are

λ_0	the vacuum wave length of the laser (20 nm/m)
n_{tpf}	the refractive index equation (20 nm/m)
t_a	the air temperature in the interferometer path (less than 1 nm/m)
t_s	the scale temperature (1 nm/m for quartz or Zerodur)
p	the atmospheric pressure in the laboratory (20 nm/m)
rh	the Relative Humidity in the measuring chamber (10 nm/m)
co_2	the carbon dioxide in the laboratory (10 nm/m)
$align.$	the interferometer and scale alignments (20 nm/m)
α	the expansion coefficient of the scale (less than one nm/m)

$u_j = 50 \text{ nm / m}$ was used in the measurements

Measurement results for: #2, 100 mm Quartz Scale, Group #1 intervals

Nominal length L (mm)	Measured deviation dL (nm)	Nominal length L (mm)	Measured deviation dL (nm)
0	0, per definition	0.6	4.9
0.1	36.0	0.7	-15.1
0.2	1.2	0.8	18.2
0.3	16.7	0.9	-11.3
0.4	4.4	1.0	30.3
0.5	-11.2		

All length deviation values are referred to the position of the zero reference line, thus the uncertainty of determination of the reference line position has to be taken into account for the uncertainty estimation of the measured deviations from nominal lengths.

Combined standard uncertainty: $u_c(dL) = [(3.1 \text{ nm})^2 + (5 \times 10^{-8} \times L)^2]^{1/2}$

Effective degree of freedom: $\nu_{\text{eff}}(dL) = 7$

Expanded uncertainty: $U_{95}(dL) = [(3.1 \text{ nm})^2 + (5 \times 10^{-8} \times L)^2]^{1/2} \times [2.36]$

Measurement results for: #2, 100 mm Quartz Scale, Group #2 intervals.

Nominal length L (mm)	Measured deviation dL (nm)	Nominal length L (mm)	Measured deviation dL (nm)
0	0, per definition	55	-131.7
5	20.7	60	-153.1
10	24.9	65	-111.2
15	-19.4	70	-129.0
20	27.3	75	-146.2
25	-116.6	80	-125.3
30	-145.8	85	-125.4
35	-119.3	90	-313.4
40	-119.3	95	-266.3
45	-183.1	100	-249.6
50	-110.8		

All length deviation values are referred to the position of the zero reference line, thus the uncertainty of determination of the reference line position has to be taken into account for the uncertainty estimation of the measured deviations from nominal lengths.

$$\text{Combined standard uncertainty: } u_c(dL) = [(3.7 \text{ nm})^2 + (5 \times 10^{-8} \times L)^2]^{1/2}$$

$$\text{Effective degree of freedom: } v_{\text{eff}}(dL) = 7$$

$$\text{Expanded uncertainty: } U_{95}(dL) = [(3.7 \text{ nm})^2 + (5 \times 10^{-8} \times L)^2]^{1/2} \times [2.36]$$

NMi-VSL Netherlands

Input quantity x_i	Distrib.	$u(x_i)$ unit	ν_i	$c_i = \partial dL / \partial x_i$	$u_i (dL) / \text{nm}$
Interferometer resolution	R	0,4 nm	inf	1	0,4 nm
Repeatability edge detection	N	12 nm	93	1	12,0 nm
Wavelength					
Laser	R	$3,1 \cdot 10^{-9}$	inf	L	$3,1 \cdot 10^{-9} \cdot L$
Air temperature	R	0,051 K	inf	$9,6 \cdot 10^{-7} \text{ K}^{-1} \cdot L$	$4,9 \cdot 10^{-9} \cdot L$
Air pressure	R	22 Pa	inf	$2,7 \cdot 10^{-9} \text{ Pa}^{-1} \cdot L$	$5,8 \cdot 10^{-8} \cdot L$
Air humidity	R	2,0 %RH	inf	$8,5 \cdot 10^{-9} \text{ %RH}^{-1} \cdot L$	$1,7 \cdot 10^{-8} \cdot L$
CO ₂ content	R	58 ppm	inf	$1,5 \cdot 10^{-10} \text{ ppm}^{-1} \cdot L$	$8,4 \cdot 10^{-9} \cdot L$
Edlen equation	R	$1,0 \cdot 10^{-8}$	inf	L	$1,0 \cdot 10^{-8} \cdot L$
Dead path ($L_{dp}=10 \text{ mm}$)					
Air temperature drift	R	0.051 K	inf	$9,6 \cdot 10^{-7} \text{ K}^{-1} \cdot L_{dp}$	0,5 nm
Air pressure drift	R	5.8 Pa	inf	$2,7 \cdot 10^{-9} \text{ Pa}^{-1} \cdot L_{dp}$	0,2 nm
Air humidity drift	R	1.7 %RH	inf	$8,5 \cdot 10^{-9} \text{ %RH}^{-1} \cdot L_{dp}$	0,1 nm
CO ₂ content drift	R	58 ppm	inf	$1,5 \cdot 10^{-10} \text{ ppm}^{-1} \cdot L_{dp}$	0,1 nm
Alignment					
Scale to SIP 400	R	$4,2 \cdot 10^{-10}$	inf	L	$4,2 \cdot 10^{-10} \cdot L$
Laser to SIP 400	R	$1,0 \cdot 10^{-10}$	inf	L	$1,0 \cdot 10^{-10} \cdot L$
Interferometer optics	R	0,1 nm	inf	1	0,1 nm
Material temperature					
Scale	R	0,087 K	inf	$5,0 \cdot 10^{-7} \text{ K}^{-1} \cdot L$	$4,3 \cdot 10^{-8} \cdot L$
Expansion coefficient	R	$1,4 \cdot 10^{-7} \text{ K}^{-1}$	inf	0,015 K	$2,2 \cdot 10^{-9} \cdot L$
Local heating	R	0,194 K	150	$5 \text{ nm} \cdot \text{K}^{-1}$	1,0 nm
Abbe error	R	17,3 nm	inf	1	17,3 nm

Combined standard uncertainty: $u_c(L) = 21 \text{ nm} + 9,0 \cdot 10^{-8} \cdot L$

Effective degree of freedom: $\nu_{\text{eff}}(dl) = 890$

Expanded uncertainty: $U_{95}(dl) = 42 \text{ nm} + 1,8 \cdot 10^{-7} \cdot L$

NPLI India

<i>Source of uncertainty</i>	x_i	$\pm u(x_i)$	ν_i	$c_i = \partial L_i / \partial x_i$	$\pm u_i(dL_i)$ <i>nm</i>
Edge detection	0 nm	144 nm	16.5	1	144
Alignment	0 nm	0.288 μ rad/m	Infinite	L	288 L
Thermal Expansion	5×10^{-7} K ⁻¹	2.8×10^{-8} K ⁻¹	Infinite	$L \text{ m} \times 0.5\text{K}$	14 L
Temperature variation	0 °C	0.28 K	Infinite	$L \text{ m} \times 5 \times 10^{-7}$ K ⁻¹	140 L
Laser interferometer	100 mm	50 nm/m	Infinite	$L \text{ m}$	50 L
Repeatability	0	187 nm	20	1	187
		<i>veff.</i>	36		
		<i>t distribution</i>	2	$u_c(dL)$	239

Combined standard uncertainty (k=1) $u_c(dL) = \pm [(236)^2 + (324L)^2]^{1/2}$

Combined standard uncertainty (k=1) $u_c(dL) = \pm 239$ nm at $L = 100$ mm

NRC Canada

No budget was reported. Only report in the form of tabular values for single measurement points was sent:

$U = 80 \text{ nm}$ (at 0,1 mm) to 89 nm (at 100 mm)

The following explanation was given:

“The NRC long-bed comparator was still under development at the time of measurement and an uncertainty model was not developed at that time. The cited uncertainty was based on repeatability & reproducibility data, plus allowances for some instrument problems we were suspecting at the time.”

NIMT Thailand

Input quantity x_i	Distrib	$u(x_i)$ unit	ν_i	c_i	u_i (dL)/ nm	
l_s	Normal	5.00E-10 λ	∞	l/λ		5.00E-10 l
δl_d	Rectangular	7.84E-09 λ	∞	l/λ		7.84E-09 l
$\delta l_{stability}$	Rectangular	1.27E-10 λ	∞	l/λ		1.27E-10 l
δl_{ip}	Rectangular	1.67E-09 λ	∞	l/λ		1.67E-09 l
δl_{is}	Rectangular	0.231 nm	∞	1	0.231	
δl_{ind}	Normal	5.814 nm	5	1	5.814	
δl_{rep}	Normal	18.000 nm	∞	1	18.000	
δl_{abbe}	Rectangular	7.136 nm	∞	1	7.136	
δl_{mis}	Rectangular	2.89E-09 l	∞	1		2.89E-09 l
δl_{cos}	Rectangular	4.41E-11 l	∞	1		4.41E-11 l
δl_{edge}	Rectangular	0.185 nm	∞	1	0.185	
δl_{α}	Rectangular	2.89E-07	∞	$2.0E-01 l$		5.77E-08 l
$\delta l_{\Delta t}$	Normal	1.00E-02	∞	$5.0E-07 l$		5.00E-09 l
δl_{drift}	Rectangular	1.15E-02	∞	$5.0E-07 l$		5.77E-09 l
$\delta l_{stability}$	Rectangular	1.15E-02	∞	$5.0E-07 l$		5.77E-09 l
$\delta l_{difference}$	Rectangular	1.73E-02	∞	$5.0E-07 l$		8.66E-09 l
$\delta l_{\alpha \Delta t}$	Rectangular	2.89E-09	∞	l		2.89E-09 l
$\delta l_{\alpha drift(\Delta t)}$	Rectangular	3.33E-09	∞	l		3.33E-09 l
$\delta l_{\alpha stability(\Delta t)}$	Rectangular	3.33E-09	∞	l		3.33E-09 l
$\delta l_{\alpha difference(\Delta t)}$	Rectangular	5.00E-09	∞	l		5.00E-09 l
δl_{uuc}	Rectangular	5.77E-11 l	∞	1		5.77E-11 l
δl_{op}	Rectangular	2.56E-09 l	∞	1		2.56E-09 l
$\delta l_{compression}$	Rectangular	5.14E-07 l	∞	1		5.14E-07 l
					408.81	2.68E-13 l^2
u_c					20.22	5.17E-07 l
$U(l_x)$				$k=2$	40.44	1.03E-06 l
					41.0	1.03E-06 l

Combined standard uncertainty: $u_c(L) = Q[20.5, 0.517 \cdot L]$ nm L indication in mm

Effective degree of freedom: $\nu_{\text{eff}}(dL) = 9893.8$

Expanded uncertainty: $U_{95}(dL) = Q[41, 1.03 \cdot L]$ nm L indication in mm

VNIIM Russia

name and symbol x_i	dist rib.	$u(x_i)$ unit	ν_i	$c_i =$ $\partial dl / \partial x_i$	$u_i(dl) / \text{nm}$
<i>Length independent</i>					
δ_{Edef} Edge geometry influence (roughness, parallelism)	N	9 nm	10	1	9
δ_{Eloc} Influence of focal length variation	N	1 μm	5	0.002	2
δ_{Ealig} Microscope axis alignment	R	1 mrad	>100	δ_{Estr}	1
δ_{Res} Interferometer resolution	N	0.1 nm	5	1	0.1
δ_{NL} Interferometer nonlinearity	N	1 nm	5	1	1
δ_{Ai} Errors due to Abbe offsets and pitch and yaw of translation stages	R	0.2 mm	>100	δ_{Erot}	1
<i>Length dependet</i>					
λ_0 vacuum wavelength of light source used for displacement measurement	N	3E-8	10	L	3E-8* L
n_{air} Index of refraction of air	N	1.3E-7	10	L	1.3E-7*L
δ_{Ii} Cosine errors of interferometer alignment	R	0.1 mrad	>100	$(\delta_{Ii}/2)$ *L	5E-9* L
δ_{Si} Errors of scale alignment	R	0.02 mrad	>100	$(\delta_{Si}/2)$ *L	4E-10*L
α Linear coefficient of thermal expansion of scale material	N	0.01 K	10	$\alpha * L$	5E-9*L
$\Delta t_s = (t_s - 20)$ is the difference of the scale temperature t_s in °C during the measurement from the reference temperature of 20 °C	N	3E-8 K ⁻¹	10	$(t_s - 20)$ * L	3E-9*L

Combined standard uncertainty: $u_c(dl) = 10 \text{ nm} + 1.5 * 10^{-7} * L$ (from 10 nm to 25 nm)

Effective degree of freedom: $\nu_{\text{eff}}(dl) = 22$

Expanded uncertainty: $U_{95}(dl) = 20 \text{ nm} + 3 * 10^{-7} * L$ (from 20 nm to 50 nm)